β-Parvin Mediates Novel Integrin Signaling Pathways During Early *Xenopus laevis* Development

By

Justin Knapp

A thesis

presented to the University of Waterloo

in fulfillment of the thesis requirement for the degree of

Doctor of Philosophy

in

Biology

Waterloo, Ontario, Canada, 2019

Examining Committee Membership

The following served on the examining committee for this thesis. The decision of the Examining Committee is by majority vote.

External Examiner	Dr. Lina Dagnino Professor
Internal-external Member	Dr. Jonathan Blay Professor
Supervisor	Dr. Mungo Marsden Associate Professor
Internal Member	Dr. Bernard Duncker Professor
Internal Member	Dr. Paul Craig Assistant Professor

Author's Declaration

I hereby declare that I am the sole author of this thesis. This is a true copy of the thesis, including any required final revisions, as accepted by my examiners. I understand that my thesis may be made electronically available to the public.

Abstract

Crosstalk between cell adhesion molecules is critical for the cell rearrangements that occur during early *Xenopus laevis* development. Cells primarily use integrin receptors to adhere to and interpret the extracellular environment, and cadherin receptors to modulate adhesion between cells. The *Xenopus laevis* gastrula provides a simple model to examine the molecular processes that regulate adhesion receptor crosstalk as epiboly and convergent extension rely on the modulation of integrin and cadherin adhesion. The adhesive crosstalk of integrin and cadherin is regulated in part by the binding of a shared pool of cytoplasmic molecules to the intracellular tail of these molecules.

β-Parvin, a scaffolding molecule, has been described to accumulate at both cell-extracellular matrix (ECM) and cell-cell junctions. β-parvin consists of two calponin homology domains (CH1 and CH2). The CH1 domain was found to regulate the recruitment of β-parvin to cell-cell borders while the CH2 domain mediates the compartmentalization of β-parvin at sites of cell-ECM adhesion. Cell adhesion assays indicate that over-expression of the CH1 domain reduces cell adhesion to a cadherin substrate, whereas over-expression of the CH2 domain reduces cell adhesion to Fibronectin (FN). Furthermore, disruption of β-Parvin signaling inhibits cell intercalation behaviours that underlie epiboly and convergent extension. This suggests that β-parvin plays a role in mediating both integrin and cadherin adhesion.

Co-immunoprecipitation analysis indicates that the CH2 domain of β-parvin regulates the association of β-parvin with the C-terminus of *Xenopus laevis* integrin-linked kinase (xILK). This interaction requires an outside/in signal originating from the ligation of integrin to FN. In addition, the recruitment of β-parvin to xILK is decreased in the presence of Activin A. This suggests that the activation state of integrin controls xILK- β-parvin interactions.

The CH1 domain of β-parvin was found to regulate the binding of β-parvin to C-cadherin and β-catenin. GST-pull-down analysis indicates that β-catenin is not required for this interaction. Activin A increases the interaction between C-cadherin and β-Parvin. In addition, β-Parvin interacts with a T-cell factor (TCF)-selective pool of β-catenin known to translocate to the nucleus. Interestingly, the nuclear localization signal (NLS) in the N-terminus appears to regulate the exclusion of β-Parvin from the nucleus.

Finally, this study also revealed the existence of a α-parvin homolog in *Xenopus laevis.* RT-PCR analysis indicates that α-parvin mRNA is expressed throughout early *Xenopus laevis* development.

The present study has for the first time described the molecular mechanisms regulating the function of β-Parvin in integrin-cadherin receptor crosstalk during *Xenopus laevis* gastrulation. These findings also demonstrate the novel finding that β-parvin actively modulates cadherin mediated cell adhesion.

Acknowledgements

My PhD would have been much more difficult had I not been blessed with the support of many people along the way. I'd like to thank my supervisor Dr. Mungo Marsden for his help both inside and outside of the lab. I very much enjoyed the conversations we had over the last four years and appreciated his unique view of the world. He was a great role model and I feel very lucky that he was my supervisor.

I would also like to thank my committee members Dr. Bernard Duncker and Dr. Paul Craig for their valuable input throughout my PhD. I must also thank my internal-external member Dr. Jonathan Blay and my external examiner Dr. Lina Dagnino for their time and constructive analysis of this thesis.

I always enjoyed chats and trips to the gym or grad house with my lab friends Cody Shirriff, Matt McLeod, Mitch Kay, Heather Ikert and Dr. James Campbell. Their company made grad school much more enjoyable.

I must also express my appreciation for my buddies Dan Bolton, Sean Lemon, and Nick Meisenheimer for their constant words of encouragement.

Finally, this thesis would not have been possible without my family. My parents, in-laws, brothers and grandparents have always supported my journey through academia. Most importantly I am extremely grateful for my best friend and biggest supporter, my wife, Cassandra Knapp. I'm very lucky to have you in my life.

Table of Contents

List of Figures

List of Tables

List of Abbreviations

ANK	ankyrin
ATCC	American Type Culture Collection
BCR	blastocoel roof
BSA	bovine serum albumin
CE	convergent extension
DMSO	dimethyl sulfoxide
DMZ	dorsal marginal zone
ECL	enhanced chemiluminescence
ESB	embryo solubilization buffer
EtBr	ethidium bromide
FBS	fetal bovine serum
FN	fibronectin
GFP	green florescence protein
GST	glutathione-s-transferase
hCG	human chorionic gonadotropin
HEPES	4-(2-hydroxyethyl)-1-piperazineethanesulfonic acid
HDAC	histone deacetylase
HRP	horseradish peroxidase
ILK	integrin-linked kinase
IPTG	Isopropyl β-D-1-thiogalactopyranoside
L-15	Leibowitz-15
LB	Luria broth
LEF	lymphoid enhancing factor
MBS	modified Barth's saline
MBT	mid-blastula transition
MEM	MOPS, EGTA, $MgSO_4$
MEMFA	MOPS, EGTA, $MgSO_4$, Formaldehyde
MMR	modified Marc's ringer
MO	morpholino oligonucleotide
MSS	modified Stearn's solution
NCoR	nuclear receptor co-repressor 1
NLS	nuclear localization signal
PBS	phosphate buffered saline
PBS-TD	phosphate buffered saline-tween-DMSO
PH	pleckstrin homology
PMSF	phenylmethane sulfonyl fluoride
PNK	polynucleotide kinase
TAE	tris/acetic acid/EDTA
TBS	tris buffered saline
TCF	T-cell factor
TE	tris EDTA

TRITC	tetramethylrhodamine-5-isothiocyanate
WMBS	whole mount blocking solution

1.0 Introduction

In multicellular organisms cell adhesion is a fundamental biological phenomenon and plays numerous roles in cell polarity, cell migration, and morphogenesis (reviewed in Parsons et al., 2010). Cells express diverse types of cell adhesion receptors to control their physical interaction with the ECM and other cells. Of these receptors, the integrin and cadherin transmembrane protein superfamilies are the best studied. The extracellular domain of integrins and cadherins mediate their ligand binding function, while the cytoplasmic domain links the extracellular environment to intracellular signaling pathways. Understanding how these pathways modulate cell adhesion is critical to our understanding of development, wound healing, inflammation, and tumour metastasis (Parsons et al, 2010).

1.1 *Xenopus laevis* gastrulation

Due to the well-characterized cell movements during gastrulation the *Xenopus laevis* embryo is widely used as a model for studying the molecular processes that regulate cell adhesion. Following fertilization, the *Xenopus laevis* embryo undergoes a series of rapid holoblastic reductive cleavages to form the blastula. During this time, the three primary germ layers ectoderm, mesoderm and endoderm are specified. Following cleavage, mass cell movements signal the initiation of gastrulation. During gastrulation, mesoderm and endoderm move to the interior of the embryo and become surrounded by ectoderm. These movements establish the mature spatial arrangement of the germ layers in the embryo. The tissue behaviours that characterize this dramatic re-

organization include: vegetal rotation, involution, epiboly, and convergent extension (Figure 1). These spatially and temporally coordinated rearrangements are dependent on the combined actions of cell adhesion, migration, shape change, and intercalation (Hardin and Keller, 1988; Winklbauer and Schürfeld, 1999; Keller et al., 2003).

Gastrulation is initiated on the dorsal side of the embryo when surface epithelial cells constrict at their apical surface and elongate in the basal direction to form bottle cells (Hardin and Keller, 1988). Concomitantly, cells on the dorsal side of the blastocoel floor begin a massive tissue rotation and move towards the animal pole, a process known as vegetal rotation (refer to Figure 1). Vegetal rotation passively draws cells of the dorsal marginal zone (DMZ) into the interior of the embryo. It also positions the anterior mesoderm in apposition to the overlying blastocoel roof (BCR), where leading edge mesendoderm cells use FN as a substrate for migration moving towards the animal pole (Winklbauer and Schürfeld, 1999). The boundary between the involuted mesoderm and overlying BCR, termed Brachet's cleft, prevents cell mixing between the pre-involution and post-involution mesoderm (Fagotto, 2014). After initial passive involution, convergent extension (CE) and epiboly continue to drive active involution of the DMZ (refer to Figure 1, Keller et al., 1992).

Epiboly is a process that results in the thinning of a multilayered epithelium through radial cell intercalation. Cells undergoing radial intercalation extend protrusions between one another and interdigitate (Szabo et al., 2016). As cells interdigitate, the number of cell layers is reduced and the tissue spreads to occupy a greater surface area. In the *Xenopus laevis* embryo the first phase of epiboly occurs in the BCR at stage 8 and

ends near the beginning of gastrulation at stage 10 (Keller, 1978). At the onset of epiboly, the BCR consists of a superficial epithelial layer and a deep cell layer, 2-4 cells deep. Interestingly during this phase of epiboly, as the deep epithelial layers thin changes in cell shapes are not observed in cells undergoing radial intercalations (Keller, 1978). The second phase of epiboly occurs in the deep layers of the pre-involution DMZ at stage 10+ (Keller, 1980). Cells extend protrusions and interdigitate to form a single layer by stage 11. At the end of gastrulation both the BCR and pre-involution DMZ consist of a superficial epithelial layer and a single deep cell layer (Keller, 1980).

Convergent extension is a process that results in the narrowing and concomitant extension of a tissue through medial-lateral (ML) cell intercalation (Tada and Heisenberg, 2012). Cells undergoing ML cell intercalations polarize along their ML axis, elongate and form stable lamellipodia that are used to attach to neighbouring cells and provide traction for individual cell movement (Keller et al., 1992; Tada and Heisenberg, 2012). At stage 10.5 pre and post-involution mesoderm undergo CE movements and continue to undergo these movements until the end of neurulation (stage 18, Keller et al, 1992). The combined movement of epiboly and CE eventually closes the blastopore.

1.2 Modulation of cell adhesion regulates cell behaviours during *Xenopus laevis* gastrulation

During early *Xenopus laevis* development the modulation of cadherin and integrin adhesions underlie the cell behaviours driving gastrulation. The cadherin superfamily controls the physical interaction between cells, and the integrins mediate adhesive

Figure 1. Tissue movements and cell behaviours during *Xenopus laevis* gastrulation. Gastrulation is initiated on the dorsal side of the embryo, indicated by the formation of elongated, bottle-shaped cells. Vegetal rotation (yellow arrows) expands the blastocoel floor and promotes initial endoderm (yellow) and mesoderm (red) internalization. Subsequent internalization of the mesoderm continues through active involution (red arrows). Mesoderm rolls over the blastopore lip to form a layer between the external ectoderm (blue) and internal endoderm (yellow). Concurrently, cells in the deep layers of the ectoderm interdigitate and undergo radial intercalation. This tissue spreads by a process called epiboly (blue arrows, stage 10.5). After radial intercalations, cells in the involuted mesoderm, polarize along their medial-lateral axis and undergo medial-lateral intercalation. This tissue converges and extends along the anterior-posterior axis by a process called convergent extension (green arrows, stage 12.5). Epiboly and convergent extension drive the closure of the blastopore. This marks the end of gastrulation. (Figure adapted from Evren, 2010 and Keller et al., 2000).

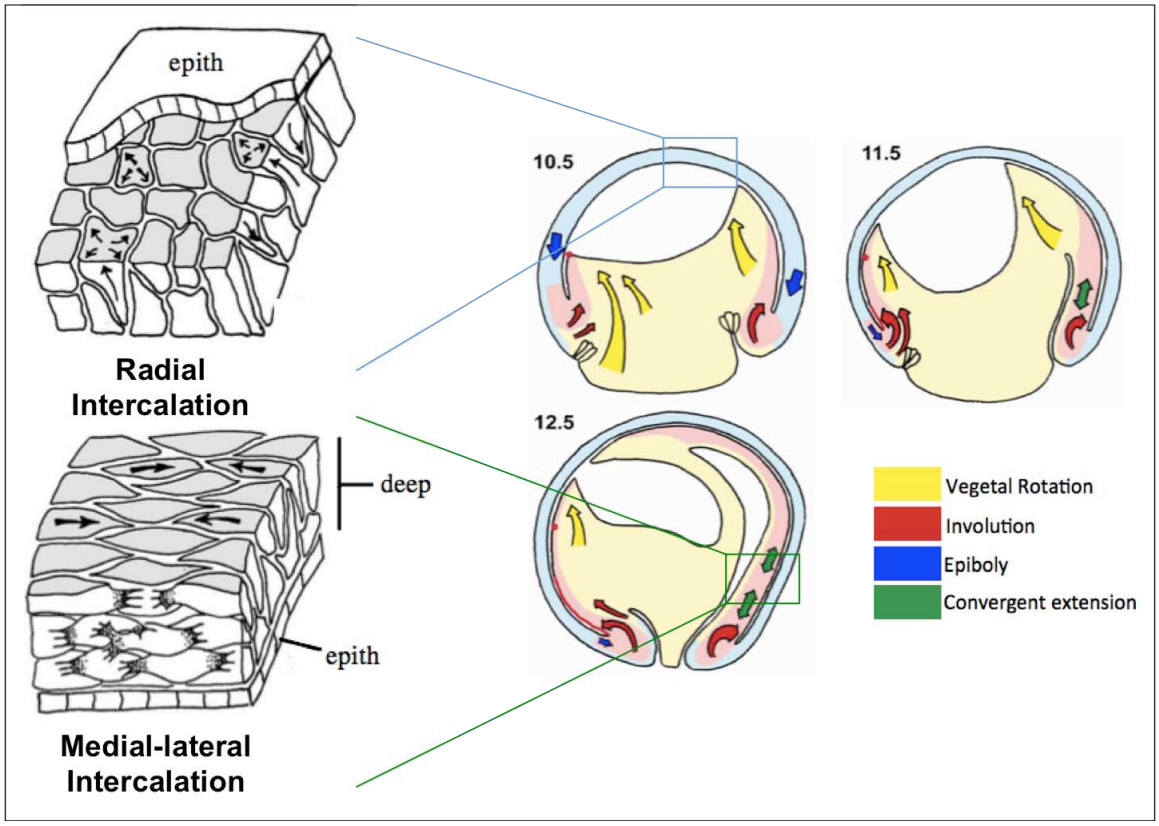
epith
Radial
Intercalation
deep
epith
Medial-lateral
Intercalation
10.5
11.5
12.5
Vegetal Rotation
Involution
Epiboly
Convergent extension

interactions between cells and the extracellular matrix (ECM). Cells use both cadherin and integrin receptors to transmit information about the immediate environment bi-directionally across the cell membrane to fine-tune behaviours as they negotiate the rapidly changing tissue arrangements observed during gastrulation.

C-cadherin is the major cadherin expressed during *Xenopus laevis* development (Levi et al., 1991; Nandadasa et al, 2009). In the BCR, C-cadherin adhesion is increased in comparison to post-involution mesoderm suggesting C-cadherin adhesion is regulated in temporal-spatial manner during *Xenopus laevis* gastrulation (Levi et al., 1991; Nandadasa et al, 2009; Lee and Gumbiner, 1995). During involution, cells pass through the Spemann organizer at the dorsal lip and receive inductive signals that result in a decrease in cadherin adhesion. This can be mimicked *in vitro* through the exposure of dissociated embryonic cells to Activin A, a TGF- β family member (Smith et al., 1990). The decrease in cadherin adhesion occurs without changes in C-cadherin surface expression, and thus reflects a change in the affinity of the receptor (Brieher and Gumbiner, 1994). These changes in cell-cell adhesion are critical during gastrulation for the proper movement of tissues.

ECM interactions driving gastrulation are dependent upon the binding of α5β1 integrin with its sole ligand, FN. Similar to cadherin adhesion, integrin adhesion is regulated in a temporal-spatial fashion in the embryo. All cells of the early embryo have the ability to adhere to FN using the RGD sequence in the cell central binding domain (CCBD). After Activin A exposure, cells can recognize a second site within the CCBD of FN called the synergy domain. These activated cells then acquire the ability to spread and

migrate on FN (Ramos and DeSimone, 1996). The molecular mechanism mediating α5β1 integrin recognition of the synergy domain is not known. As the cell surface expression of α5β1 integrin is unchanged during these events it suggests that changes in integrin adhesive properties are responsible (Ramos and DeSimone, 1996). It is known that the binding of intracellular signaling complexes to the integrin tail may regulate these changes (refer to section 1.4.3).

Integrin and cadherin receptors are capable of propagating biochemical signals bi-directionally across the cell membrane and have been demonstrated to recruit and activate a common set of signaling molecules (Weber et al., 2011; Mui et al., 2016). This co-regulation has been termed crosstalk. There are three modes of adhesive crosstalk: Input-output signaling, lateral coupling and convergent signaling. Input-output signaling involves long-range interactions where signaling from one adhesion receptor modulates the expression or activity another. Convergent signaling occurs when adhesion receptors signal to common downstream effector molecules allowing for redundant, additive or synergistic mechanisms. Lastly, lateral coupling allows for signaling in the absence of cell adhesion, through the interaction with other transmembrane proteins, cytoplasmic adaptors or scaffolding proteins (Weber et al., 2011). The regulation of cell adhesion during early *Xenopus laevis* development involves each mode of crosstalk.

1.3 The cadherin superfamily

The cadherin superfamily of calcium dependent, homophilic cell-cell adhesion molecules consists of the classical cadherins, desmosomal cadherins, atypical cadherins and proto-cadherins (Kraft et al., 2012). The classical cadherins are transmembrane

proteins that form a protein complex through parallel (cis) dimer formation. The extracellular domain mediates cell-cell interactions through homophilic (trans) binding. Receptor clustering enhances the adhesive strength of cadherin (Gumbiner, 2000). Cadherin dimer formation initiates the recruitment and binding of catenins (β, p120, plakoglobin) to highly conserved domains in the cytoplasmic tail. β-catenin and plakoglobin (PG) bind to the more distal region known as the catenin-binding-domain (CBD) while p120-catenin binds a membrane proximal region known as the juxtamembrane domain (JMD). The cadherin-catenin cytoplasmic complex can connect to and modulate cytoplasmic signaling pathways as well as cytoskeletal assembly (Kraft et al., 2012; Weber et al., 2011). Both β-catenin and PG mediate the association between cadherins and the actin cytoskeleton at adherens junctions (McCrea and Gottardi, 2015). PG can also facilitate the association of cadherins with intermediate filaments at desmosomal junctions (Leonard et al, 2008). Thus the recruitment of cytoplasmic assemblies to the intracellular domain of cadherins is directly responsible for the adhesive properties of these receptors.

β-catenin was first isolated in association with the cytoplasmic domain of classical cadherins and is the founding member of the Armadillo family of structural proteins (reviewed in Fagotto, 2013). In addition to roles in cadherin-mediated adhesion, β-catenin is a key signal transducer of the canonical WNT signaling pathway (reviewed in Gumbiner, 2005; McCrea and Gottardi, 2015). When stabilized in the cytosol by Wnt signals, β-catenin associates with T-cell factor (TCF) or leukocyte enhancing factor (LEF) transcription factors, translocates to the nucleus and alters gene expression (McCrea et

al., 2015). In HEK 293 cells, cytoplasmic β-catenin can exist as a TCF-selective pool that is targeted to the nucleus and a distinct non-overlapping population that can interact with cadherin (Gottardi and Gumbiner, 2004). It was subsequently found that E-cadherin phosphorylation permits cadherin binding of β-catenin that would have otherwise been TCF selective. Therefore, these pools of β-catenin appear to be distinguished through the ligand and not β-catenin itself. A similar scenario appears to be true in *Xenopus laevis* as C-cadherin acts as a stoichiometric inhibitor of β-catenin transcriptional signaling, suggesting that cadherins and xTCF compete for the same pool of cytoplasmic β-catenin (Fagotto et al, 1996). A competitive relationship between C-cadherin and xTCF binding is supported by the observation that they both bind to extensively overlapping regions along β-catenin (Howard et al, 2011; Gottardi and Gumbiner, 2001). Taken together, cadherin cytoplasmic tail conformation appears to control in part the cytoplasmic populations of β-catenin involved in cell adhesion and gene expression.

1.3.1 Cadherin adhesion regulates cell behaviors during *Xenopus laevis* gastrulation

Three cadherin receptors are expressed in the early *Xenopus laevis* embryo, C-, E- and N-cadherin. C-cadherin is ubiquitously expressed in the embryo. Blastomeres express maternally derived C-cadherin, while C-cadherin in the gastrula is zygotically expressed (Heasman et al., 1994). Expression of E-cadherin is observed at the start of gastrulation but is restricted to animal cells that give rise to the superficial ectoderm. The underlying cells of this epithelium pre-dominantly express C-cadherin. N-cadherin is not expressed until neurulation and expression is restricted to the neural plate

(Nandadasa et al, 2009). Therefore, C-cadherin is the primary cadherin expressed in tissues undergoing morphogenic processes during *Xenopus laevis* gastrulation.

Precise control of cadherin adhesion is required for proper cell movements during gastrulation. Experimentally reducing C-cadherin activity using a truncated C-cadherin construct (Lee and Gumbiner, 1995), or increasing C-cadherin activity using an activating antibody (Zhong et al., 1999) inhibits medial-lateral cell intercalations required for CE. The modulation of cadherin adhesion is also required for FN assembly along the BCR (Dzamba et al., 2009). Ectopic expression of cadherin in the BCR increases tissue tension and leads to the precocious assembly of FN (Dzamba et al., 2009). Conversely, reducing cadherin adhesion with a dominant negative construct inhibits fibrillogenesis. This indicates that cadherin mediated cell-cell adhesion contributes to tensile forces required to assemble FN (discussed in section 1.5.2; Dzamba et al., 2009). More recently, the recruitment of PG to C-cadherin was demonstrated to establish directed protrusive behaviour of cells within the post-involution mesoderm (Weber et al, 2012). It was also determined that PG-C-cadherin complexes recruit keratin intermediate filaments under integrin mediated tension to drive this behavior (Weber et al, 2012). This indicates that C-cadherin regulated cell behaviours play major roles in diverse phenomena that occur during gastrulation.

The above interactions indicate that a regulated communication between integrin and cadherin is required for proper morphogenesis in *Xenopus laevis*. Inhibiting α5β1 signals, using β1 cytoplasmic domain dominant negative constructs (HAβ1) during gastrulation blocks FN matrix assembly (Marsden and DeSimone, 2001) an integrin

mediated process, as well as epiboly and CE tissue movements requiring changes dependent on cell-cell adhesion (discussed in section 1.4.3). This crosstalk between cell-ECM and cell-cell adhesion appears to be direct as inhibiting α5β1 signals reduces the adhesion of embryonic cells to a cadherin substrate (Marsden and DeSimone, 2003).

The existence of an adhesive crosstalk during *Xenopus laevis* gastrulation is further supported by the observation that FAK, an integrin associated molecule, is required for the ML protrusive polarity in post-involution mesoderm and is required for the assembly of C-cadherin adhesion complexes in this tissue (Bjerke et al., 2014). In cell culture, FAK associates with VE-cadherin in growth factor stimulated endothelial cells. Here, FAK phosphorylates β-catenin and facilitates its dissociation from cadherin, resulting in reduced junctional stability (Chen et al., 2012). Thus it appears that receptor crosstalk is mediated in part through the direct localization of molecules at integrin and cadherin adhesions.

1.4 The integrin superfamily

Integrins are heterodimeric cell-ECM adhesion molecules formed through the association of α and β subunits. In mammals there are 18 α-subunits and eight β-subunits that can combine to form 24 distinct receptors. A much more limited repertoire is present in invertebrates. *Drosophila melanogaster* expresses five α-subunits and two β-subunits, while *Caenorhabditis elegans* express only 2 α-subunits and 1 β-subunit (Hynes, 2002). Therefore the variety of integrin heterodimers has increased as the body plan of multicellular organisms has increased in complexity.

Furthermore, the diversity of integrins is directly related to the diversity of ECM molecules (discussed in section 1.4.1; Hynes and Zhao, 2000).

Each integrin heterodimer possesses different ligand specificity and tissue expression patterns (reviewed in Hynes, 2002). The binding affinity of individual integrin heterodimers for their extracellular ligand depends on the conformation of the extracellular domain and the clustering of integrins. Integrins exist in a continuum of conformations that are regulated by stimuli originating both outside (outside/in signaling) and inside the cell (inside/out signaling; reviewed in Shattil et al., 2010 and Bouvard et al, 2013). Outside/in signaling transmits biochemical signals from the extra-cellular ligands through integrins into the cell. Ligand binding induces a conformational change in the integrin heterodimer and stimulates the recruitment of cytoplasmic protein complexes. Inside/out activation involves the binding of cytoplasmic integrin activators (such as talin and kindlin) to conserved motifs in the cytoplasmic tails of β-integrins. Activator binding leads to conformational changes in the integrin heterodimer and increases extracellular ligand binding affinity (Shattil et al., 2010). Once activated, integrins are capable of mediating ECM assembly, cell adhesion as well as cell migration. The binding of cytoplasmic proteins such as filamin, ICAP1 and SHARPIN can inhibit integrin activation. SHARPIN directly interacts with the cytoplasmic tails of α-integrins and blocks the recruitment of talin to β-integrins (Rantala et al., 2011). Therefore the activity of integrin receptors is mediated through a complex set of signaling pathways.

1.4.1 The extracellular matrix

The extracellular matrix is the non-cellular environment present in all tissues and organs in part composed of several distinct families of proteins (glycoproteins, proteoglycans, glycosaminoglycans; reviewed in Frantz et al., 2010; Rozario and DeSimone, 2010). There are a greater diversity of ECM molecules found in vertebrates than invertebrates, this is reflected in the range of integrins found in these organisms. (reviewed in Hynes and Zhao, 2000). *Drosophila melanogaster* and *Caenorhabditis elegans* express the basic constituents of a basement membrane, however, many ECM molecules critical for vertebrate development such as FN are not present. It is suggested that FN co-evolved with the elaboration of complex vasculature (Hynes and Zhao, 2000).

The ECM not only provides the physical scaffold for cells and tissues but also initiate critical signaling pathways in diverse cellular processes (reviewed in Rozario and DeSimone, 2010). The extracellular environment is highly dynamic and constantly remodeled by cells that come into contact with it. Differences in the density, composition and architecture, termed the “matrix-topography”, have functional consequences on cell behaviours. For example, the assembly and remodeling of FN during *Xenopus laevis* gastrulation are essential for the cell behaviours underlying collective cell migration, epiboly and CE (reviewed in Rozario and DeSimone, 2010; Nagel and Winklbauer, 2018)

1.4.2 Integrin mediated fibronectin assembly

Three integrins are expressed in the early *Xenopus laevis* embryo: α5β1, α3β1 and αVβ3 (Joos et al., 1995; Alfandari et al., 1995; Joos et al., 1998). Of the three, α5β1

integrin is the only functional heterodimer for FN during early *Xenopus laevis* development (Hoffstrom, 2002). Fibronectin is secreted as a soluble dimer by all cells of the blastula stage embryo (Lee et al., 1984). In the blastula, all cells express α5β1 integrin and all cells lining the blastocoel are in contact with soluble FN (Lee et al., 1984), however FN assembly only occurs on the BCR, suggesting spatially restricted signaling pathways regulate FN assembly.

FN assembly requires cell contractility. In cell culture, increasing cell contractility by transfecting cells with constitutively active Rho GTPase promotes FN assembly, while treating cells with inhibitors of cell contractility (BDM and H7) decreases the incorporation of FN into fibrils (Zhong et al., 1998). A similar process occurs in the *Xenopus laevis* embryo. FN fibrillogenesis along the blastocoel roof is a multi-step process. Initially BCR cells use α5β1 integrin to bind soluble FN. α5β1 bound FN has a compact structure that prevents matrix formation in solution, therefore FN is observed as punctae on the surface of these cells (Winklbauer, 1998). As gastrulation proceeds, increases in cadherin adhesion and Pak activation result in peripheral F-actin accumulation. Subsequent myosin-light chain II phosphorylation increases cellular contractility and tension across the BCR (Dzamba et al., 2009). The cadherin-mediated tension across BCR cells is transmitted to FN through α5β1-actin linkages. This increased tension unfolds bound FN dimers and promotes self-assembly of insoluble fibrils (Figure 2; Dzamba et al., 2009).

1.4.3 Integrin mediated adhesion regulates cell behaviours during gastrulation

The FN matrix defines tissue boundaries in the embryo. At these boundaries,

Figure 2. FN assembly during *Xenopus laevis* gastrulation requires integrin and cadherin adhesion. A) At the onset of gastrulation, FN assembly is spatially restricted to the inner surface of the blastocoel roof (BCR) and tissue boundaries separating pre and post-involution mesoderm (inner surface of blue tissue) B) An example of FN matrix as indicated by the black box in panel A. C) Cartoon model of FN matrix assembly as depicted in panel B. Molecular mechanisms promoting FN fibrillogenesis. BCR cells use α5β1 integrin to bind FN dimers. Increases in C-cadherin mediated cell-cell adhesion increases the tension across the BCR. This is associated with increased F-actin at the cell periphery. Tissue tension is then transmitted to FN through α5β1-FN complexes. The unfolding of FN exposes masked self-interaction sites that promote FN-FN interactions and initiates matrix assembly. (Panel A adapted from Evren, 2010).

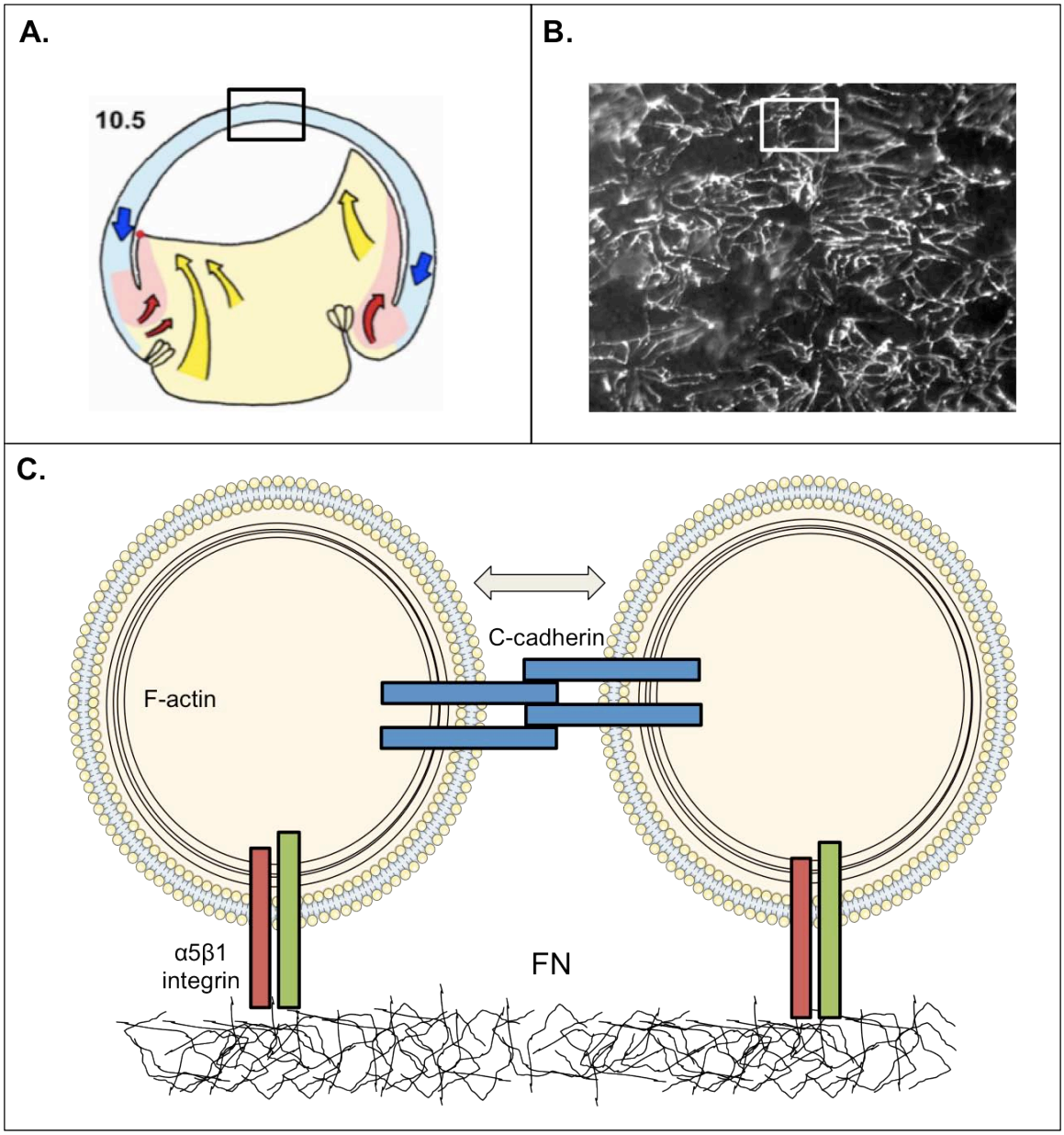
A.
10.5
B.
C.
C-cadherin
F-actin
α5β1
integrin
FN

α5β1 integrin transmits signals from FN into the cell to drive the cell intercalations that underlie epiboly and CE (Marsden and DeSimone, 2001; Davidson et al., 2006). Inhibiting FN matrix formation with function-blocking antibodies inhibits radial cell intercalations driving the second phase of epiboly in the DMZ (Keller, 1978; Marsden and DeSimone, 2001). While FN is not required for thinning of the animal cap at the beginning of gastrulation, inhibiting matrix assembly results in subsequent tissue thickening (Marsden and DeSimone, 2001). Therefore, FN is required in the DMZ to support intercalation behaviours, while in the BCR FN maintains these movements. Furthermore, morpholino oligonucleotide (MO) knockdown of FN results in the loss of medial-lateral cell protrusions required for CE (Davidson et al., 2006). Taken together, these findings indicate that FN is essential for the cell intercalation behaviours during gastrulation. Interestingly a FN matrix in itself does not appear to be required for these cell behaviours. Rozario et al., 2009, experimentally separated FN ligation at the cell surface from assembly of a fibrillar matrix using a 70kD N-terminal domain of FN as a competitive inhibitor of FN matrix assembly. Inhibition of FN assembly has no effect on medial-lateral cell intercalations in *ex vivo* explants (Rozario et al, 2009). This indicates that α5β1-FN ligation is permissive for the cell intercalations that drive CE. As all cells in the embryo are exposed to soluble FN it may well be that once incorporated into a matrix FN exposes masked sites that are responsible for these signals.

As described above, the signals initiated from α5β1-FN ligation are transmitted into the cell to drive the cell behaviours underlying epiboly and CE (Marsden and DeSimone, 2001; Davidson et al., 2006). Signaling from both the α and β cytoplasmic

domains of α5β1 integrin are responsible for these behaviors. Inhibiting α5β1 signals, using β1 cytoplasmic domain dominant negative constructs (HAβ1) inhibits FN matrix assembly, epiboly in the pre-involution DMZ (Marsden and DeSimone, 2001) as well as medial-lateral cell intercalations that drive CE in both the post-involution mesoderm and neural tissues. In experiments utilizing chimeric integrin molecules, consisting of different α cytoplasmic domains, distinct α cytoplasmic tails were found to contribute to the modulation of integrin function during *Xenopus laevis* gastrulation (Na et al., 2003). While all chimeras with a full-length α cytoplasmic domain were able to support migration on FN after exposure to Activin A, signaling downstream of α5, and α6 cytoplasmic tails uniquely support FN assembly (Na et al., 2003). Thus α cytoplasmic domain specific inside/out signaling is essential for FN assembly.

1.5 Integrin-linked kinase

Signals associated with the cytoplasmic domain of integrins are essential for the regulation of receptor adhesive activity (refer to section 1.5.2). Initial integrin ligation to the ECM promotes the clustering of integrins and the recruitment of multi-protein complexes to the cytoplasmic domain. These integrin assemblies are known as focal adhesions and are known to contain at least 150 different signaling and scaffolding molecules. Focal adhesions are dynamic structures with highly regulated turnover of these protein assemblies (reviewed in Legate et al., 2006; Wolfenson et al., 2013; Shattil et al., 2010). One of these protein complexes is the ILK-PINCH-parvin (IPP) complex and the focus of my thesis is ILK and parvin.

Integrin linked kinase (ILK) was identified in a yeast two-hybrid screen for proteins that interact with the cytoplasmic domain of β1 integrin and was also found capable of interacting with β3 integrin (Hannigan et al., 1996). ILK contains five tandem N-terminal ankyrin (ANK) domains, a central pleckstrin homology (PH) domain and a C-terminal domain that shares significant homology to Serine/Threonine protein kinases (refer to Figure 3; Hannigan et al., 1996). While the kinase domain of ILK displays homology to protein kinases, there have been several conflicting reports examining ILK kinase activity (reviewed in Dagnino, 2011).

Despite conflicting data on whether ILK functions as a kinase, the scaffold function of ILK is essential for the function of ILK at sites of integrin adhesion (reviewed in Boulter and Obberghen-Schilling, 2005; Legate et al., 2006). In *Drosophila* ILK is recruited to integrins at muscle attachment sites (MAS) and focal contact-like structures in the wing epithelium, where it plays essential roles in maintaining the link between integrin and the actin cytoskeleton (Zervas et al., 2011; Vakaloglou et al., 2012). Introduction of a null mutation in *ilk* resulted in the breakage of integrin adhesions and actin was observed to aggregate rather than extend as fibrils along the length of the cells (Zervas et al., 2011). In cultured keratinocytes, inactivation of *ilk* produced cells incapable of spreading on an ECM substrate and the cells displayed a rounded morphology with abnormal membrane protrusions (Nakrieko et al., 2008b). Furthermore, ILK-deficient keratinocytes were unable to sustain directed migration suggesting a potential role in developing polarity. Indeed, ILK is necessary for the acquisition of front-rear polarity and forward movement (Ho and Dagnino, 2012).

Figure 3. Structure of β-Parvin and ILK. β-Parvin consists of two nuclear localization signals (black rectangles) in the amino terminus and two calponin homology domains (CH1 and CH2). The CH2 domain binds to the kinase domain (KINASE) in the carboxy terminus of integrin-linked kinase (ILK). ILK consists of five tandem ankryin repeat (ANK) domains, a central pleckstrin homology domain (PH) and an integrin-binding domain (INT) found within the c-terminal kinase domain. Green and red indicate non-conserved domains in β-Parvin and ILK.

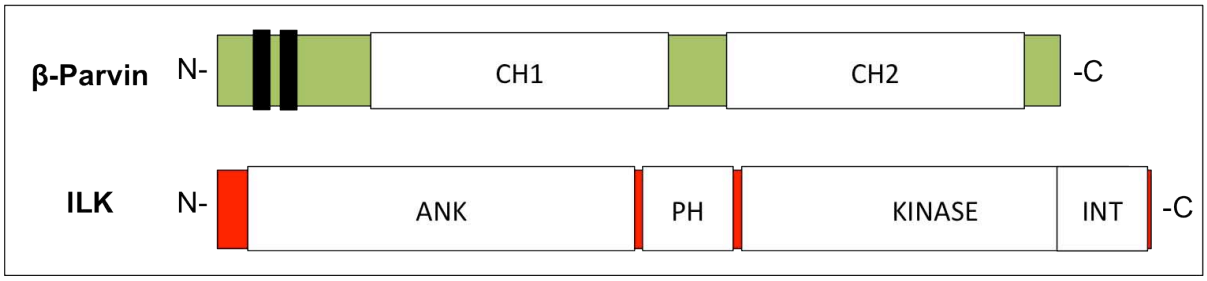
β-Parvin
N-
CH1
CH2
-C
ILK
N-
ANK
PH
KINASE
INT
-C

In addition to its function at sites of integrin adhesion, ILK has been reported to influence cell-cell adhesions and is also actively transported into the nucleus (Wu et al., 1998; Yusunaga et al., 2005; Nakrieko et al, 2008a). In cultured keratinocytes, ILK was found to change subcellular distribution during keratinocyte differentiation from focal adhesions to cell borders (Vespa et al., 2005). Interestingly, a point mutation in ILK that abolishes recruitment to focal adhesions doesn't disrupt compartmentalization at cell-cell junctions. Therefore, the domain mediating recruitment to integrin is separate from the domain responsible for localization at cell borders. Furthermore, the recruitment to cell borders does not depend on the association of ILK with PINCH or parvin, suggesting novel interactions may regulate cell junction recruitment (Vespa et al., 2005). ILK has been demonstrated to modulate cell-cell adhesion *in vitro* and *in vivo*. In cell culture, over-expression of ILK deletion constructs unable to localize to cell borders impaired the formation of cell-cell contacts. In support of a role in cell-cell contacts, junctional proteins β–catenin and occludin display abnormal localization in the absence of ILK. Cortical actin fibers critical for nascent junction formation also failed to develop properly in these cells (Vespa et al., 2005). Therefore, ILK plays a critical role in the events required for the formation of cell-cell junctions in cultured cells.

In the developing *Xenopus laevis* embryo, morpholino (MO) mediated knockdown of ILK decreased the adhesion of embryonic cells to a FN substrate and produced gross embryonic defects similar to those observed with disruption of integrin-ECM signaling such as delayed blastopore closure and truncated extension of the dorsal axis (Yusunaga et al., 2005; Marsden et al., 2001). Furthermore, ILK knockdown decreased cell-cell

adhesion and tissues were observed to dissociate into single cells (Yusunaga et al., 2005). These results indicate that ILK may be involved in regulating both cell-ECM and cell-cell adhesions.

1.6 Parvin

The parvins are a family of scaffolding proteins involved in linking the ECM to intracellular signaling pathways through $\beta 1$ and $\beta 3$ integrins (reviewed in Sepulveda and Wu, 2006). In mammals three parvin isoforms α, β, γ are expressed from separate genes (Olski, et al., 2001). Parvins do not possess enzymatic activity, but act as scaffolding proteins to assemble cytoplasmic complexes (Sjoblom, et al., 2008). α-Parvin and β-Parvin are ubiquitously expressed, whereas γ-Parvin expression is restricted to lymphoid and hematopoietic tissues (Sepulveda and Wu, 2006).

The most distinct feature of the parvins is the presence of two tandem calponin homology (CH) domains: an N-terminal (CH1) domain and a C-terminal (CH2) domain (refer to Figure 3). CH domains are found in diverse proteins and can serve drastically different functional roles. CH domains are one of approximately 12 protein domains shared by both signaling and cytoskeletal proteins (Gioma, et al., 2001). The presence of tandem calponin homology domains has been associated with the formation of an actin-binding domain (ABD). α and β-Parvin possess unconventional CH domains that do not contain a consensus ABD (Gioma, et al., 2001).

In *Drosophila,* the recruitment of parvin (only a single parvin gene is present in *Drosophila*) and ILK to integrin is tissue specific (Vakaloglou et al., 2012). During *Drosophila* development, ILK is essential for parvin stability and accumulation at muscle

adhesion sites, however parvin is not required for ILK recruitment. Introduction of a null mutation in *parvin* resulted in similar phenotypes to those observed in *ilk* null embryos suggesting that the two molecules collaborate in regulating the stability of integrin adhesion (refer to section 1.6; Vakaloglou et al., 2012). At focal contact-like structures in the wing epithelium, ILK and parvin are interdependent for recruitment to integrin as parvin knockdown reduces the recruitment of ILK to integrin. Furthermore, parvin plays a role in stabilizing ILK in the wing epithelium as parvin knockdown decreases ILK expression. Similarly, in cultured mouse myoblast cells the interaction of ILK and parvin precedes recruitment to integrin. Disrupting the interaction between ILK and parvin impairs the recruitment of ILK to focal adhesions (Zhang et al., 2002). The differential recruitment of parvin suggests that there are tissue specific signals that control parvin and ILK interactions.

α -parvin was first identified as a rat complementary DNA (cDNA) (Nikolopoulos and Turner, 2000). Another group of researchers independently identified α-Parvin by yeast 2-hybrid assay using a bait construct encoding the C-terminus of human ILK. The CH2 domain was determined to mediate the interaction of α-Parvin with ILK and recruit α-Parvin to focal adhesions. Furthermore, α-Parvin potentially plays a crucial role in the in the regulation of cell-ECM adhesion as over-expression of the CH2 domain in CHO cells reduced the ability of cells to adhere to and spread on collagen. Examination of the cytoskeleton revealed that CH2 domain over-expression delayed stress fiber formation (Tu et al., 2000; Clarke et al, 2004). Thus it would appear that the interaction of the CH2

domain of α-Parvin with the kinase domain of ILK plays a role maintaining integrin-cytoskeletal connections.

Shortly after the characterization of α-Parvin, β-Parvin was identified via yeast 2-hybrid assay using a bait construct encoding full length human ILK (Yamaji et al., 2001). Similar to α-Parvin the CH2 domain of β-Parvin was also found to mediate the recruitment of β-Parvin to focal adhesions and mediate the interaction with ILK. β-Parvin is observed in membrane blebs during the early stages of cell spreading suggesting that it is recruited into nascent cell-ECM adhesion structures. CH2 domain over-expression had deleterious effects on cell adhesion. Cells were observed to remain in a circular or oval shape with deficient membrane extensions, spreading and lamellipodium maturation. Therefore, β-Parvin plays an essential role in the establishment of cell-ECM adhesions.

Although structurally similar, α and β-Parvin have been demonstrated to play distinct roles in regulation of cell behaviour. Given that α and β-Parvin interact with ILK and localize to focal adhesions, it was hypothesized that these molecules may play antagonistic roles (Zhang et al., 2004). Indeed, α and β-Parvin competitively bind ILK and the expression level of each protein was found to control the ratio of the complex (Zhang et al., 2004). Although structurally similar, α and β-Parvin have been demonstrated to play distinct roles in regulation of cell behaviour. While α-Parvin does not appear to have an effect on cell survival β-Parvin is pro-apoptotic (Zhang et al., 2004).

In addition to the role at focal adhesions, α and β-Parvin have also been observed at cell borders (Pitter, et al., 2018) and in the nucleus (Olski et al., 2001; Johnstone et al., 2008). Despite prominent localization, a role in the nucleus has not been determined. At endothelial cell borders, α and β-Parvin maintain the integrity of cell-cell junctions. The depletion of α and β-Parvin in endothelial cells during mouse development results in diffuse and discontinuous VE-cadherin distribution leading to cell-cell junction destabilization and the loss of apical-basal polarity (Pitter, et al., 2018). These defects are similar to the phenotypes observed in endothelial cells lacking β1 integrin suggesting adhesive crosstalk, through parvin, plays a role in maintaining the integrity of endothelial cell-cell adhesion (Pitter, et al., 2018).

1.7 Disrupting β-parvin signaling inhibits gastrulation

During early *Xenopus laevis* development β-Parvin mRNA is expressed in the dorsal tissues of the gastrula stage embryo. β-Parvin mRNA is found within the BCR and also in the pre-and post-involution DMZ (Studholme, 2013). Therefore, *beta-parvin* is expressed in tissues that regulate FN assembly and tissues undergoing radial and medial-lateral cell intercalations. When β-Parvin deletion constructs were transfected into *Xenopus laevis* A6 cells, the CH2 domain was recruited to focal adhesions while the CH1 domain was not (Studholme, 2013), consistent with observations in other cell culture models (Olski et al., 2001). Interestingly, the CH1 domain of β-Parvin was found to accumulate at nascent cell boundaries in re-associating embryonic cells suggesting that the CH1 domain of β-Parvin may recruit β-Parvin to sites of cell-cell adhesion (Studholme, 2013).

β-Parvin plays an important role in regulating morphogenic processes during gastrulation as over-expression of either the CH1 or CH2 domain of β-Parvin produced tissue level defects resembling a failure in epiboly and CE. Disruption of β-Parvin signaling also resulted in embryos with a truncated anterior-posterior axis (Studholme, 2013). The inhibition of FN assembly produces similar defects (Marsden and DeSimone, 2001) and the observed phenotypes may be an indirect consequence of disrupting β-Parvin. Over-expression of the CH1 or CH2 domain does inhibit FN assembly along the BCR, however they act through distinct mechanisms (Studholme, 2013). The CH2 domain associates with xILK and inhibits integrin-FN interactions while the CH1 domain inhibits FN assembly downstream of receptor ligand interactions. Interestingly the CH2 domain inhibits matrix assembly and all associated cell movements (epiboly and CE), while the CH1 domain permits CE in the absence of a FN matrix (Studholme, 2013). This suggests that β-Parvin may be a key player in the signaling pathway involved in cell-cell adhesion downstream of integrin.

A potential mechanism to explain the tissue level defects observed in β-Parvin morphant embryos is the ability of β-Parvin to modulate the activation of Rho GTPases. In cell culture the CH1 domain of β-Parvin interacts with α Pix, a guanine nucleotide exchange factor (GEF) that activates Rho GTPases, at the leading edge of lamellipodia (Mishima et al, 2004). Over-expression of CH1 increased the level of active Rac while CH2 over-expression increased the level of active RhoA (Studholme, 2013). Therefore, it is plausible that β-Parvin may directly activate Rho GTPases during *Xenopus laevis* gastrulation to regulate cell behaviour

1.8 Summary

The tissue movements and cell behaviours that underlie *Xenopus laevis* morphogenesis are well characterized and are dependent on the regulation of integrin and cadherin adhesion. While there is abundant evidence that there is crosstalk between integrins and cadherins, the molecules and mechanisms are not as well characterized. The *Xenopus laevis* embryo provides a simple model to examine the molecules that play a role in mediating a receptor crosstalk. The tissue level defects produced by disrupting β-Parvin signaling during *Xenopus laevis* development have been examined (Studholme, 2013). These tissue level defects suggest that β-Parvin has pleiotropic effects and modulates cell adhesion through multiple mechanisms. Therefore, I hypothesize that β-Parvin acts to regulate the dynamic interplay between integrin and cadherin receptors during *Xenopus laevis* gastrulation. I tested this by examining the signaling pathways β-Parvin participates in as well as its molecular interactions

2.0 Materials and Methods

2.1 Materials

2.1.1 Reagents

Table 1. Reagents

Chemical	Company
Agarose	Bioshop, Burlington, ON
Benzocaine	Sigma-Aldrich, Oakville, ON
BMPurple α-Parvin-Substrate	Roche, Mississauga, ON
Digoxigenin labeling mix	Roche, Mississauga, ON
DTT (Dithiothreitol)	Bioshop, Burlington, ON
Coomassie Brilliant Blue R-250 Dye	Thermo Fisher Scientific, Mississauga, ON
Ethidium Bromide (EtBr)	Bioshop, Burlington, ON
Halt™ Protease inhibitor cocktail (100X)	Thermo Fisher Scientific, Mississauga, ON
IPTG (Isopropyl β-D-1-thiogalactopyranoside), Ultra Pure	TekNova, Hollister, CA
Leibowitz-15 (L-15) Medium	Thermo Fisher Scientific, Mississauga, ON
Nitrocellulose membrane	GE Healthcare, Mississauga, ON
Paraformaldehyde	Bioshop, Burlington, ON
Ponceau S	Bioshop, Burlington, ON
Ruby Red 5K-dextran	Molecular Probes, Eugene, OR
Tween 20	Sigma-Aldrich, Oakville, ON
Triton X 100	Sigma-Aldrich, Oakville, ON

2.1.2 Buffers and solutions

Table 2. Buffer and solution recipes used in molecular biology protocols

Buffer/Solution	Recipe
BABB	1:2 (v/v) mixture of benzyl alcohol: benzylbenzoate

Blocking solution (Western blot)	5% powdered milk, 0.1% tween-20, in TBS
Coomassie de-stain	10% glacial acetic acid, 40% MeOH
Coomassie stain stain	0.1% Coomassie Brilliant Blue R-250 Dye, 10% glacial acetic acid, 40% MeOH
Cysteine Solution (2%)	1g l-cysteine, 50mL 0.1x MBS, pH: 8.3 with NaOH
ECL solution #1	2.5 mM luminol, 0.4 mM p-cumaric acid, 100 mM Tris-HCl
ECL solution #2	0.02% H_2O_2, 100 mM tris-HCl
ESB	50 mM tris pH: 7.5, 100 mM NaCl, 1% trition X 100, 1x Halt™ Protease inhibitor cocktail
GST-pull-down lysis buffer	50mM tris pH: 7.5, 100mM NaCl, 0.5mM MgCl2, 1% trition X 100, 1x Halt™ Protease inhibitor cocktail
HEPES lysis buffer	20mM HEPES pH: 7.5, 120mM NaCl, 10% glycerol, 2mM EDTA, 0.5% NP-40, 1x Halt™ Protease inhibitor cocktail
LB medium	1% bactotryptone, 1% NaCl, 0. 5% yeast extract
LB-Amp	LB-medium, 50 mg/ml ampicillin
LB-Amp-agar plates	1.5% agarose, LB-medium, 50 mg/ml ampicillin
L-15 complete cell culture media	66% L-15, 10% FBS, 1% penicillin/streptomycin
MBS (1x)	88 mM NaCl, 1 mM KCl, 0.7 mM $CaCl_2$, 1 mM $MgSO_4$, 5 mM HEPES (pH 7.8), 2.5 mM $NaHCO_3$
MMR (1x)	0.1 M NaCl, 2.0 mM KCl, 1 mM $MgSO_4$, 2 mM $CaCl_2$, 5 mM HEPES (pH 7.8), 0.1 mM EDTA
MEM (10x)	1 M MOPS, 20 mM EGTA, 10 mM MgSO4 pH 7.4
MEMFA	3.7% formaldehyde, 1x MEM

MSS-	3.75 mM NaCl, 0.01mM Na_2SO_4, 0.25 mM HEPES, 0.12 mM KCl, 30mM Na_2HPO_4, 0.07mM K_2HPO_4, pH: 8.3
MSS+	MSS-, 1mM $CaCl_2$, 0.5mM $MgCl_2$
PBS (10x)	27 mM KCl, 1.37 mM NaCl, 20 mM KH2PO4, 100 mM Na2HPO4, pH: 7.4
PBST (1x)	PBS, 0.1% tween-20
PBS-TD	PBS, 1% tween-20, 1% DMSO
SDS sample buffer (5x)	312.5 mM tris-HCl pH 6.8, 1% SDS, 25% glycerol, 0.015% bromophenol Blue, 12.5% β-mercaptoethanol
SSC (20x)	3 M NaCl, 0.3 M sodium citrate, pH 7.5
STE lysis buffer	10mM tris-HCl, 1mM EDTA, 150mM NaCl, pH: 8.0, 1x Halt™ Protease inhibitor cocktail.
TAE (1x)	40 mM tris-acetate, 1 mM EDTA
TBS (1x)	2 mM tris, pH 7.5, 30 mM NaCl
TBST	2 mM tris, pH 7.5, 30 mM NaCl, 0.1% Tween20
TE	10 mM tris-HCl, 1 mM EDTA, pH 8.0
WMBS	PBS, 1% tween-20, 1% DMSO, 0.1M glycine, 2% powdered milk, 5% lamb serum
Western Blot running buffer	24.8 mM tris, 192 mM glycine, 0.1% SDS
Western Blot transfer buffer	24.8 mM tris, 192 mM glycine, 20% methanol

2.1.3 Proteins and enzymes

Table 3. Proteins and Enzymes used in molecular biology protocols

Protein/Enzyme	Company
Activin A	R&D Systems, Burlington, ON
BamH1, EcoR1, Not1, Stu1 and Xba1 restriction enzymes	New England Biolabs, Ipswich, MA
Bovine serum albumin	Bioshop, Burlington, ON
DNaseI (RNase Free)	New England Biolabs, Ipswich, MA
FC-cadherin	Gift from Barry Gumbiner, University of Virginia
Glutathione-Uniflow Resin	BD Biosciences, Mississauga, ON
Human chorionic gonadotropin (hCG)	Chorulon; Intervet, Kirkland, QC
Human Plasma FN	BD Biosciences, Mississauga, ON
Phusion DNA polymerase	New England Biolabs, Ipswich, MA
Phusion High-Fidelity PCR Master Mix with HF Buffer	New England Biolabs, Ipswich, MA
Polynucleotide Kinase (PNK)	Fermentas, Burlington, ON
Proteinase K	Bioshop, Burlington, ON
Protein A Agarose Beads	Agarose Beads Technology, Doral, FL
Protein G Agarose Beads	Agarose Beads Technology, Doral, FL
ProtoScript® II Reverse Transcriptase	New England Biolabs, Ipswich, MA
RiboLock RNase inhibitor	Thermo Fisher Scientific, Mississauga, ON
Rhodamine-phalloidin	Molecular Probes, Eugene, OR
Taq DNA polymerase	New England Biolabs, Ipswich, MA
T3, T7 and SP6 RNA polymerases	New England Biolabs, Ipswich, MA
T4 DNA Ligase	New England Biolabs, Ipswich, MA

2.1.4 Antibodies

Table 4. Antibodies and working dilutions used for western blots and immunoprecipitations

Antibody (Cat #)	Species	Working Dilution	Company
α-Digoxigenin-AP Fab fragments (11093274910)	sheep	1:10000 (ISH)	Roche, Mississauga, ON
α-GFP 7.1 and 13.1 (11814460001)	mouse	1:2000 (WB) 1:1000 (IP) 1:1000 (ICC)	Roche, Mississauga, ON
goat-α-mouse Alexa Fluor®	mouse	1:1000 (ICC)	Invitrogen, Burlington, ON

488 (A11029)			
goat-α-mouse-HRP (115035146)	mouse	1:5000 (WB)	Jackson ImmunoResearch, West Grove, PA
goat-α-rabbit Alexa Fluor® 546 (A11035)	rabbit	1:1000 (ICC)	Invitrogen, Burlington, ON
goat-α-rabbit-HRP (111035144)	rabbit	1:5000 (WB)	Jackson ImmunoResearch, West Grove, PA
α-γ-catenin (610523)	mouse	1:1000 (WB)	BD Biosciences, Mississauga, ON
α-β-catenin (C2206)	rabbit	1:5000 (WB) 1:1000 (IP)	Sigma-Aldrich, Oakville, ON
α-β-catenin (610153)	mouse	1:1000 (WB)	BD Biosciences, Mississauga, ON
α-HA 12CA5 (11583816001)	mouse	1:1000 (WB) 1:500 (IP)	Roche, Mississauga, ON
α-DYKDDDDK Tag FG4R (MA1-91878)	mouse	1:500 (IP)	Thermo Fisher Scientific, Mississauga, ON
α-X-CAD	rabbit	1:2500 (WB) 1:1000 (IP)	Gift from B. Gumbiner, University of Virginia.
α-FN 32FJ	rabbit	1:1000 (ICC)	Gift from D. DeSimone, University of Virginia.

2.1.5 Oligonucleotides

The following oligonucleotides were ordered from Sigma Life Science and used to subclone or perform site directed mutagenesis. The restriction enzyme site included in the primer sequence used to subclone the each gene is underlined.

Table 5. PCR primers used to subclone and perform site-directed mutagenesis

Clone	Primers	Restriction Enzymes	Template
Flag – xILK pCS2+	**ILK Flag Forward** 5’ CCGAATTC ATG GACTACAAGGACGACGATGACAAG GATGACATTTTCGCTCAGTGTCG 3’ **ILK reverse Xba** 5’ CGCTCTAGATTTCTCCTGCATCTTCTCCAG 3’	5’ EcoR1 – 3’ Xba1	xILK pSPORT

Flag – xILK Δ KINASE pCS2+	**ILK Flag Forward** 5’ CCGAATTC ATG GACTACAAGGACGACGATGACAAG GATGACATTTTCGCTCAGTGTCG 3’ **Kinase deletion reverse** 5’ GCTCTAGACCAACGTCCCTTCCAGAGCT 3’	5’ EcoR1 – 3’ Xba1	xILK pSPORT
Flag – xILK ΔINT pCS2+	**ILK Flag Forward** 5’ CCGAATTCATGGACTACAAGGACGACGATGAC AAGGATGACATTTTCGCTCAGTGTCG 3’ **Integrin deletion reverse** 5’ GCTCTAGACACGTCCCAAAGCAGAACGG 3’	5’ EcoR1 – 3’ Xba1	xILK pSPORT
Flag – xILK ΔANK pCS2+	**ANK delete forward** 5’CCGAATTCATGGACTACAAGGACGACGATGACA AGGGCACCCTGAATAAACAGGCTG 3’ **ILK reverse Xba** 5’ CGCTCTAGATTTCTCCTGCATCTTCTCCAG 3’	5’ EcoR1 – 3’ Xba1	xILK pSPORT
Flag – xILK E359K pCS2+	**ILK E359K Forward** 5’ CGTGGGTGGCACCTAAAGCGCTGCAGAAACG 3’ **ILK E359K Reverse** 5’ CGTTTCTGCAGCGCTTTAGGTGCCACCCACG 3’	5’ EcoR1 – 3’ Xba1	xILK pSPORT
β-Parvin pCS2+HA	**bparvin forward** 5’ CCGGATCCATGTCCAGCACCCCAGTC 3’ **Bparvin GFP Reverse** 5’ CCAGGCCTGTCGAGGTGCTTGTACTTTG 3’	5’ BamH1 – 3’ Stu1	β-Parvin pCMV SPORT 6
RP1 pCS2+HA	**bparvin forward** 5’ CCGGATCCATGTCCAGCACCCCAGTC 3’ **B-parvin RP1 reverse** 5’ CCAGGCCTCTTCACTACTACCACTTGTACAC 3’	5’ BamH1 – 3’ Stu1	β-Parvin pCMV SPORT 6
RP2 pCS2+HA	**B-Parvin RP2 Forward** 5’ CCGGATCCATGAAGAAACGCGAGGGGC 3’ **B-parvin GFP Reverse** 5’ CCAGGCCTGTCGAGGTGCTTGTACTTTG 3’	5’ BamH1 – 3’ Stu1	β-Parvin pCMV SPORT 6
xCad ΔBcat pGEX?	**xC-Cad Bcat FWD** 5’ GAAGCTGCATCGCTCAGCT 3’ **xC-Cad Bcat REV** 5’ AGCTGCATCCAAGTTCTCATC 3’	5’ EcoR1 – 3’ Xba1	xCadherin pGEX KG

xCad ΔJMD pGEX?	**xC-Cad JMD FWD** 5’ CACAGAGGCCTAGATTCTCGT 3’ **xC-Cad JMD REV** 5’ ATCCCTGGTATCATCCTCTGGC 3’	5’ EcoR1 – 3’ Xba1	xCadherin pGEX KG

The following oligonucleotides were ordered from Sigma Life Science and used to perform RT-PCR.

Table 6. PCR primers used to perform RT-PCR

Template	Primers
alpha-parvin	**Alpha-parvin FWD** 5’ CCGGATCCGCAACGTCCCCCCAAAAATCTCC 3’ **Alpha-parvin REV** 5’ GGCTCGAGCTCCACGCTTCTGTACTTGGTG 3’
beta-parvin (L+S)	**bparvin forward** 5’ CCGGATCCATGTCCAGCACCCCAGTC 3’ **Bparvin GFP Reverse** 5’ CCAGGCCTGTCGAGGTGCTTGTACTTTG 3’
beta-parvin (S)	**parvin gen F** 5’ GCTGATAAGACTGAGCTTCAG 3’ **parvin gen R** 5’ AGTCAAGGTGCTTGTACTTTG 3’

2.1.6 Plasmids

Table 7. Plasmid constructs

Plasmid	Source
pCS2+	Gift from DL Turner, University of Michigan
pCS2+GFP N1	Gift from Jeff Miller
pCS2+HA	Gift from Pierre McCrea, University of Texas
xILK pCS2+GFP N1	Justin Knapp - Subcloned from Flag – xILK pCS2+ (5’ EcoRI – 3’ Xba1)
xILK E359K pCS2+GFP N1	Justin Knapp - Subcloned from Flag – xILK E359K pCS2+ (5’ EcoRI – 3’ Xba1)
β-Parvin pCS107 cGFP	Hyder Al-Attar, University of Waterloo
β-Parvin pCS2+GFP N1	Catherine Studholme, University of Waterloo
RP1 pCS2+GFP N1	Catherine Studholme, University of Waterloo
PINCH pCS2+GFP N1	Bhanu Pilli, University of Waterloo

β-Parvin pCMV SPORT 6 (Clone ID: 5542473)	Open Biosystems, Huntsville, AL
xILK pSPORT (NM_001092516.1)	Open Biosystems, Huntsville, AL
xCadherin pGEX KG	Gift from Cara Gottardi, Northwestern University
TCF pGEX KG	Gift from Cara Gottardi, Northwestern University
β1-Intergin pGEX KG	Gift from Hélène Cousin, University of Massachusetts Amherst
HA- β1 pCS107	Mungo Marsden, University of Waterloo
HA pCS107	Mungo Marsden, University of Waterloo

2.1.7 Morpholino oligonucleotides

The following morpholino oligonucleotide was purchased from Gene Tools LLC (Philomath, OR, USA).

β-Parvin MO2: 5’ GAG CTG AAG CTC AGT CTT ATC AGC A 3’

2.1.8 Bacteria

Table 8. Bacteria used to propagate plasmid and express protein

Species	Genotype	Source
E.Coli (DH5α)	F^- ϕ80*lac*ZΔM15 Δ(*lac*ZYA-*arg*F)U169 *rec*A1 *end*A1 *hsd*R17(r_K^-, m_K^+) *pho*A *sup*E44 λ^- *thi*-1*gyr*A96 *rel*A1	ATCC, Rockville, MD
E.Coli (BL21 DE3)	F^- *omp*T *hsd*S_B (r_B^-, m_B^-) *gal dcm*	Gift from Barb Moffatt, University of Waterloo

2.1.9 Kits

Table 9. Molecular biology kits

Kit	Company
Ambion MEGAclear	Thermo Fisher Scientific, Mississauga, ON
Geneaid Gel/PCR DNA Fragments Extraction	Froggabio, North York, ON
Geneaid PCR Clean up	Froggabio, North York, ON
High-Speed Plasmid Mini	Froggabio, North York, ON

2.2 Molecular cloning

2.2.1 Subcloning

β-Parvin, *Xenopus laevis* integrin-linked kinase (xILK) and *Xenopus laevis* cadherin intracellular domain (xCad) were isolated by polymerase chain reaction (PCR) using primers and template listed in Table 5 in the following reaction and cycle conditions:

1x HF Buffer	3 min at 95°C
0.2 μM FWD Primer	**30 s at 95°C**
0.2 μM REV Primer	**30 s at 50-60°C (Repeat 24-28x)**
1 mM dNTPs	**15-60 s at 72°C**
1.25 units Phusion DNA polymerase (NEB,	5 min at 72°C
Water up to 50 μl Total Volume	

The vector (Table 7) and PCR product were then sequentially digested using restriction enzymes listed in Table 5 or 7 using the following reaction:

1X Buffer (specific to restriction enzyme)
10 units restriction enzyme (listed in Table 5; NEB)
1-5 μg DNA
Water up to 50 μl Total Volume

The reactions were incubated at 37°C for 1.5 h and purified using a Gel/PCR DNA Fragments Extraction kit. The purified digests were run on a 1% agarose TAE gel containing ethidium bromide, and visualized using the U:Genius (Syngene) gel doc station. The purified vector and insert were then ligated in a molar ratio of 1:3 respectively using T4 DNA ligase in the following reaction:

10-50 ηg digested vector
50-90 ηg digested insert
1X T4 buffer
800 units T4 DNA ligase (NEB, Ipswich, MA)
20 μl Total Volume

The reaction was incubated at room temperature for 3 h and transformed into competent DH5α *E.coli* using standard methods (Promega).

2.2.2 Site-directed mutagenesis

Site-directed mutagenesis was used to alter beta-parvin (β-Parvin), *Xenopus laevis* integrin-linked kinase (xILK) and *Xenopus laevis* cadherin intracellular domain (xCad) by introducing a substitution or deleting domains. To introduce a substitution in xILK (xILK E359K), a PCR reaction was carried out as described in section 2.2.1, using primers ILK E359K forward and ILK E359K reverse, followed by Dpn1 digestion for 1 h at 37°C to remove template plasmid. The reaction was then purified using the Geneaid PCR cleanup kit and transformed into competent DH5α *E.coli*. To introduce a deletion, an inverse PCR reaction was performed (Sambrook and Russell, 2006) using primers listed in Table 5, followed by Dpn1 treatment. The reaction products were separated on a 1% agarose TAE gel and the band representing the deletion product was purified using the Geneaid Gel/PCR DNA Fragments Extraction kit. 100 ηg of the purified DNA was phosphorylated using polynucleotide kinase (PNK) according to manufacturers protocol and purified using the Geneaid PCR Clean up kit. The phosphorylated DNA was then ligated with T4 DNA ligase for 3 h at room temperature and transformed into competent DH5α *E.coli.* Substitution and deletion constructs were verified through sequencing (Robarts Research Institute, London, ON).

2.3 Generation of *in vitro* transcripts

RNA for microinjection was *in vitro* transcribed using a linearized plasmid containing an Sp6 phage promoter upstream of the gene of interest. 1μg of plasmid DNA was linearized with Not1 HF restriction enzyme, purified using the Gel/PCR DNA Fragments Extraction kit and used in the following transcription reaction:

1x RNA polymerase reaction buffer (NEB, Ipswich, MA)
1 mM of each RTP (rUTP, rATP, rCTP)
0.1 mM rGTP
1 mM of m7G(5')ppp(5')G RNA Cap Structure Analog (NEB, Ipswich, MA)
40 units of Ribolock RNase inhibitor (Thermo Fisher Scientific, Mississauga, ON)
40 units SP6 RNA Polymerase (NEB, Ipswich, MA)
1 μg linearized plasmid DNA (16μl maximum)
50 μl Total Volume at 37°C for 30 min

After 30 min, 0.5 mM of rGTP was added to the reaction and incubated at 37°C for 1 h. The plasmid DNA was then degraded with DNase1 (RNase free; New England Biolabs, Ipswich, MA) and the reaction was purified using the Ambion MEGAclear kit (Thermo Fisher Scientific, Mississauga, ON) followed by ammonium acetate precipitation. The purified RNA was resuspended in water and checked for quality, using agarose gel electrophoresis, and concentration and purity using an Ultraspec 2100 pro spectrophotometer (GE Healthcare, Mississauga, ON). Stocks of RNA were aliquoted and stored at -80°C until needed.

2.4 RT-PCR

DNA transcripts were amplified from cDNA acquired at various stages of *Xenopus laevis* development. Total RNA was extracted using a standard protocol (Chomczynski and Sacchi, 1987). Integrity of the RNA was determined by the presence of 28S and 18S

rRNA bands as visualized on a 1% agarose gel. The concentration and purity was determined using an Ultraspec 2100 pro spectrophotometer (GE Healthcare, Mississauga, ON). To synthesize cDNA, 2 μg of total RNA was used in a reaction with ProtoScript® II Reverse Transcriptase according to manufacturers protocols. A PCR reaction was performed using primers listed in Table 6. The reaction products were separated on a 1% agarose gel and visualized using EtBr.

2.5 Embryology

2.5.1 Culture of *Xenopus laevis* embryos

Xenopus laevis were acquired from Nasco Scientific (Fort Atkinson, WI) and housed in the Biology Aquatic Facility at The University of Waterloo. To obtain oocytes, female *Xenopus laevis* are injected with 20 units of human chorionic gonadotropin (hCG) sub-cutaneously four to seven days before inducing ovulation. To initiate ovulation, females were injected with 400 units of hCG and oocytes were obtained by gently squeezing (manual stripping) the females. Male *Xenopus laevis* were anesthetized in 0.1% benzocaine and testes surgically removed and stored in L-15 complete media. Oocytes were fertilized *in vitro* using a small piece of minced testes in 1x Modified Barth's Saline (MBS) for three-five min. The dish was then flooded with water and left for 20 min. Following cortical rotation fertilized oocytes were dejellied by gentle swirling in 0.1x MBS supplemented with 2% L-cysteine. Once dejellied, embryos were then rinsed in 0.1x MBS and allowed to develop.

2.5.2 Microinjection

Microinjection of *in vitro* transcribed mRNA, morpholino oligonucleotides and purified protein was performed using a Narishige IM300 pressure injector (Narishige International USA, East Meadow, NY) using extended glass capillaries made using the Narishige PC-10 puller (Narishige International USA, East Meadow, NY). Embryos were injected in 0.5x MBS/4% Ficoll 400 solution. *In vitro* transcribed mRNA or morpholino oligonucleotides were injected into animal caps of one-cell stage embryos or the future dorsal side of two and four-cell stage embryos. Injection of 0.05 to 0.5ng of xILK, BP, RP1 and RP2 RNA did not cause a defect in the embryo (sub phenotypic) and were used in immunocytochemistry and co-immunoprecipitation experiments. Embryos were then transferred to 0.1x MBS and allowed to develop to the desired stage. Embryos were then fixed in MEMFA for 1 h at room temperature and the injection targeting and gross phenotype was visualized using a Zeiss Lumar V12 fluorescence stereomicroscope (Carl Zeiss Canada Ltd., Mississauga, ON) with Zeiss Axiovision 4.7 (Carl Zeiss Canada Ltd., Mississauga, ON) or QCapture Pro (Qimaging, Surrey, BC) software respectively.

2.5.3 Immunocytochemistry and microscopy of embryos

To visualize cell boundaries, embryos were injected 30 min after fertilization with ruby red 5K-dextran. Embryos were subsequently injected with RNA as described. For FN staining, embryos were cultured until stage 12 and fixed in 2% trichloroacetic acid (TCA) for 1 h at room temperature. Fixed embryos were then washed in 1x PBS/0.1% tween20, three times for 20 min, and animal caps were excised. The animal caps were blocked in 1x PBS/0.1% tween20/1% Bovine serum albumin (BSA) for 1 h at

room temperature and then stained with α-FN 32FJ polyclonal antibody for 1 h at room temperature. After staining, caps were washed three times for 10 min with 1x PBS/0.1% tween20 and then incubated with Alexa Fluor® 488-conjugated goat-α-rabbit secondary antibody for 1 h at room temperature followed by three washes in PBS. The caps were then mounted on glass slides and imaged using a Zeiss Axiovert 200 inverted microscope (Carl Zeiss Canada Ltd., Mississauga, ON) using Openlab imaging software (PerkinElmer Inc., Waltham, MA).

When staining bisected embryos, embryos were cultured to the desired stage and fixed in MEMFA for 1 h at room temperature. After fixing, embryos were softened by rinsing in 1x PBS/0.1% tween20, three times for 20 min, and bisected along the sagittal plane to view the dorsal lip. The embryos were then rinsed in PBS-TD once for 10 min and then blocked for 4 h at room temperature in whole mount blocking solution (WMBS). They were then incubated with primary antibody in WMBS overnight at 4°C followed by six, 1 h washes in PBS-TD at room temperature. This was followed by incubation with fluorophore-conjugated secondary antibody in WMBS overnight at 4°C. The embryos were washed six times for 1 h in PBS-TD and then rinsed three times for 20 min in 100% methanol. They were then transferred to a glass bottom microscope slide and washed in BABB solution three times for 20 min. Embryos were immediately viewed using a Zeiss LSM 510 confocal microscope (Carl Zeiss Canada Ltd., Mississauga, ON) with ZEN 2009 software (Carl Zeiss Canada Ltd., Mississauga, ON).

2.5.4 Animal cap manipulations

In experiments examining protein-protein interactions in pre vs. post involution tissue, animal caps of embryos microinjected with RNA were excised at stage 8 in 1x MBS and cultured in 0.5x MBS with or without 20 units/mL Activin A for 30 min at room temperature. Animal caps were then transferred to fresh 0.5x MBS and allowed to recover overnight at 18°C. Animal caps were collected and used for co-immunoprecipitation experiments.

2.5.5 Cell adhesion assays

Fibronectin and Fc-cadherin were used as substrates for adhesion assays. Flame-sterilized acid-washed 25-mm round coverslips (Thermo Fisher Scientific, Mississauga, ON) were glued (Norland optical adhesive 68, Norland Products Inc., Cranbury, NJ) to the bottom of a 60-mm Petri dish (Sarstedt) and coated for 16-18 h at 4°C with 25 µg/mL human plasma FN or 0.25 µg/mL FC-cadherin in 1x PBS. The substrates were then blocked in 1 mg/mL BSA in 1x PBS and washed three times for 10 min in MSS+.

Animal caps were excised from stage 11 embryos and the cells dissociated in MSS-. The cells were rinsed in MSS+ and plated on substrates in MSS+ and left for 20 min at room temperature to allow for adhesion. After 20 min the Petri dish was rinsed with MSS+, washing away non-adherent cells. Images were collected pre and post-wash on a Zeiss Axiovert 200 inverted microscope, (Carl Zeiss Canada Ltd., Mississauga, ON) using Openlab imaging software (PerkinElmer Inc., Waltham, MA). Cells were counted pre and post-wash.

2.6 Protein analysis

2.6.1 Western blotting

For protein isolation, an equivalent number of embryos from each experimental treatment were lysed using 10 µl ESB/embryo and homogenized by pipetting using a 100 µl tip. Protein isolate was cleared by centrifugation at 14,000 rpm (20,800 x g) for 15 min at 4°C. The supernatant was removed and then denatured by the addition of 5x SDS sample buffer and heated at 95°C for five min. Embryo protein equivalents were separated by sodium dodecyl-sulphate polyacrylamide gel electrophoresis (SDS-PAGE), using acrylamide gels, at a constant voltage of 150 V using the Mini-Protean 3 system (Bio-Rad, Mississauga, ON). Protein was transferred to a nitrocellulose membrane at a constant voltage of 100 V for 60 min in the Mini-Protean 3 system (Bio-Rad, Mississauga, ON). PonceauS staining was used to assess transfer efficiency and the membrane was incubated overnight at 4°C in blocking solution. Membranes were incubated with primary antibody in blocking solution either overnight at 4°C or for 1 h at room temperature. Membranes were then washed three times for 10 min in blocking solution followed by incubation with HRP-conjugated secondary antibody for 1 h at room temperature. Membranes were washed twice with blocking solution for 10 min and rinsed twice for 5 min in TBS. The protein bands were visualized by chemiluminescence. Membranes were exposed to equal volumes of ECL solution 1 and 2 for one to two min and protein was detected using RXB X-ray film (Labscientific, Highlands, NJ) or via signal accumulation on the Gel Doc XR+ System (Biorad, Mississauga, ON) using Image Lab 5.2.1 (Biorad, Mississauga, ON) software.

2.6.2 Co-immunoprecipitation analysis

For co-immunoprecipitations protein was isolated from embryos as described in section 2.6.1. 2% of each protein isolate (total lysate sample) was collected and frozen at -80°C. The remaining protein isolate was added to 500 µl of ESB and incubated with 20 µl of a 50% slurry of Protein A or G Agarose beads with rocking for 1 h at 4°C. Beads were removed by centrifugation and lysate incubated with primary antibody with rocking at 4°C overnight. After primary incubation, 25 µl of a 50% slurry of Protein A or G Agarose beads added to the lysate and rocked for 2 h at 4°C to recover primary antibody complexes. The mixture was centrifuged for 1 min at 3000 rpm and supernatant removed. The beads were then washed three times in 500µl of cold ESB and resuspended in 40 µl ESB (pull-down sample). The total lysate and pull-down samples were then subjected to SDS-PAGE and western blot analysis as described in section 2.6.1.

2.6.3 Protein expression

Prior to expression, constructs were transformed into competent BL21 (DE3) *E.coli*, as detailed in the results section, and spread onto Luria broth (LB) + ampicillin (Amp) agar plates for selection. A single colony was used to inoculate 3 mL of LB + Amp broth and incubated at 30°C with shaking for 16-18 h. The cells were then sub-cultured 1:100 into 100 mL of fresh LB + Amp broth and grown at 37°C until the cells reached an optical density $(OD)_{600}$ of 0.4-0.6. Protein expression was induced by the addition of 0.4 mM Isopropyl β-D-1-thiogalactopyranoside (IPTG) and incubated at 37°C for 2 h. Cultures were then divided into 20 mL aliquots, centrifuged to remove supernatant, and

froze at -80°C until needed. To confirm protein expression, 1 mL of culture was pelleted in a microfuge tube by centrifugation at 14,000rpm (20,800 x g) for 1 min and resuspended in 5x SDS sample buffer heated to 95°C. The tube was then vortexed and heated at 95°C for 5 min. Protein was separated by SDS-PAGE, using 10% acrylamide gels at a constant voltage of 150V. Proteins were visualized with Coomassie stain.

2.6.4 Protein purification

To purify GST-xCad and GST-xCad Δβcat 20mL culture aliquots were resuspended in 1 mL HEPES lysis buffer (without detergent). The samples were then sonicated and centrifuged at 14,000rpm (20,800 x g) for 15 min at 4°C. The supernatant was transferred to a new microfuge tube and NP-40 was added to a final concentration of 0.5%. The lysate was then incubated with 100 µl of a 50% slurry of Glutathione-Uniflow Resin and rocked for 2 h at 4°C. The mixture was centrifuged for one min at 3,000 rpm (956 x g) and supernatant removed. The beads were then washed five times in cold HEPES lysis buffer with 0.5% NP-40, followed by three washes in cold HEPES lysis buffer without NP-40. The purified protein was stored as a 50% slurry at 4°C and used within one week. To confirm successful purification, 10 µl of the 50% bead slurry was subjected to SDS-PAGE and then proteins were visualized with Coomassie stain.

2.6.5 GST-pull-down assay

For protein isolation, an equivalent number of embryos from each experimental treatment were lysed using 10 µl GST-pull-down lysis buffer/embryo and homogenized by pipetting. 2% of each protein isolate (total lysate sample) was collected and frozen at

-80°C. The remaining protein isolate was added to 500 µl of GST-pull-down lysis buffer and incubated with 20 µl of a 50% slurry of purified GST bound Glutathione-Uniflow Resin and rocked for 1 h at 4°C. Beads were removed by centrifugation and lysate incubated overnight with 25 µl of a 50% slurry of purified GST fusion protein bound Glutathione-Uniflow Resin. The mixture was centrifuged for 1 min at 3000 rpm and supernatant removed. The beads were then washed three times in 500 µl of cold GST-pull-down lysis buffer and resuspended in 40 µl of buffer (pull-down sample). The total lysate and pull-down samples were then subjected to SDS-PAGE and western blot analysis as described in section 2.6.1.

2.6.6 Densitometry

Densitometric analysis was performed using Image J software (Version 1.49; National Institute of Health). The band intensity in each condition was expressed as the percentage mean relative density of the maximum value in each experiment. Vertical error bars represent standard deviations. Significance ($p<0.05$) was determined using one-way ANOVA with Tukey's post hoc test.

3.0 Results

3.1 β-Parvin regulates integrin and cadherin mediated adhesion

It has been previously described that disrupting β-Parvin function affects cell adhesion and subsequently gastrulation (Studholme, 2013). One of the unresolved issues in this study was the role that β-Parvin played in cell-ECM and cell-cell adhesion. I used cell adhesion assays to examine the effect of GFP tagged full-length β-Parvin, a CH2 deletion (RP1) as well as a CH1 deletion (RP2) over-expression on cadherin and integrin adhesion. (Figure 4A). To assess α5β1 integrin (since α5β1 is the only active integrin during *Xenopus laevis* gastrulation, it will be referred to hereafter as integrin) function cells obtained from dissociated embryos injected with control GFP or one of the GFP tagged β-Parvin constructs were plated on FN. The percentage of cells remaining attached to the substrate after washing was calculated. 92% of control GFP (GFP), GFP-β-Parvin (BP) and GFP-RP1 (RP1) cells plated on FN remained attached (Figure 4B). GFP-RP2 (RP2) over-expressing cells display an apparent decrease in adhesion (86%). However, the decrease in RP2 over-expressing samples is not a statistically significant decrease when compared to control GFP, BP and RP1.

To assess cadherin function cells were plated on a cadherin fusion protein (Fc-Cadherin) (Refer to section 2.5.5). Cells were obtained as described above. When plated on a cadherin substrate, 98% of cells over-expressing GFP, 97% over-expressing BP and 98% over-expressing RP2 remain attached (Figure 4C). RP1 over-expressing cells show a statistically significant decrease in adhesion (88%) compared to control GFP, BP and RP2

Figure 4. β-Parvin regulates integrin and cadherin mediated adhesion. A) Schematic of β-Parvin displaying the location of both calponin homology (CH) domains and the composition of the RP1 (aa. 1-212) and RP2 (aa. 213-365) deletion constructs. Nuclear localization signals are indicated with black rectangles. Embryonic cells were dissociated and plated on a Fibronectin (B) or cadherin (C) substrate. Cells were counted pre and post wash and the results are expressed as the percentage of cells remaining adhered to the substrate. B) Cells over-expressing GFP-RP2 (RP2) display a significant decrease in adhesion to FN in comparison to GFP-β-Parvin (BP) and GFP-RP1 (RP1) over-expressing cells. C) Cells over-expressing GFP-RP1 (RP1) display a significant decrease in adhesion to a cadherin substrate in comparison to GFP, GFP-β-Parvin (BP) and GFP-RP2 (RP2). Vertical error bars indicate standard deviations. Significance ($p<0.05$) was determined using one-way ANOVA with Tukey's post hoc test and is represented by an asterisk. These data represent 3 separate experiments (>100 cells/experiment)

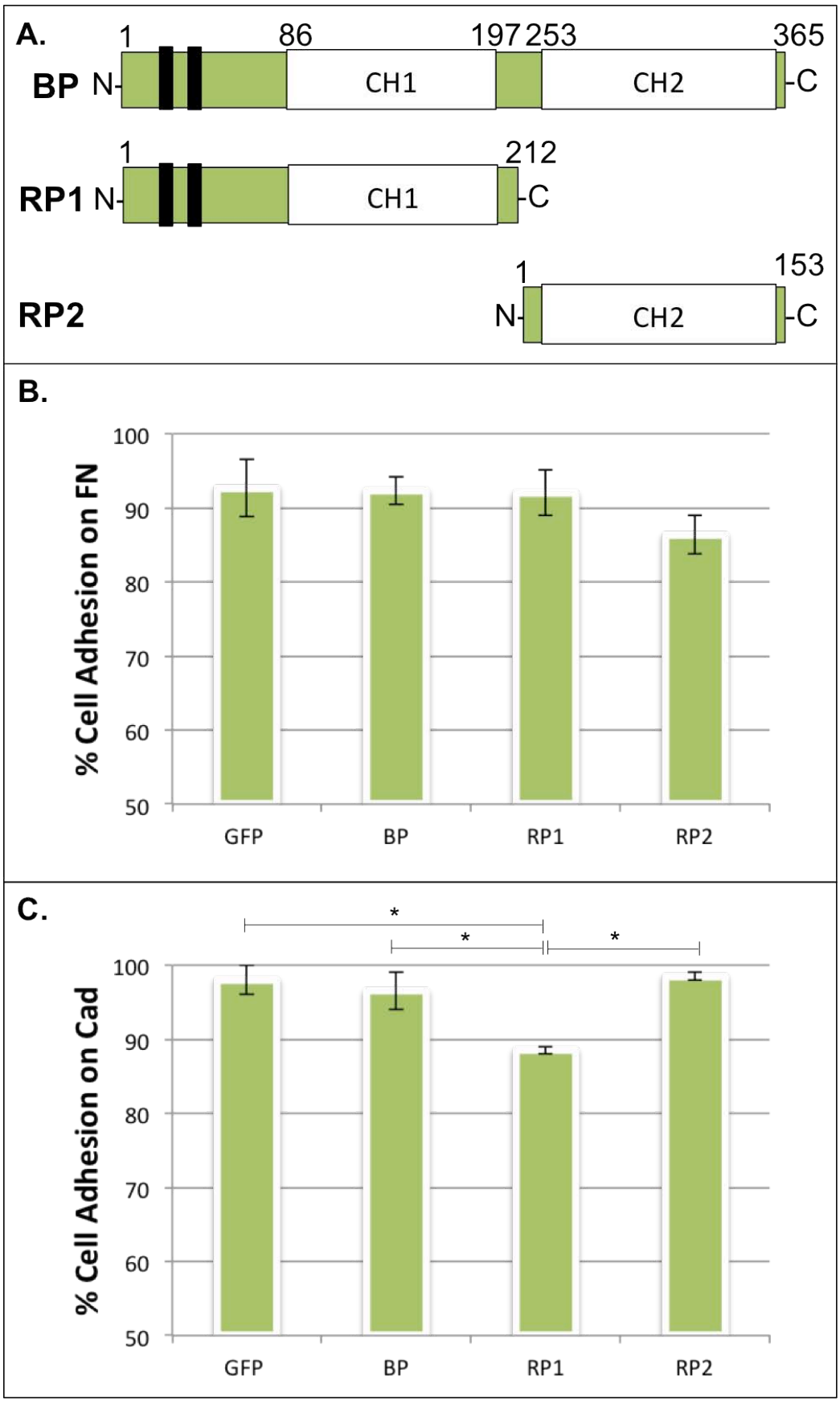
A.
1
86
197
253
365
BP
N-
CH1
CH2
-C
1
212
RP1
N-
CH1
-C
1
153
RP2
N-
CH2
-C
B.
% Cell Adhesion on FN
100
90
80
70
60
50
GFP
BP
RP1
RP2
C.
*
*
*
% Cell Adhesion on Cad
100
90
80
70
60
50
GFP
BP
RP1
RP2

($p<0.05$, n=3). Taken together, these results suggest that the RP1 and RP2 regions of β-Parvin may regulate cadherin and integrin based adhesions respectively.

3.2 β-Parvin compartmentalization is regulated during *Xenopus laevis* gastrulation

Previous work in our laboratory demonstrated that the RP1 and RP2 deletion constructs of β-Parvin display different subcellular localization. In *Xenopus laevis* A6 kidney epithelial cells, full-length β-Parvin and RP2 localize to sites of integrin ligation known as focal adhesions. RP1 localizes to the leading edge of migrating A6 cells and is recruited to nascent cell-cell adhesions in re-associating *Xenopus laevis* embryonic cells (Studholme, 2013). Knowing that the two CH domains mediate compartmentalization *in vitro* and *ex vivo*, I then asked whether the CH domains perform a similar function *in vivo*. Immunocytochemistry was performed on gastrula stage embryos injected with <0.05 ng of control GFP (GFP), GFP-β-Parvin (BP), GFP-RP1 (RP1), or GFP-RP2 (RP2) RNA. 0.05 ng RNA does not cause a defect in the embryo and can be used to view compartmentalization. Injections were targeted to allow for expression of the fusion proteins in the pre or post-involution mesoderm. In pre (Figure 5) and post-involution mesoderm (Figure 6), GFP and BP are diffusely expressed throughout the cells. RP2 is also expressed diffusely throughout the cells but exhibits accumulation along the FN lined cleft in pre-involution mesoderm, suggesting recruitment to sites of integrin-FN ligation (Figure 5). RP1 displays an increased accumulation at the periphery of the cells in both pre and post-involution mesoderm in comparison to the other constructs (Figure 5 and 6). Additionally, RP1 appears to display a relative decrease in nuclear localization in both tissues in comparison to control GFP, BP and RP2 (Figure 5 and 6). This result

Figure 5. β-Parvin CH domains regulate compartmentalization of β-Parvin in pre-involution mesoderm**.** Control GFP (GFP) and GFP-β-Parvin (BP) are diffusely expressed throughout the cells. GFP-RP2 (RP2) exhibits minor accumulation at the boundary between pre and post-involution mesoderm. GFP tagged RP1 (RP1) displays increased compartmentalization at the periphery of cells. RP1 also displays a relative decrease in nuclear localization when compared to control GFP, BP and RP2 and appears to accumulate in a ring around the nucleus. The white box represents the area of the magnified panel on the right. Scale bars represent 100μm.

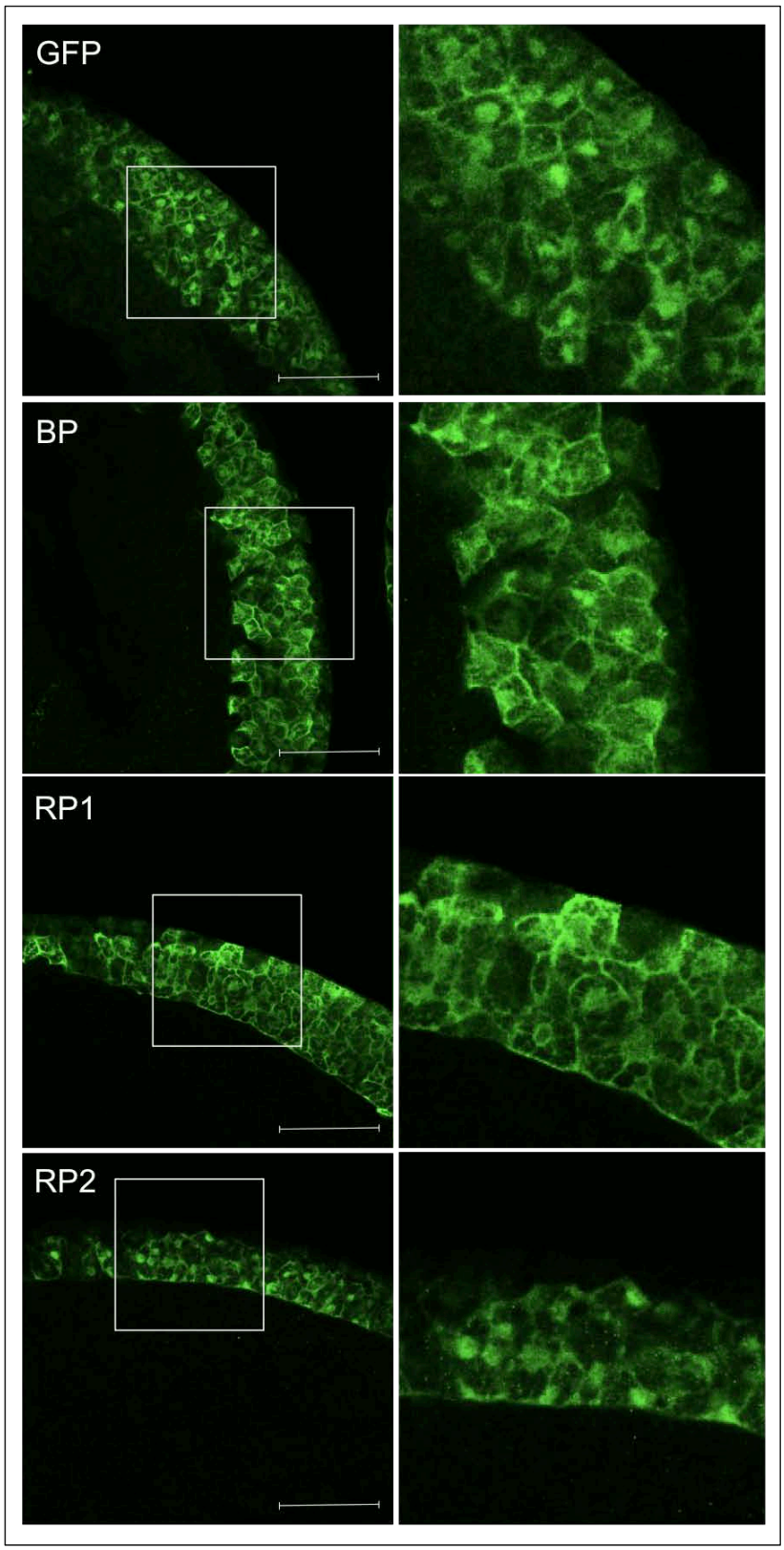
GFP
BP
RP1
RP2

Figure 6. β-Parvin CH domains regulate compartmentalization of β-Parvin in post-involution mesoderm. Control GFP (GFP), GFP-β-Parvin (BP) as well as GFP-RP2 (RP2) are diffusely expressed throughout the cells. GFP tagged RP1 (RP1) displays increased compartmentalization at the periphery of cells. RP1 also displays a relative decrease in nuclear localization when compared to control GFP, BP and RP2 and appears to accumulate in a ring around the nucleus. The white box represents the area of the magnified panel on the right. Scale bars represent 100μm.

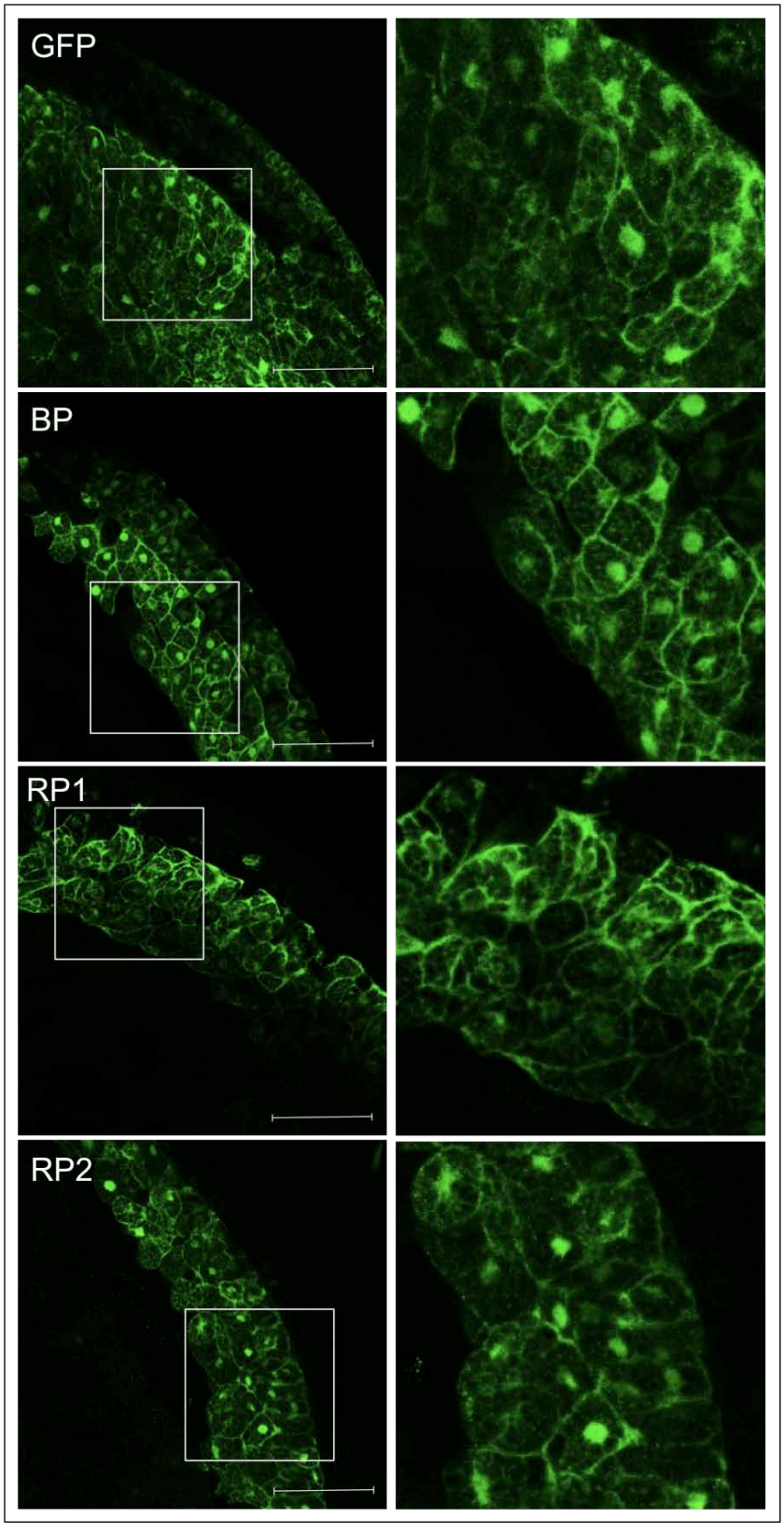
GFP
BP
RP1
RP2

was confirmed using HA tagged RP1 and RP2 constructs (Appendix A, Figure A1). This suggests that the nuclear localization of β-Parvin is regulated through sequences associated with carboxy terminus of the protein.

3.3 RP1 and RP2 over-expression inhibits cell polarization and epiboly

In the next phase of this study I asked whether the compartmentalization of β-Parvin was correlated to cell behaviours during gastrulation. During normal gastrulation, the BCR and pre-involution dorsal marginal zone (DMZ) thins through radially directed cell intercalations that drive epiboly. Following radial intercalations, convergent extension (CE) lengthens the anterior-posterior body axis through medial-lateral cell intercalations (Keller et al, 1992).

I employed confocal microscopy to examine cell shapes and tissue thickness in pre and post-involution DMZ. Embryos were injected with control GFP, or GFP tagged β-Parvin constructs. All embryos display a pre-involution DMZ that is 4-5 cell layers thick at stage 10.5 (Figure 7). During this stage, cells are undergoing well-established radial intercalation movements indicated by the presence of interdigitating cells. These cells display a “sharks tooth” appearance. Control GFP (GFP) and GFP-β-Parvin (BP) expressing embryos display interdigitating cells in the pre-involution DMZ (Figure 7). As a result, by stage 12.5, the DMZ has thinned to 2-3 cell layers (Figure 8). However, when GFP-RP1 (RP1) or GFP-RP2 (RP2) is over-expressed, cells do not interdigitate (Figure 7) and the DMZ remains 4-5 cell layers thick (Figure 8). The thickness of the DMZ in RP1 and RP2 injected embryos at stage 12.5 is statistically different compared to control GFP and BP overexpressing embryos (Figure 9, $p<0.05$, $n>3$). This suggests that signaling

Figure 7. β-Parvin regulates radial intercalation in the pre-involution DMZ. Stage 10.5 embryos. Pre-involution DMZ is 4-5 cell layers thick in embryos over-expressing control GFP (GFP), and GFP tagged full-length β-Parvin (BP), RP1 (RP1) and RP2 (RP2). Cells over-expressing GFP and BP are undergoing radial intercalations, indicated by interdigitating cells in the deep cell layers of the pre-involution DMZ (outlined in magnified right panels). Cells over-expressing RP1 and RP2 are disorganized and do not display cell shapes required for radial intercalation movements. Cells in the post-involution mesoderm have started to develop polarity (increased length/width ratio) in GFP and BP over-expressing embryos. Cells are rounded in RP1 and RP2 over-expressing embryos. The white box represents the area of the magnified panel on the right. Double-headed white arrow represents the thickness of the pre-involution DMZ and the single headed white arrow points to the involuted mesoderm. Scale bars represent 100μm.

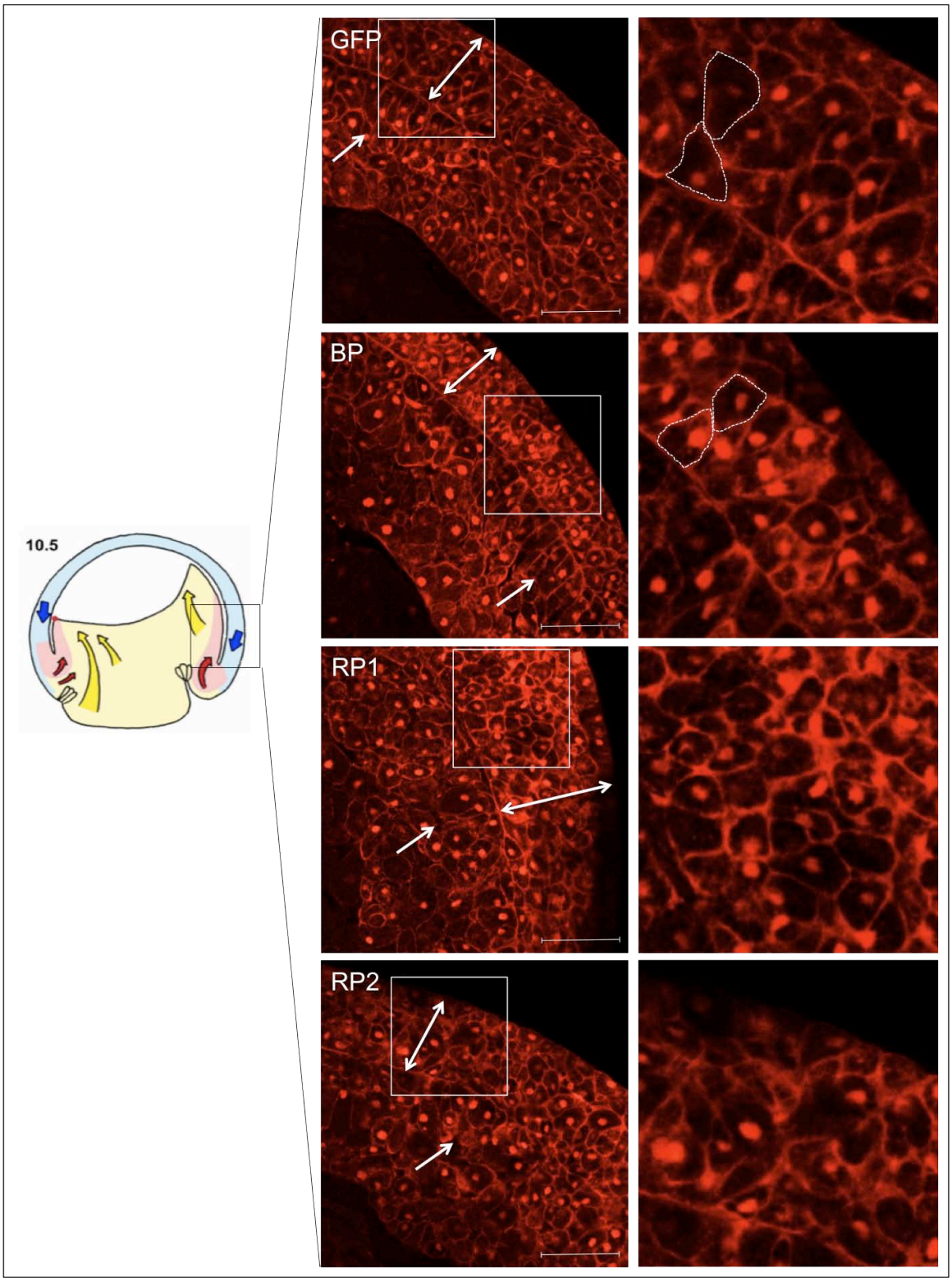
10.5
GFP
BP
RP1
RP2

Figure 8. β-Parvin regulates medial-lateral intercalation in the post-involution DMZ. Stage 12.5 embryos. Embryos over-expressing control GFP (GFP) and GFP tagged β-Parvin (BP) have undergone epiboly and the pre-involution DMZ has thinned to 2-3 cell layers thick while cells in the post-involution DMZ are have developed polarity (increased length/width ratio) required for CE medial-lateral cell intercalations. The pre-involution DMZ in GFP tagged RP1 (RP1) or RP2 (RP2) over-expressing embryos remains 4-5 cell layers thick and the cells in the post-involution DMZ are round in shape. The white box represents the area of the magnified panel on the right. Double-headed white arrow represents the thickness of the pre-involution DMZ. Scale bars represent 100µm.

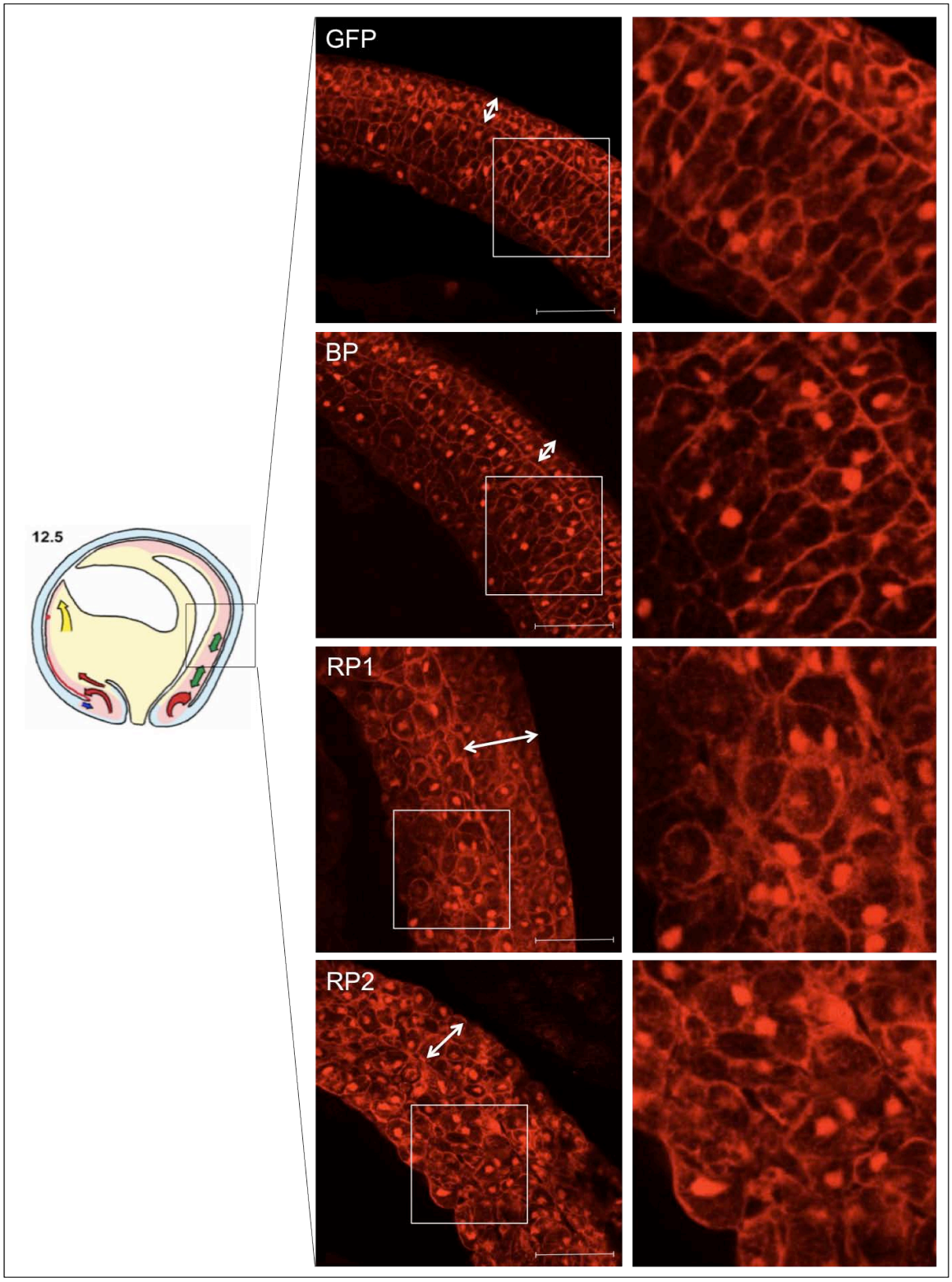
12.5
GFP
BP
RP1
RP2

Figure 9. RP1 and RP2 influence DMZ tissue thickness and post-involution mesoderm polarization. A) The pre-involution DMZ layer thickness is represented by average number of cells at both stage 10.5 (green) and stage 12.5 (red). The DMZ in all conditions is 4-5 cell layers thick at stage 10.5. In GFP (GFP) and GFP-β-Parvin (BP) over-expressing embryos, this layer thins to 2-3 cell layers thick at stage 12.5. The DMZ remains 4-5 cell layers thick at stage 12.5 in embryos over-expressing GFP-RP1 (RP1) or GFP-RP2 (RP2). B) The polarization of cells in the post-involution mesoderm is represented by average length/width ratio of cells in stage 12.5 embryos. Cells in control GFP (GFP) and BP over-expressing embryos display an average length/width ratio of 2.34 and 2.53 respectively. RP1 and RP2 cells do not acquire polarity and display an average length/width ratio of 1.21 and 1.41. Vertical error bars indicate standard deviations. Significance ($p<0.05$) was determined using one-way ANOVA with Tukey's post hoc test and is represented by an asterisk. These data are representative of atleast 3 separate experiments.

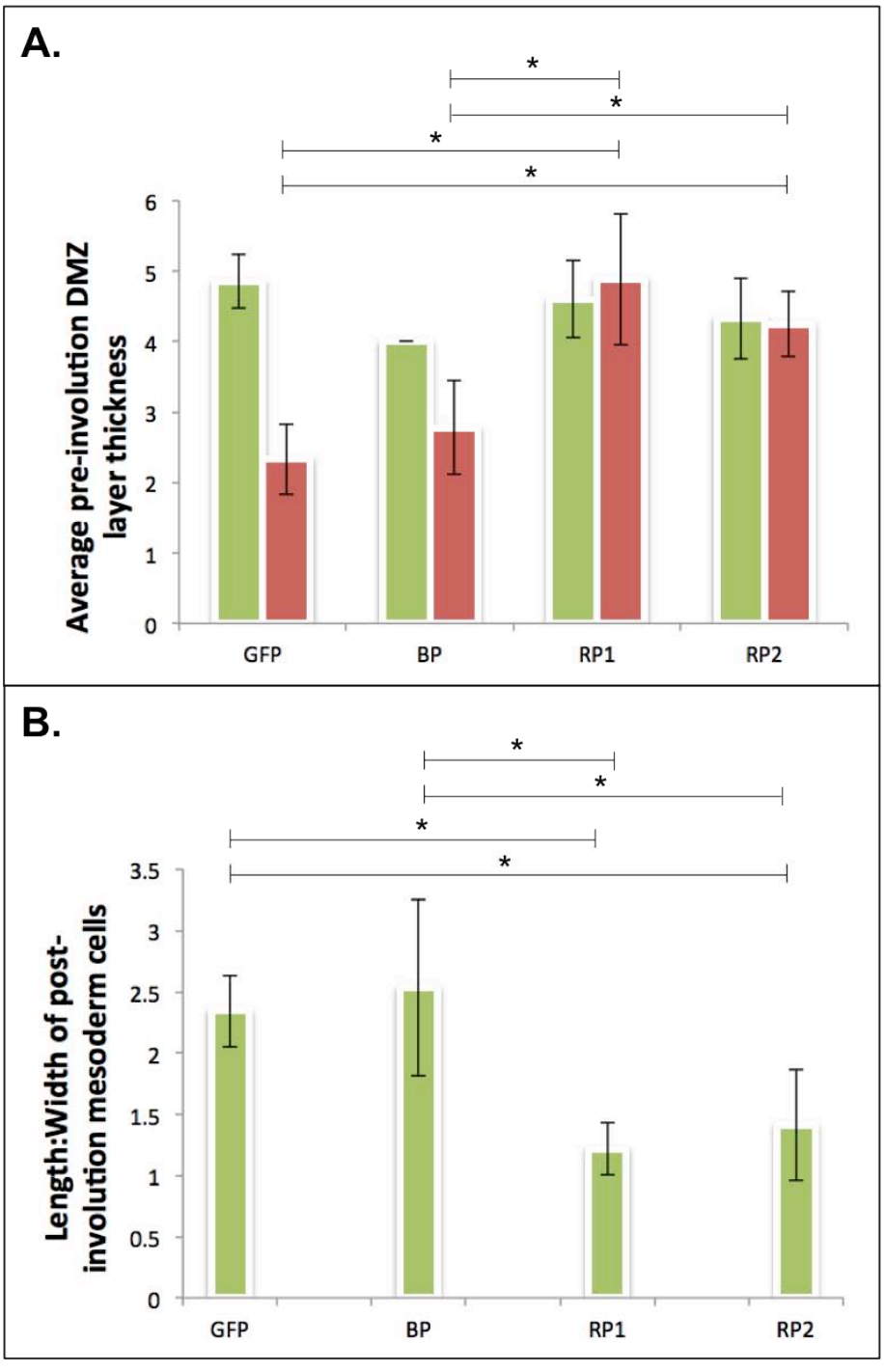
A.
Average pre-involution DMZ layer thickness
0
1
2
3
4
5
6
GFP
BP
RP1
RP2
*
*
*
*
B.
Length:Width of post-involution mesoderm cells
0
0.5
1
1.5
2
2.5
3
3.5
GFP
BP
RP1
RP2
*
*
*
*

downstream of β-Parvin is required for radial intercalations that result in DMZ thinning.

Cell intercalations driving CE in the post-involution DMZ also require polarized cell movements. As cells begin to intercalate they elongate and display an increased length/width ratio. Post-involution DMZ cells in control GFP and BP over-expressing embryos begin to develop polarity at stage 10.5, characterized by a rectangular shape (Figure 7). At stage 12.5 cells are undergoing well-established CE movements. Control GFP and BP over-expressing cells display similar length/width ratios of 2.34 and 2.53 respectively (Figure 8 and Figure 9). However, in embryos over-expressing RP1 or RP2, cells are rounded and do not develop an elongated shape (Figure 8). A statistically significant difference in the length/width ratio of cells in RP1 (1.21) and RP2 (1.41) expressing embryos was found when compared to control GFP and BP embryos (Figure 9). This suggests that β-Parvin is required for the development of cell polarity in the post-involution DMZ.

3.4 The RP2 region of β-Parvin mediates the interaction with xILK

The above results indicated that β-Parvin regulates cell behaviours during gastrulation and this is in part mediated through integrin. As β-Parvin interacts with β1 and β3 integrin tails through a complex with ILK, I asked if this interaction was important during gastrulation using co-immunoprecipitation assays (Hannigan et al, 1996)**.** To this end, I isolated the xILK CDS and generated a FLAG tagged construct (FLAG-xILK, refer to section 2.1.5). Embryos were then co-injected with FLAG-xILK and either GFP-β-Parvin, GFP-RP1 or GFP-RP2 RNA and cultured until stage 11. Constructs were injected at sub phenotypic amounts (0.5 ng) to avoid extraneous interactions. FLAG-xILK was

immunoprecipitated from embryo lysate and GFP tagged β-Parvin constructs detected by western blot. GFP-β-Parvin and GFP- RP2 are pulled down in a complex with FLAG-xILK, while GFP-RP1 is not (Figure 10). This demonstrates that the CH2 domain of β-Parvin is necessary for the interaction with xILK.

Having defined the domain of β-Parvin that mediates the interaction with xILK, I then used xILK deletion constructs to map the domain(s) that interact with β-Parvin. I created xILK deletion constructs as described in section 2.2.1 (Figure 11A). These individual xILK constructs were co-injected with β-Parvin-GFP. After immunoprecipitation of FLAG-xILK constructs, western blot analysis revealed that GFP tagged β-Parvin (BP-GFP) was associating with full-length-xILK and the xILK ΔANK construct (Figure 11B-C). However, there was no interaction with the construct deleting the c-terminal kinase domain (ΔKIN). To further characterize the interaction with the kinase domain I made an E to K point mutation at amino acid 359 of xILK using site-directed mutagenesis (refer to section 2.2.2). This mutation has been shown to abolish interaction with β-Parvin in tissue culture (Yamaji et al., 2001). As expected, immunoprecipitated FLAG xILK E359K revealed no association with β-Parvin. These data indicate that during gastrulation β-Parvin interacts with xILK through the kinase domain. Interestingly, when I immunoprecipitate a xILK construct that lacks the distal integrin binding domain (ΔINT), I do not retrieve GFP-BP (Figure 11B). This would suggest the xILK-integrin interactions are critical for xILK-β-Parvin complex formation.

Figure 10. The RP2 region of β-Parvin mediates association with xILK. Embryos were co-injected with FLAG-xILK and either GFP-β-Parvin (BP), GFP-RP1 (RP1) or GFP-RP2 (RP2) and cultured until stage 11. FLAG-xILK was immunoprecipitated from protein lysate using a mouse anti-FLAG antibody. The immunoprecipitated samples were then subjected to SDS-PAGE and western blot analysis to detect BP, RP1 and RP2 proteins. BP, RP1 and RP2 are equally expressed in embryos (Lysate). BP and RP2 were pulled down in a complex with FLAG-xILK (IP). Black triangles indicate complexed proteins. FLAG antibody heavy chain runs at 55kDa and is indicated with an outlined triangle.

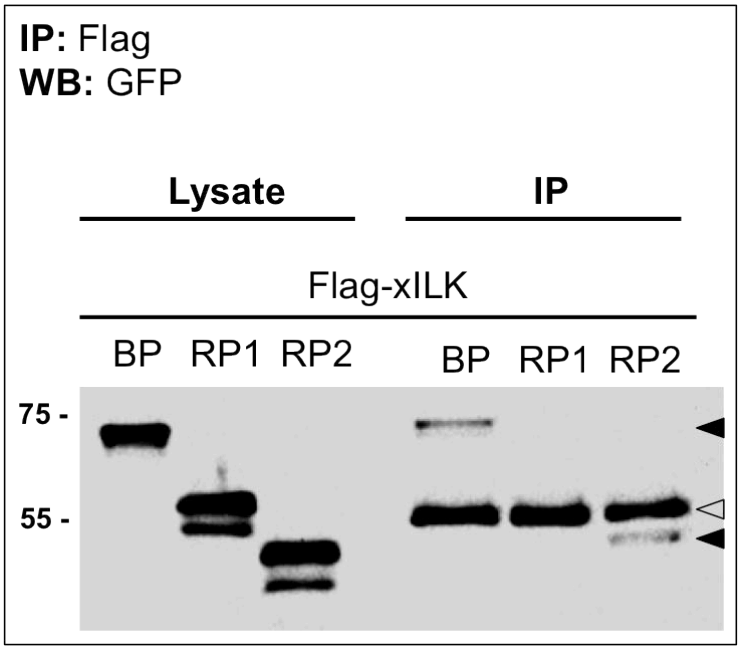
IP: Flag
WB: GFP
Lysate
IP
Flag-xILK
BP RP1 RP2 BP RP1 RP2
75 -
55 -

Figure 11. xILK kinase domain mediates β-Parvin association. A) Schematic of xILK (452 amino acids) deletion constructs. The E359K point mutation is indicated with an asterisk. Embryos were co-injected with β-Parvin-GFP (BP-GFP) and one of the FLAG-xILK constructs and cultured until stage 11. B-C) FLAG-xILK constructs were immunoprecipitated from protein lysate using a mouse anti-FLAG antibody. The immunoprecipitated samples were then subjected to SDS-PAGE and western blot analysis to detect BP-GFP. BP-GFP is equally expressed in embryo lysate (Lysate). BP-GFP is immunoprecipitated with full-length xILK (xILK) and xILK ΔANK (ΔANK, IP) but not with xILK ΔINT (ΔINT), xILK ΔKIN (ΔKIN) or xILK E359K (E359K).

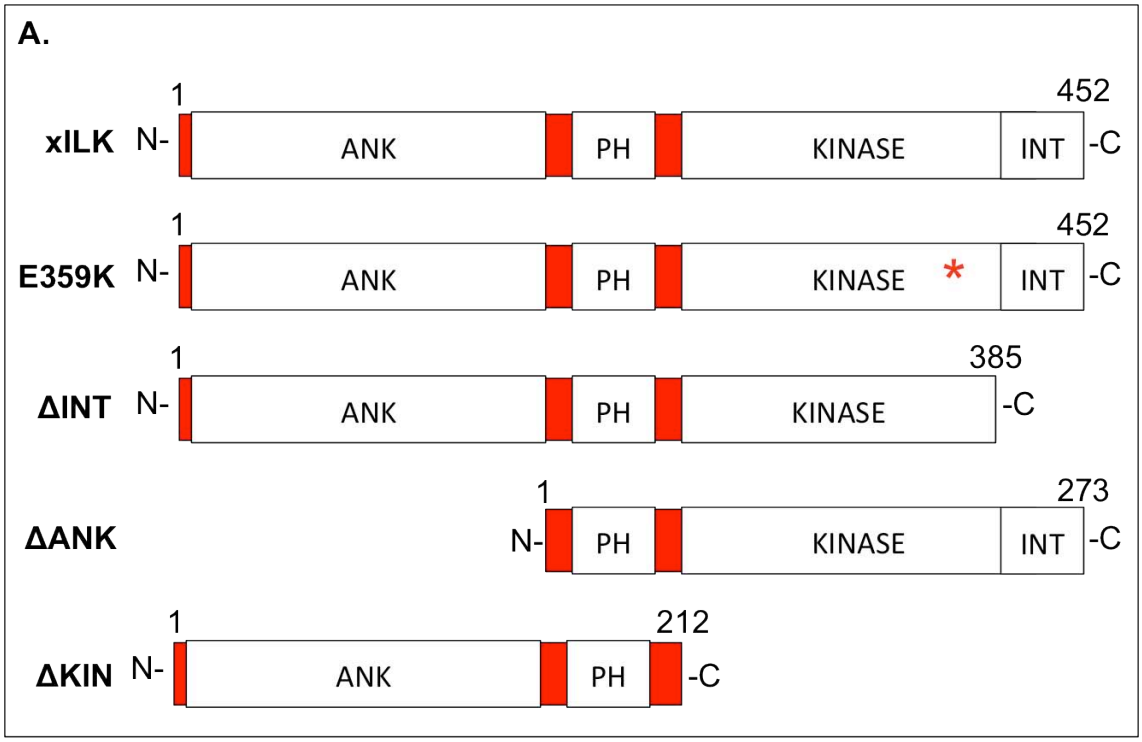
A.
xILK
N-
1
452
ANK
PH
KINASE
INT
-C
E359K
N-
1
452
ANK
PH
KINASE
*
INT
-C
ΔINT
N-
1
385
ANK
PH
KINASE
-C
ΔANK
1
273
N-
PH
KINASE
INT
-C
ΔKIN
N-
1
212
ANK
PH
-C

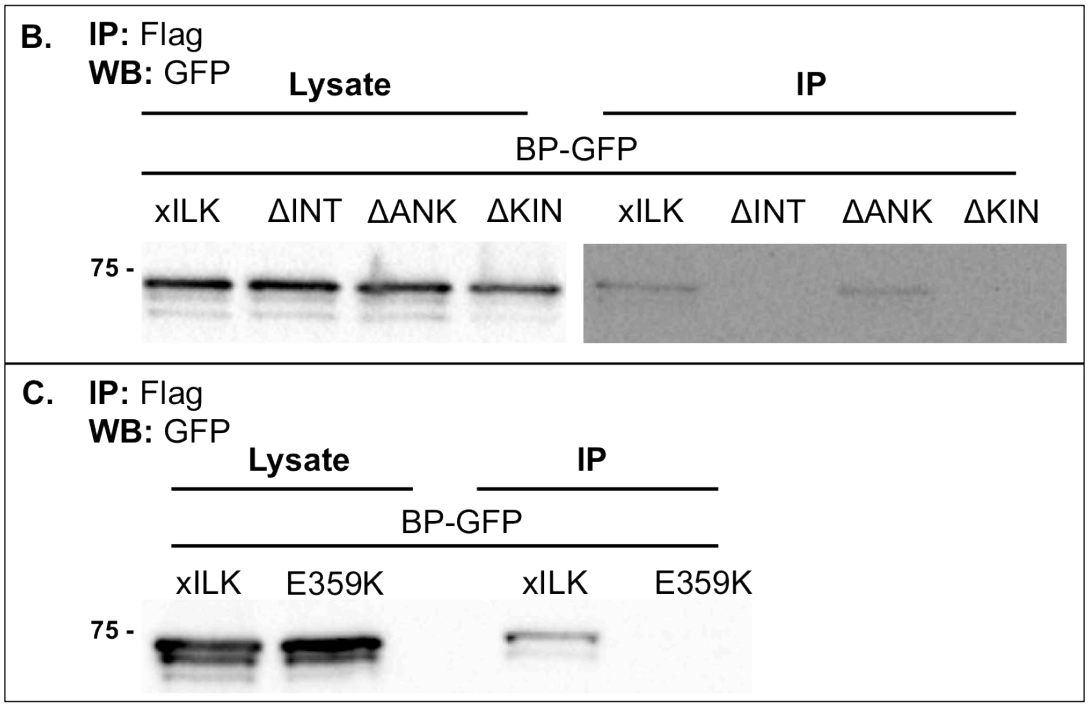
B.
IP: Flag
WB: GFP
Lysate
IP
BP-GFP
xILK
ΔINT
ΔANK
ΔKIN
xILK
ΔINT
ΔANK
ΔKIN
75 -
C.
IP: Flag
WB: GFP
Lysate
IP
BP-GFP
xILK
E359K
xILK
E359K
75 -

3.5 The xILK-β-Parvin complex formation is regulated in the embryo

Given the finding that β-Parvin-xILK complex formation requires xILK-Integrin interaction, it was of interest to determine how this interaction was regulated. Integrin receptors can transduce bidirectional signals across the cell membrane (Wolfenson et al., 2013). Integrins can be activated by outside/in signaling, when the extracellular domain binds an ECM ligand or by inside/out signals when intracellular activators bind the cytoplasmic domain (Wolfenson et al., 2013). Both forms of signal initiation result in the formation of protein complexes at the integrin cytoplasmic tail. I assessed whether FN-Integrin ligation was required for β-Parvin-xILK interaction. To do this, ectodermal cells were excised from stage 8 embryos, plated on poly L lysine (PLL) or FN and cultured until sibling embryos reached stage 11. PLL is a highly charged substrate that mediates non-specific cell adhesion, while integrin mediated cell adhesion is assessed through a FN substrate. GFP-β-Parvin was co-immunoprecipitated with xILK when cells were cultured on FN but not when cultured on PLL (Figure 12). This indicates that FN-integrin ligation appears to recruit β-Parvin to xILK.

β-Parvin is expressed in ectoderm as well as both pre and post-involution mesoderm (Studholme, 2013). Therefore I asked whether tissue patterning played a role in the recruitment of β-Parvin to integrin cytoplasmic tails. Ectodermal cells were excised from stage 8 embryos and cultured in the presence or absence of Activin A. Activin A is a TGF-beta family member that induces a mesodermal cell fate in naive ectodermal cells (Smith et al., 1990). Animal caps treated with Activin A demonstrated a decrease in β-Parvin immunoprecipitated with xILK (Figure 13A). Densitometric analysis

Figure 12. FN ligation is required for xILK-β-Parvin interaction. Embryos were co-injected with GFP-β-Parvin and FLAG-xILK and cultured until stage 8. Animal caps were dissociated and cells plated on PLL or FN and cultured until sibling embryos reached stage 11. FLAG-xILK was immunoprecipitated from protein lysate using a mouse anti-FLAG antibody. The immunoprecipitated samples were then subjected to SDS-PAGE and western blot analysis to detect GFP-β-Parvin. GFP-β-Parvin is equally expressed in cells plated on PLL (PLL) and FN (FN, Lysate). GFP-β-Parvin is immunoprecipitated with xILK when cells are plated on FN (FN) (IP).

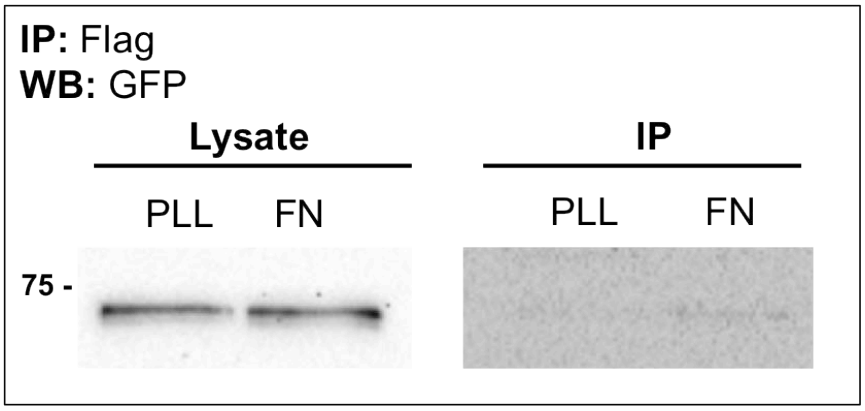
IP: Flag
WB: GFP
Lysate
IP
PLL
FN
PLL
FN
75 -

Figure 13. Activin A decreases xILK-β-Parvin interaction. Embryos were co-injected with GFP-β-Parvin and FLAG-xILK and cultured until stage 8. The animal cap of stage 8 embryos were excised and separated into 2 groups: Activin A (+A) or No Activin A (-A). The Activin A group animal caps were treated with 20 units/mL Activin A for 30 min at room temperature and then allowed to recover overnight at 18°C. A) FLAG-xILK was immunoprecipitated from protein lysate using a mouse anti-FLAG antibody. The immunoprecipitated samples were then subjected to SDS-PAGE and western blot analysis to detect GFP-β-Parvin. β-Parvin is equally expressed in embryos cultured in the presence (+A) or absence (-A) of Activin A (Lysate). β-Parvin is immunoprecipitated significantly less (66%, $p<0.05$) when animal caps are cultured in the presence of Activin A (+A) than when cultured in the absence (-A, IP) B) Densitometric analysis of immunoprecipitated GFP-β-Parvin. The results are expressed as % mean relative density compared to maximum density (-A) as indicated in the horizontal axis legend. These data are representative of 3 separate experiments.

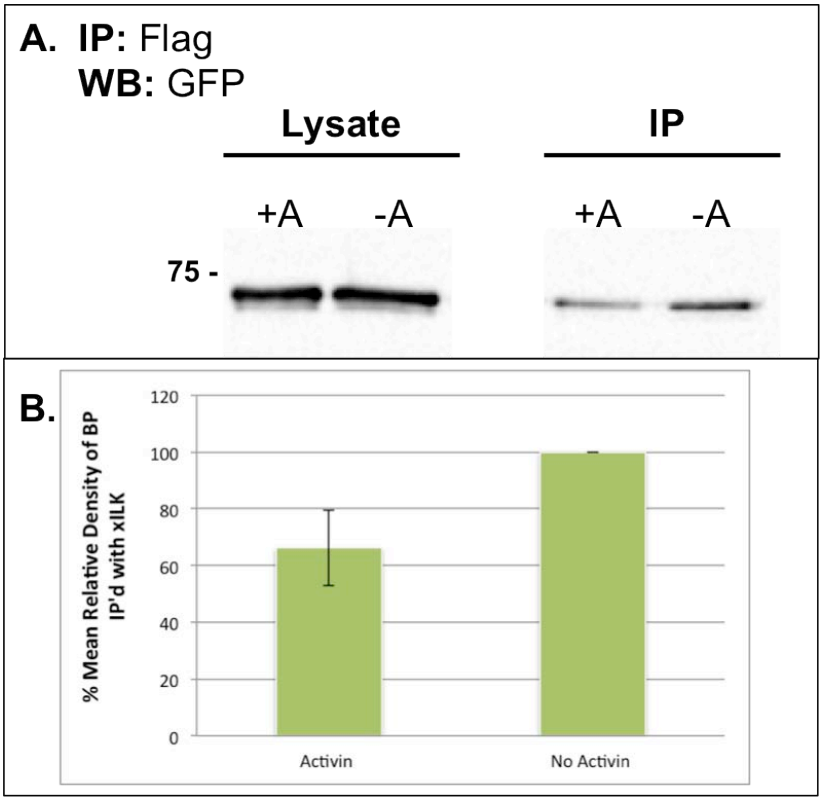
A.
IP: Flag
WB: GFP
Lysate
IP
+A
-A
+A
-A
75 -
B.
% Mean Relative Density of BP IP'd with xILK
120
100
80
60
40
20
0
Activin
No Activin

revealed that Activin A reduced the level of β-Parvin detected to 66% of that found in animal caps cultured in the absence of Activin A (Figure 13B). Therefore, Activin A decreases the recruitment of β-Parvin to xILK.

3.6 The RP1 region of β-Parvin mediates the interaction with C-Cadherin

In previous experiments, the RP1 region of β-Parvin was found to localize to the cell periphery in pre and post-involution mesoderm (Figure 5 and 6) and also decrease the ability of dissociated embryonic cells to adhere to a cadherin substrate (Figure 4C). While we know the association with integrin is mediated through xILK (Figure 10), the connection to cadherin has not been described. Given this, I examined the association of β-Parvin with C-cadherin in embryos via co-immunoprecipitation. Embryos were injected at the 1-cell stage with a control GFP (GFP), a full length GFP-β-Parvin (BP), a CH2 deletion (RP1) as well as a CH1 deletion (RP2). C-cadherin was immunoprecipitated from embryo lysate obtained from stage 11 embryos and western blot was used to detect GFP tagged β-Parvin fusion proteins. BP, and to a lesser extent RP1, are pulled down in a complex with C-cadherin, while RP2 is not (Figure 14A). These novel results were confirmed with HA tagged β-Parvin, RP1 and RP2 constructs (Figure 14B). Full-length β-Parvin-HA (BP) and RP1-HA (RP1) are retrieved by C-cadherin, but RP2-HA (RP2) is not. Co-immunoprecipitation of β-catenin was used as a positive control and was found in a complex with C-cadherin in all conditions (Figure 14A). Given that ILK was previously shown to localize to and regulate cell-cell adhesions (Vespa, 2005), I hypothesized that ILK could be physically linking β-Parvin to C-cadherin. Therefore, I immunoprecipitated C-cadherin and looked for an association with xILK. I found that

Figure 14. The RP1 region of β-Parvin mediates the interaction with C-cadherin. Embryos were injected with control GFP, GFP-β-Parvin, GFP-RP1, GFP-RP2, GFP-β-Parvin, β-Parvin-HA, RP1-HA or RP2-HA and cultured until stage 11. C-cadherin was immunoprecipitated from protein lysate using a rabbit anti-cadherin antibody. The immunoprecipitated samples were then subjected to SDS-PAGE and western blot analysis to detect β-catenin (positive control) using a mouse anti- β-catenin antibody, GFP, GFP-β-Parvin, GFP-RP1, GFP-RP2 proteins using a mouse anti-GFP antibody and GFP-β-Parvin, β-Parvin-HA, RP1-HA or RP2-HA proteins using a mouse anti-HA antibody. A) Control GFP (GFP), GFP-β-Parvin (BP), GFP-RP1 (RP1) and GFP-RP2 (RP2) are equally expressed in embryos (Lysate). β-catenin is immunoprecipitated with C-cadherin in all conditions (white triangle, IP). BP and RP1 are immunoprecipitated with C-cadherin (black triangles, IP). B) β-Parvin-HA (BP), RP1-HA (RP1) or RP2-HA (RP2) are equally expressed in embryos (Lysate). BP and RP1 are immunoprecipitated with C-cadherin (black triangles, IP).

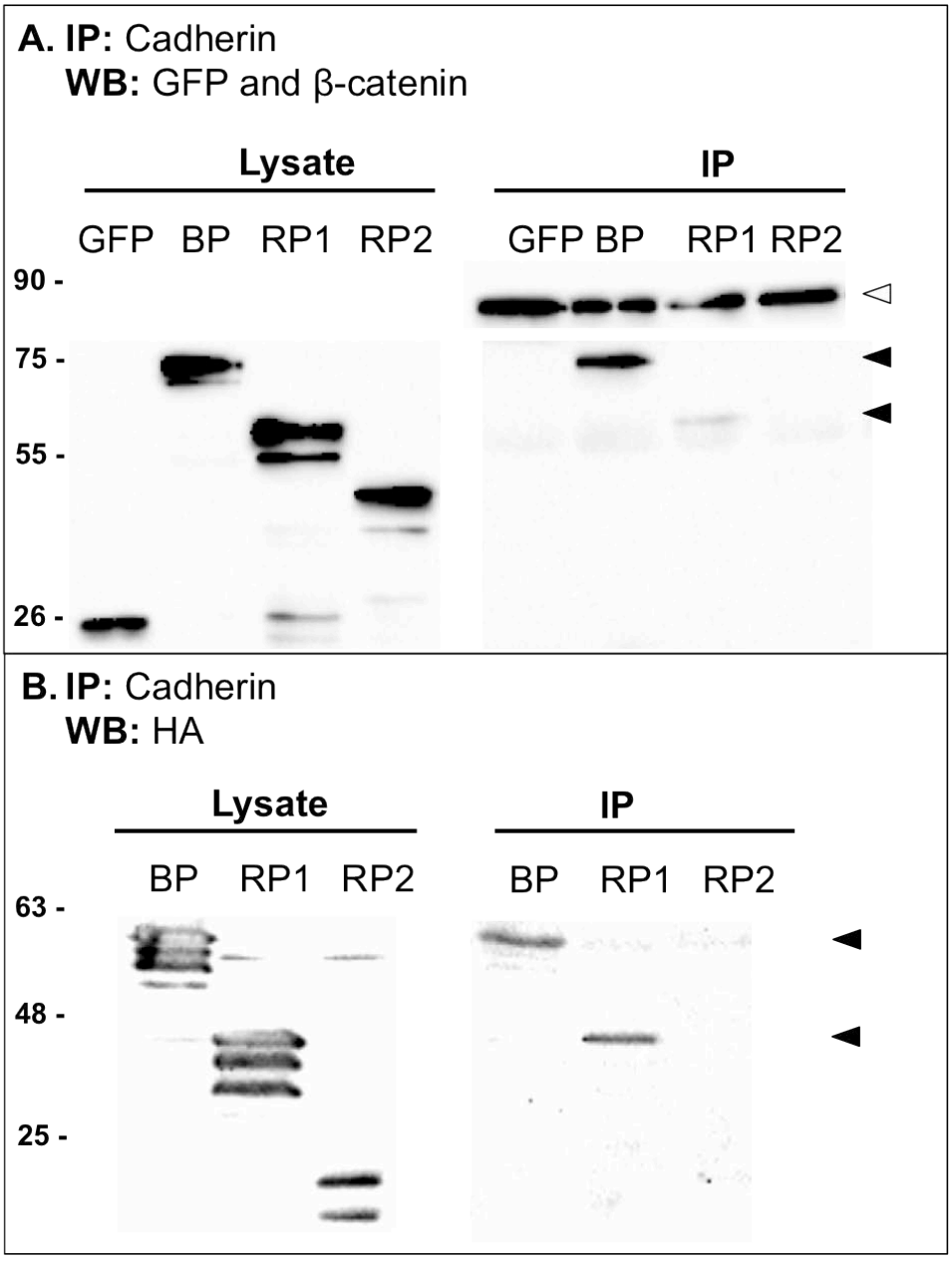
A. IP: Cadherin
WB: GFP and β-catenin
Lysate
IP
GFP BP RP1 RP2
GFP BP RP1 RP2
90 -
75 -
55 -
26 -
B. IP: Cadherin
WB: HA
Lysate
IP
BP RP1 RP2
BP RP1 RP2
63 -
48 -
25 -

GFP-xILK was not pulled down in a complex with C-cadherin (Figure 15). This indicates that xILK does not physically link β-Parvin to C-cadherin. Alternatively, xILK could competitively regulate the interaction between β-Parvin and C-cadherin. To investigate this, I co-injected embryos with β-Parvin-GFP (BP-GFP) and either Flag-xILK or Flag-xILK E359K and detect the amount of BP-GFP immunoprecipitated with C-cadherin in both conditions. BP-GFP is equally pulled down in a complex with C-cadherin in both conditions (Figure 16A). Densitometric analysis revealed that in FLAG-xILK and FLAG-xILK E359K injected embryos, BP-GFP immunoprecipitated with C-cadherin at levels of 98% and 100% respectively (Figure 16B). Therefore the interaction between β-Parvin and C-cadherin is not regulated through xILK.

3.7 β-Parvin-Cadherin complex formation is regulated in the embryo

Tissue patterning regulates cadherin adhesion to control cell movements during gastrulation. Ectodermal cells of the pre-involution DMZ have high C-cadherin adhesion, while a decrease in C-cadherin adhesion is found in the post-involution mesoderm (Lee and Gumbiner, 1995; Gumbiner, 2000). Given the finding that the β-Parvin-C-cadherin complex exists and reduces cadherin adhesion during *Xenopus laevis* gastrulation, I asked if tissue patterning influenced the interaction between β-Parvin and C-cadherin. As described in section 3.4, Activin A can be used to pattern *ex vivo* tissues. Following Activin A treatment, increased levels of β-Parvin-GFP were co-immunoprecipitated with C-cadherin (Figure 17A). Densitometric analysis revealed that cells cultured in the presence of Activin A increased the interaction of β-Parvin-GFP and C-cadherin by 28% when compared to cells that had not been exposed to Activin A (Figure 17B).

Figure 15. ILK does not interact with C-cadherin. Embryos were injected with control GFP or GFP-xILK and cultured until stage 11. C-cadherin was immunoprecipitated from protein lysate using a rabbit anti-cadherin antibody. The immunoprecipitated samples were then subjected to SDS-PAGE and western blot analysis to detect GFP-xILK protein using a mouse anti-GFP antibody. Control GFP (GFP) and GFP-xILK (GFP-xILK) are expressed in embryos (Lysate). Both GFP and GFP-xILK are not co-immunoprecipitated with C-cadherin.

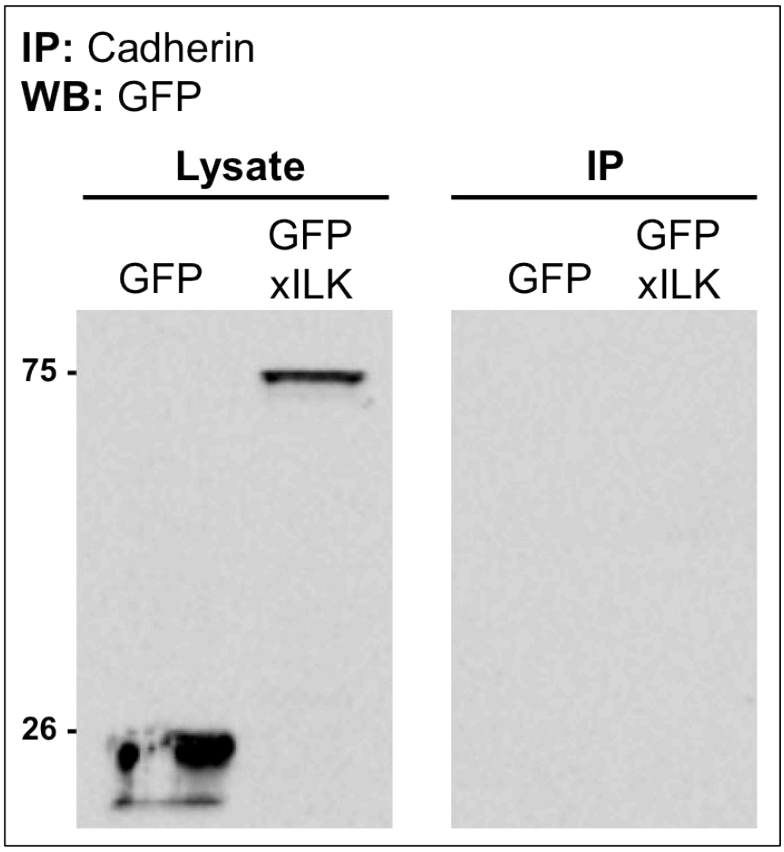
IP: Cadherin
WB: GFP
Lysate
IP
GFP
GFP xILK
GFP
GFP xILK
75 -
26 -

Figure 16. xILK does not regulate β-Parvin-C-cadherin interaction. Embryos were co-injected with β-Parvin-GFP (BP-GFP) and either FLAG-xILK or FLAG-xILK E359K. C-cadherin was immunoprecipitated from protein lysate using a rabbit anti-cadherin antibody. The immunoprecipitated samples were then subjected to SDS-PAGE and western blot analysis to detect BP-GFP using a mouse anti-GFP antibody. BP-GFP is equally expressed in FLAG-xILK (xILK) and FLAG-xILK E359K (E359K) co-injected embryos (Lysate). BP-GFP was equally immunoprecipitated with C-cadherin when co-injected with xILK or E359K with a % mean relative density compared to E359K of 98% and 100% respectively. B) Densitometric analysis of immunoprecipitated BP-GFP. The results are expressed as % mean relative density compared to E359K as indicated in the horizontal axis legend. These data are representative of 3 separate experiments.

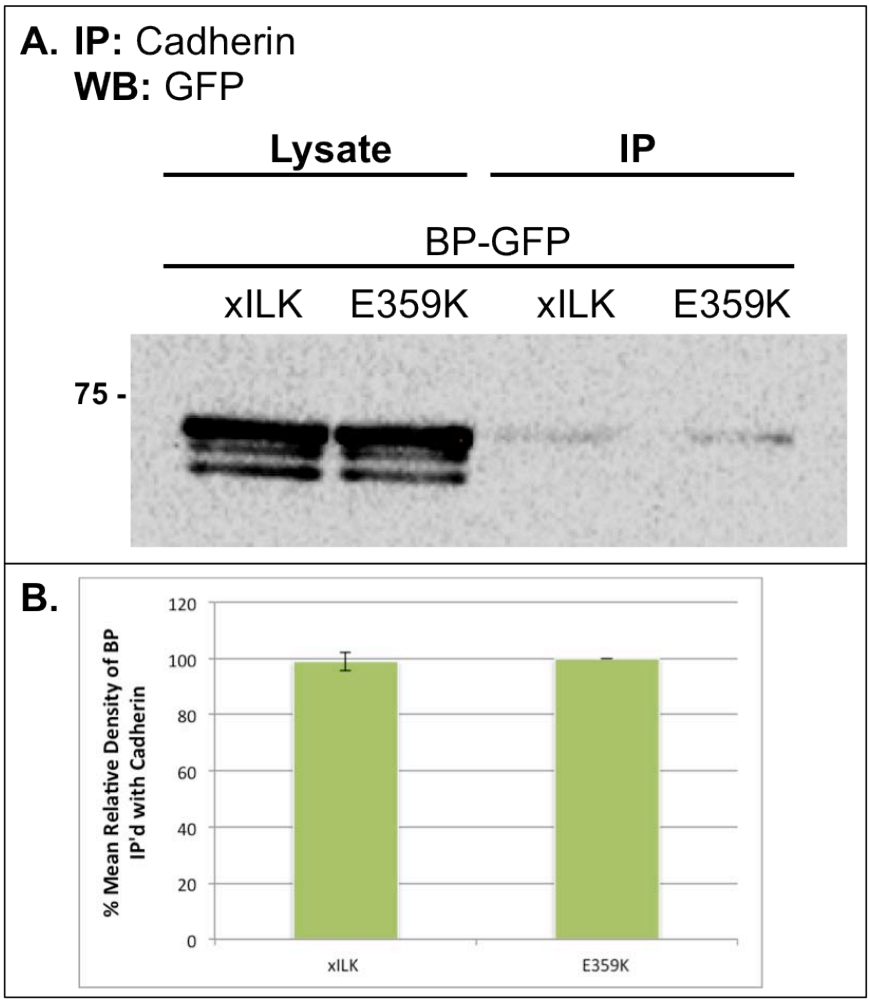
A. IP: Cadherin
WB: GFP
Lysate
IP
BP-GFP
xILK
E359K
xILK
E359K
75 -
B.
% Mean Relative Density of BP IP'd with Cadherin
120
100
80
60
40
20
0
xILK
E359K

Figure 17. Activin A increases β-Parvin-C-cadherin interaction. Embryos were injected with β-Parvin-GFP and cultured until stage 8. The animal cap of stage 8 embryos were excised and separated into 2 groups: Activin A (+A) or No Activin A (-A). The Activin A group animal caps were treated with 20 units/mL Activin A-A for 30 min at room temperature and then allowed to recover overnight at 18°C. A) C-cadherin was immunoprecipitated from protein lysate using a rabbit anti-cadherin antibody. The immunoprecipitated samples were then subjected to SDS-PAGE and western blot analysis to detect β-Parvin-GFP. β-Parvin-GFP is equally expressed in embryos cultured in the presence (+A) or absence (-A) of Activin A (Lysate). Activin A treatment increases the association of β-Parvin with C-cadherin by 28% compared to animal caps cultured in the absence of Activin A (IP). B) Densitometric analysis of immunoprecipitated β-Parvin-GFP. The results are expressed as % mean relative density compared to maximum density (-A) as indicated in the horizontal axis legend. These data are representative of 3 separate experiments.

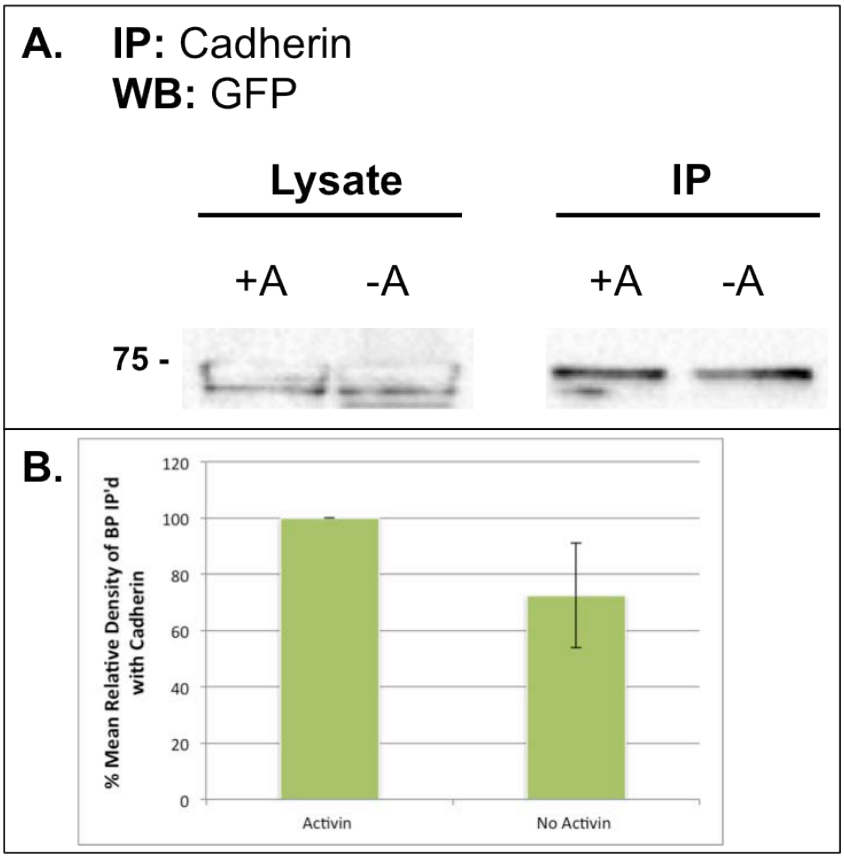
A.
IP: Cadherin
WB: GFP
Lysate
IP
+A
-A
+A
-A
75 -
B.
% Mean Relative Density of BP IP'd with Cadherin
120
100
80
60
40
20
0
Activin
No Activin

This data indicates that Activin A mediated mesodermal patterning regulates β-Parvin-C-cadherin interactions.

3.8 The RP1 region of β-Parvin mediates the interaction with β-catenin

Cadherins associate with the cytoskeleton by recruiting and binding catenin family members, such as β-catenin and Plakoglobin (PG, also known as γ-catenin) (reviewed in McCrea and Gottardi, 2015). Catenins then recruit cytoskeleton filaments to sites of cell-cell contact to enable cell-cell adhesion, cell mobility and provide a scaffold for cell signaling complexes at the cell membrane (McCrea and Gottardi, 2015). I therefore asked if the interaction between β-Parvin and C-cadherin was mediated through catenins. Initially I looked at a potential interaction with PG. Control GFP and GFP tagged β-Parvin constructs were immunoprecipitated from embryo lysate and western blot was performed to detect PG (Figure 18). PG was detected in embryos, but was not immunoprecipitated with any of the β-Parvin constructs (Figure 18A). Figure 18B confirms that control GFP and GFP tagged β-Parvin constructs were retrieved from embryo lysate. Therefore, β-Parvin does not interact with PG.

Since β-Parvin does not interact with PG, I asked whether β-Parvin associates with β-catenin. Control GFP and GFP tagged β-Parvin constructs were immunoprecipitated from embryo lysate and western blot was performed to detect β-catenin (Figure 19). β-catenin was pulled down with both GFP tagged β-Parvin (BP) and RP1 (RP1, Figure 19A). A trace amount of β-catenin was also retrieved with GFP tagged RP2 (RP2). Figure 19B confirms that control GFP and GFP tagged β-Parvin constructs were retrieved from embryo lysate. Since it was unexpected to recruit β-catenin with

Figure 18. β-Parvin does not interact with Plakoglobin. A) Embryos were injected with control GFP, GFP-β-Parvin, GFP-RP1, GFP-RP2 and cultured until stage 11. Control GFP, GFP-β-Parvin, GFP-RP1, and GFP-RP2 were immunoprecipitated from protein lysate using a mouse anti-GFP antibody. The immunoprecipitated samples were then subjected to SDS-PAGE and western blot analysis to detect PG using a mouse anti-Plakoglobin antibody. A) PG is equally expressed in embryos (Lysate). PG is not immunoprecipitated with control GFP (GFP), GFP-β-Parvin (BP), GFP-RP1 (RP1) or GFP-RP2 (RP2, IP). B) Control GFP (GFP), GFP-β-Parvin (BP), GFP-RP1 (RP1) and GFP-RP2 (RP2) were immunoprecipitated from embryo lysate (IP).

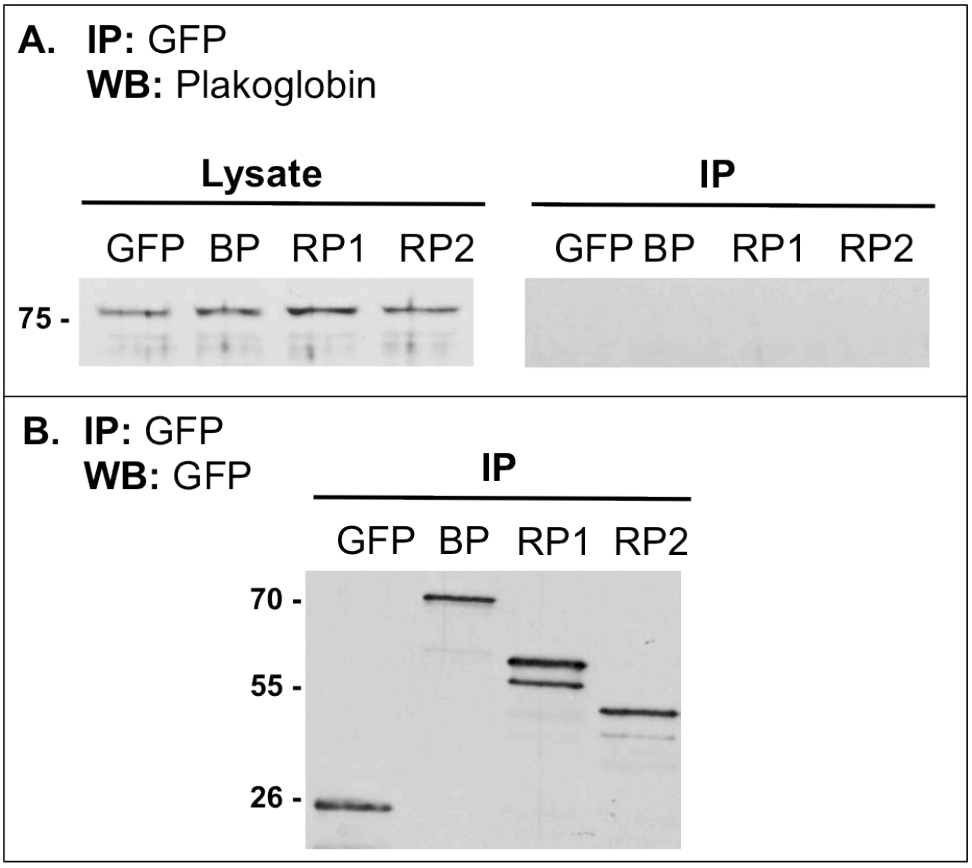
A.
IP: GFP
WB: Plakoglobin
Lysate
IP
GFP BP RP1 RP2
GFP BP RP1 RP2
75 -
B.
IP: GFP
WB: GFP
IP
GFP BP RP1 RP2
70 -
55 -
26 -

Figure 19. The RP1 region of β-Parvin mediates β-catenin interaction. A) Embryos were injected with control GFP, GFP-β-Parvin, GFP-RP1, GFP-RP2 and cultured until stage 11. Control GFP, GFP-β-Parvin, GFP-RP1, and GFP-RP2 were immunoprecipitated from protein lysate using a mouse anti-GFP antibody. The immunoprecipitated samples were then subjected to SDS-PAGE and western blot analysis to detect β -catenin using a rabbit anti-β-catenin antibody. A) β-catenin is equally expressed in embryos (Lysate). β-catenin is immunoprecipitated with GFP-β-Parvin (BP) and GFP-RP1 (RP1, IP). A small amount of β-catenin is immunoprecipitated with GFP-RP2 (RP2, IP). B) Control GFP (GFP), β-Parvin, RP1 and RP2 were immunoprecipitated from embryo lysate (IP). C) Embryos were injected with GFP-β-Parvin, GFP-RP1, GFP-RP2 and cultured until stage 11. β-catenin was immunoprecipitated from protein lysate using a rabbit anti-β-catenin antibody. The immunoprecipitated samples were then subjected to SDS-PAGE and western blot analysis to detect GFP-β-Parvin, GFP-RP1 or GFP-RP2 proteins using a mouse anti-GFP antibody. GFP-β-Parvin (BP), GFP-RP1 (RP1) and GFP-RP2 (RP2) are equally expressed in embryos (Lysate). BP and RP1 are immunoprecipitated with β-catenin (IP). A non-specific band running just above the expected molecular weight of RP2 is not expected to mask the interaction.

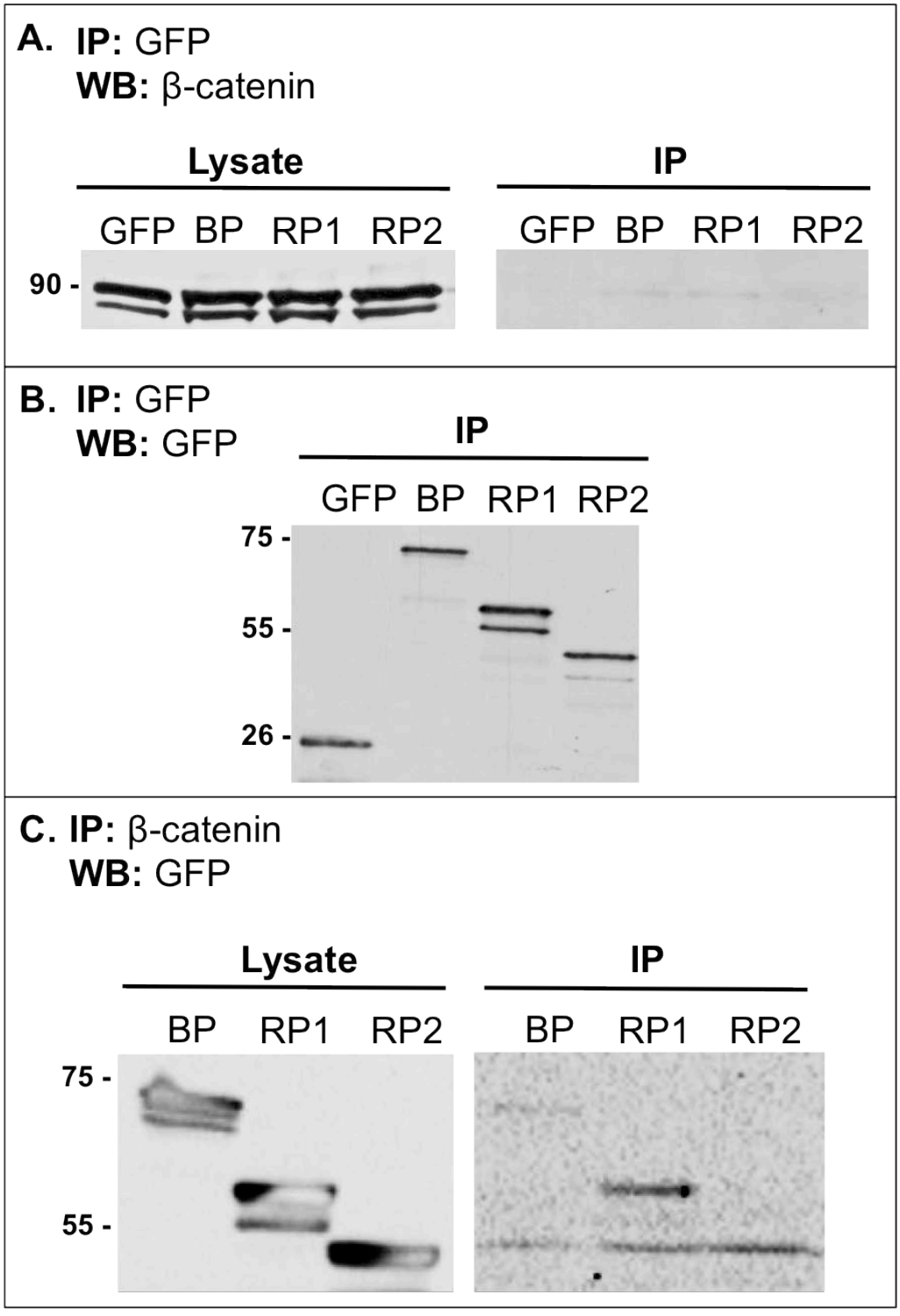
A. IP: GFP
WB: β-catenin
Lysate
IP
GFP BP RP1 RP2
GFP BP RP1 RP2
90 -
B. IP: GFP
WB: GFP
IP
GFP BP RP1 RP2
75 -
55 -
26 -
C. IP: β-catenin
WB: GFP
Lysate
IP
BP RP1 RP2
BP RP1 RP2
75 -
55 -

both domains of β-Parvin, the reverse immunoprecipitation experiment was completed to further examine molecular associations. β-catenin was immunoprecipitated from embryo lysate overexpressing control GFP or a GFP tagged β-Parvin constructs and western blot was used to detect GFP tagged proteins (Figure 19C). GFP-β-Parvin (BP) and GFP-RP1 (RP1) were pulled down with β-catenin, while GFP-RP2 (RP2) was not (Figure 19C). These experiments reveal the β-Parvin and β-catenin are part of a complex that is likely mediated through the CH1 domain. This interaction could be mediated through C-cadherin as described in section 3.6 or β-Parvin could be interacting directly β-catenin.

3.9 β-catenin is not required for β-Parvin-C-cadherin interaction

The results above indicate that β-Parvin interacts with both C-cadherin and β-catenin however it does not provide insight into the inter-molecular interactions. Catenins (β-catenin, PG and p120 catenin) are recruited to highly conserved domains in the cytoplasmic tail of cadherin (McCrea and Gottardi, 2015). β-catenin binds to the distal β-catenin binding domain (BCAT), while p120-catenin binds a juxtamembrane domain (JMD) (Gumbiner, 2005). Given this, I generated C-cadherin deletion constructs removing these conserved domains (Figure 20A). I used the GST fusion proteins to probe lysate obtained from stage 11 embryos expressing HA tagged β-Parvin. A robust interaction was observed between β-catenin and the GST- C-Cadherin (CAD) and GST-CAD ΔJMD (ΔJMD) constructs. As expected, no β-catenin was pulled down with GST-CAD ΔBCAT (ΔBCAT). Interestingly, all GST-CAD fusion proteins pulled down β- Parvin-HA (Figure 20B). Densitometric analysis reveals that ΔJMD retrieves more β-Parvin-

Figure 20. β-catenin is not required for β-Parvin-C-cadherin interaction. A) Schematic of C-cadherin cytoplasmic domain (152 amino acids), C-cadherin juxtamembrane domain deletion (ΔJMD, 131 amino acids) and beta-catenin binding domain deletion (ΔBCAT, 131 amino acids) constructs. B) Embryos were injected with β-Parvin-HA and cultured until stage 11. Isolated protein lysate was then incubated with purified GST bound Glutathione-Uniflow Resin to inhibit non-specific protein interactions and then probed with purified GST-C-cadherin (CAD), GST-CAD ΔJMD (ΔJMD) or GST-CAD ΔBCAT (ΔBCAT) bound Glutathione-Uniflow Resin. Isolated proteins were then subjected to SDS-PAGE and western blot analysis to detect β-catenin (positive and negative control) using a mouse anti- β-catenin antibody or β-Parvin-HA using a mouse anti-HA antibody. Ponceau images displays equal protein loading (Lysate) and the expression of each purified GST fusion protein (GST-Pull-down). β-Parvin-HA is equally expressed in embryos (WB, Lysate, black triangle). β-catenin is pulled down with CAD and ΔJMD (WB, GST-Pull-down, white triangle). β-Parvin-HA is pulled down with CAD, ΔJMD and ΔBCAT (GST-Pull-down, black triangle). C). Densitometric analysis of isolated β-Parvin-HA. The results are expressed as % mean relative density compared to CAD as indicated in the horizontal axis legend. ΔJMD retrieved the most β-Parvin-HA from embryo lysate. CAD and ΔBCAT retrieved 73% and 17% of β-Parvin-HA respectively when compared ΔJMD. These data are representative of 3 separate experiments.

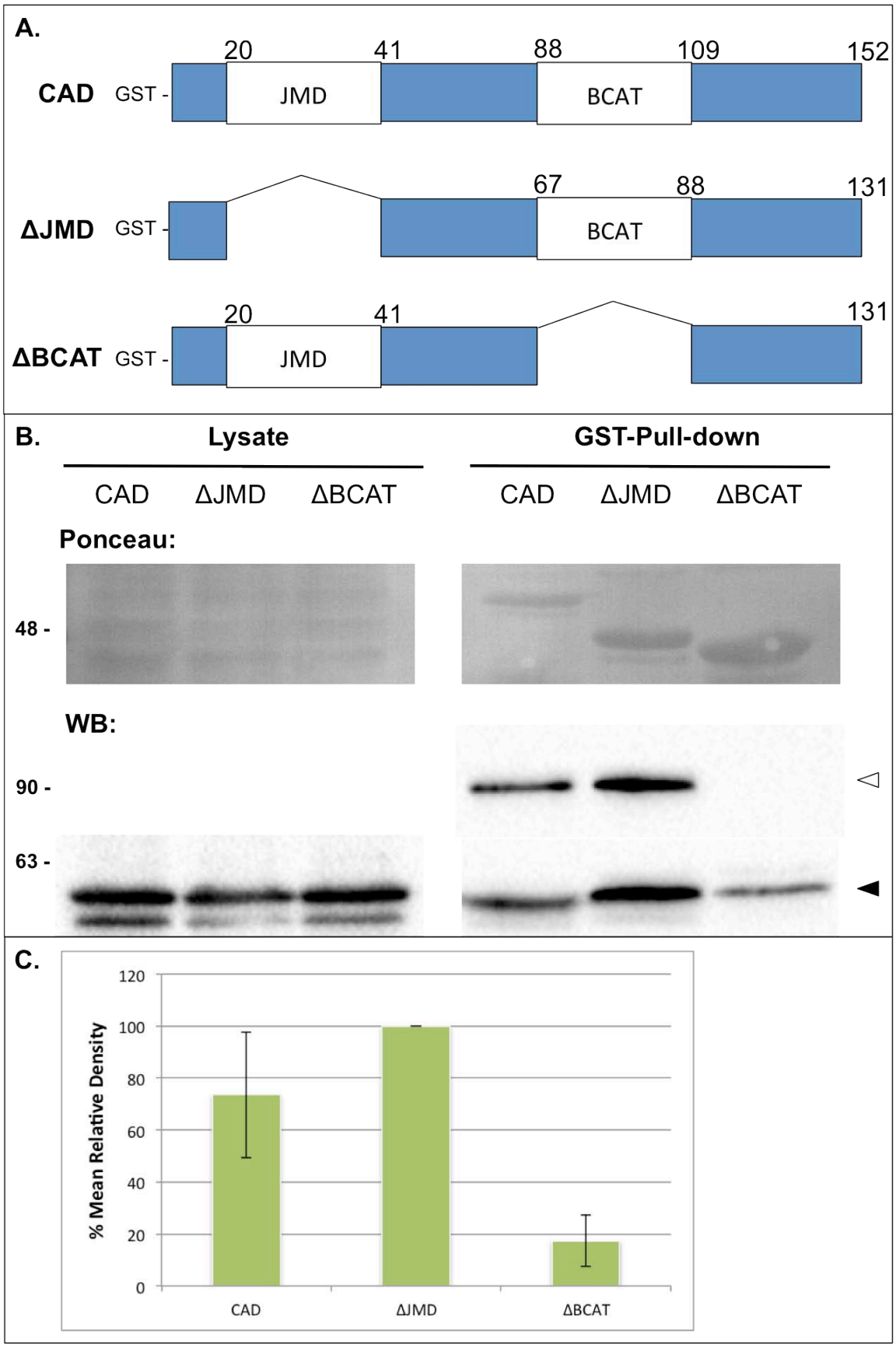
A.
CAD
GST -
20
41
88
109
152
JMD
BCAT
ΔJMD
GST -
67
88
131
BCAT
ΔBCAT
GST -
20
41
131
JMD
B.
Lysate
GST-Pull-down
CAD
ΔJMD
ΔBCAT
CAD
ΔJMD
ΔBCAT
Ponceau:
48 -
WB:
90 -
63 -
C.
% Mean Relative Density
120
100
80
60
40
20
0
CAD
ΔJMD
ΔBCAT

HA than full length CAD. Furthermore, ΔBCAT pulls down even less than full length CAD (Figure 20C). This suggests that the JMD domain is a negative regulator, while the BCAT domain is a positive regulator of β-Parvin binding, but neither is required. In addition, β-catenin is also not essential for the association of β-Parvin and C-cadherin however could potentially act to enhance the interaction between β-Parvin and the C-cadherin cytoplasmic tail. It remains unknown whether this is due to the structural constraints of the construct or whether β-catenin itself is playing an influential role.

3.10 β-Parvin associates with multiple cytoplasmic β-catenin populations

Based on the results above β-Parvin can interact with C-cadherin, and this interaction may be influenced by β-catenin. Therefore I performed experiments to help clarify the interaction between β-Parvin and β-catenin (Figure 21A). In cell culture, cytoplasmic β-catenin can exist as a TCF-selective group that is targeted to the nucleus and a population that can interact with cadherin (Gottardi and Gumbiner, 2004). When embryo lysate is probed with GST-CAD a robust interaction with the soluble pool of β-catenin is observed (Figure 21B). A sequential pull-down using GST-CAD reveals that the initial pull-down has completely removed β-catenin competent to bind cadherin from the lysate. However, a sequential pull-down with GST-xTCF (GST-TCF) reveals a second population of β-catenin with distinct binding properties (Figure 21B). Therefore, during *Xenopus laevis* development, β-catenin exists in at least two pools that can be distinguished by their association with C-cadherin and xTCF. Knowing that I can segregate these two pools of β-catenin, I asked whether β-Parvin preferential binds to a particular either or both of

Figure 21. β-catenin exists in two distinct populations during *Xenopus laevis* gastrulation. A) Schematic displaying sequential pull-down experimental workflow. Protein lysate was isolated from stage 11 embryos and incubated with GST-CAD (GST CAD) bound Glutathione-Uniflow Resin (Pull-down #1). The supernatant was then transferred to another microfuge tube and probed with either GST-CAD (GST CAD) or GST-TCF (GST TCF, Pull-down #2). B) Isolated proteins from each pull-down were subjected to SDS-PAGE and western blot analysis to detect β-catenin using a mouse anti-β-catenin antibody. Ponceau image displays the expression of each purified GST fusion protein. GST CAD pulls down β-catenin (WB, Pull-down #1). GST TCF pulls down β-catenin in Pull-down #2 (WB), but GST CAD does not.

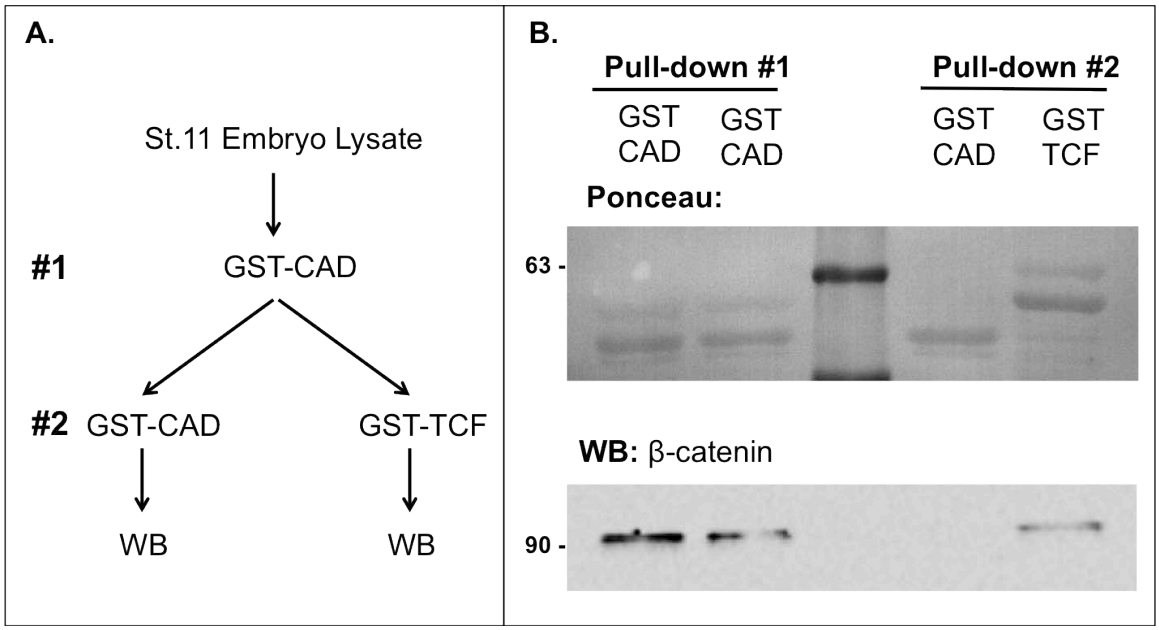
A.
St.11 Embryo Lysate
#1
GST-CAD
#2
GST-CAD
GST-TCF
WB
WB
B.
Pull-down #1
Pull-down #2
GST
CAD
GST
CAD
GST
CAD
GST
TCF
Ponceau:
63 -
WB: β-catenin
90 -

these forms. Lysate obtained from embryos overexpressing an HA tagged β-Parvin (BP-HA) was sequentially probed with GST-CAD and GST-TCF. BP-HA was pulled down in by both GST-CAD and GST-xTCF (GST-TCF, Figure 22). This finding demonstrates that β-Parvin does not selectively bind to one pool of β-catenin and suggests a direct interaction between β-Parvin and β-catenin.

3.11 α-Parvin is expressed during *Xenopus laevis* development

Our laboratory has looked for a α-Parvin ortholog in *Xenopus laevis,* however, at that time genomic sequence data at the *alpha-parvin* locus was incomplete. Recently, sequence data has become available, from Xenbase (J-strain v9.1) that reveals a α-Parvin ortholog. I used *in silico* analyses to compare *Xenopus laevis* α-Parvin to known α-Parvin orthologs. *Homo sapiens* α-Parvin shared the highest amino acid identity at 94.1%, while the percent identity with *Mus musculus* and *Gallus gallus* was also high at 92.5% and 91.8% respectively. Also, the percent identity with *Danio rerio* was 87.6% and *Drosophila melanogaster* showed the greatest divergence at 56.4% identity (Table 10). Multiple sequence alignment of α-Parvin sequences shows that the location of the nuclear localization signals and calponin homology domains are conserved across species (Figure 23). Therefore, there does not appear to be any structural differences in α-Parvin across metazoans. Significantly, *Xenopus laevis* α-Parvin and β-Parvin share 72.3% identity (Table 10) with particularly high conservation (90%) within the CH2 domain (Figure 24A). The fact that *Xenopus laevis* α-Parvin shares higher identity to other α-Parvin orthologs than to *Xenopus laevis* β-Parvin confirms that it represents a true α-Parvin. A phylogenetic tree was constructed to view evolutionary relationships

Figure 22. β-Parvin interacts with GST-C-cadherin and GST-xTCF pools of β-catenin. Embryos were injected with β-Parvin-HA and cultured until stage 11. Isolated protein lysate was incubated with purified GST bound Glutathione-Uniflow Resin to inhibit non-specific protein interactions and then probed with purified GST-CAD (GST CAD) or GST-TCF (GST TCF) bound Glutathione-Uniflow Resin. Isolated proteins were then subjected to SDS-PAGE and western blot analysis to β-Parvin-HA using a mouse anti-HA antibody. Ponceau image displays the expression of each purified GST fusion protein. β-Parvin-HA is expressed in embryos (Lysate). β-Parvin-HA is pulled down with both GST CAD and GST TCF (GST-Pull-down).

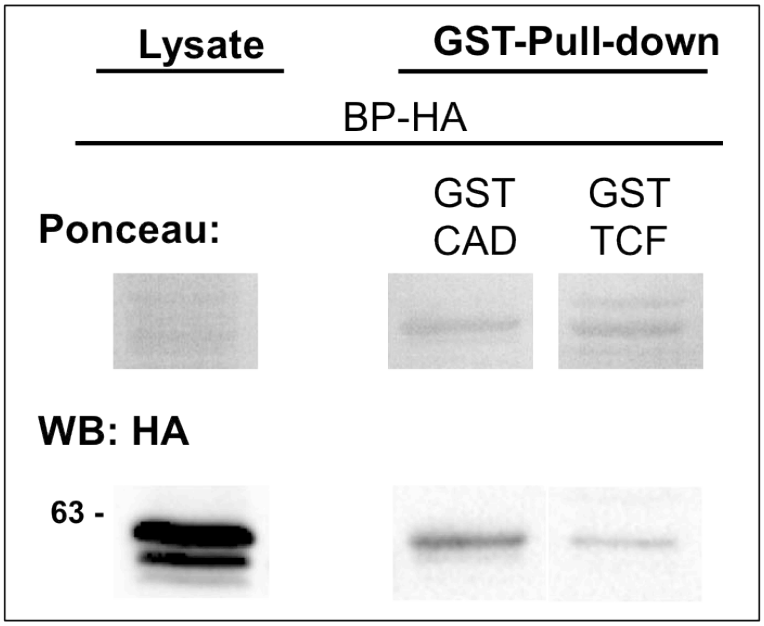
Lysate
GST-Pull-down
BP-HA
Ponceau:
GST CAD
GST TCF
WB: HA
63 -

Figure 23. α-Parvin amino acid multiple sequence alignment. Alignment of *Drosophila melanogaster* (Genbank accession number NM_134508.3), *Danio rerio* (Genbank accession number NM_001002872.2), *Xenopus laevis* (Genbank accession number XP_018115789.1), *Gallus gallus* (Genbank accession number XM_025151217.1), *Homo sapiens* (Genbank accession number NM_018222.5), and *Mus musculus* (Genbank accession number AF237774) α-Parvin amino acid sequences was performed using Clustal Omega (http://www.ebi.ac.uk/Tools/msa/clustalo/). Identical amino acids, conservative amino acid substitutions and semi-conservative substitutions are represented by an asterisk, colon and period under the sequence respectively. Deletions in the sequence are denoted by a dash in the sequence. Double lines above the sequence mark putative nuclear localization signals and calponin homology domains 1 and 2 are highlighted.

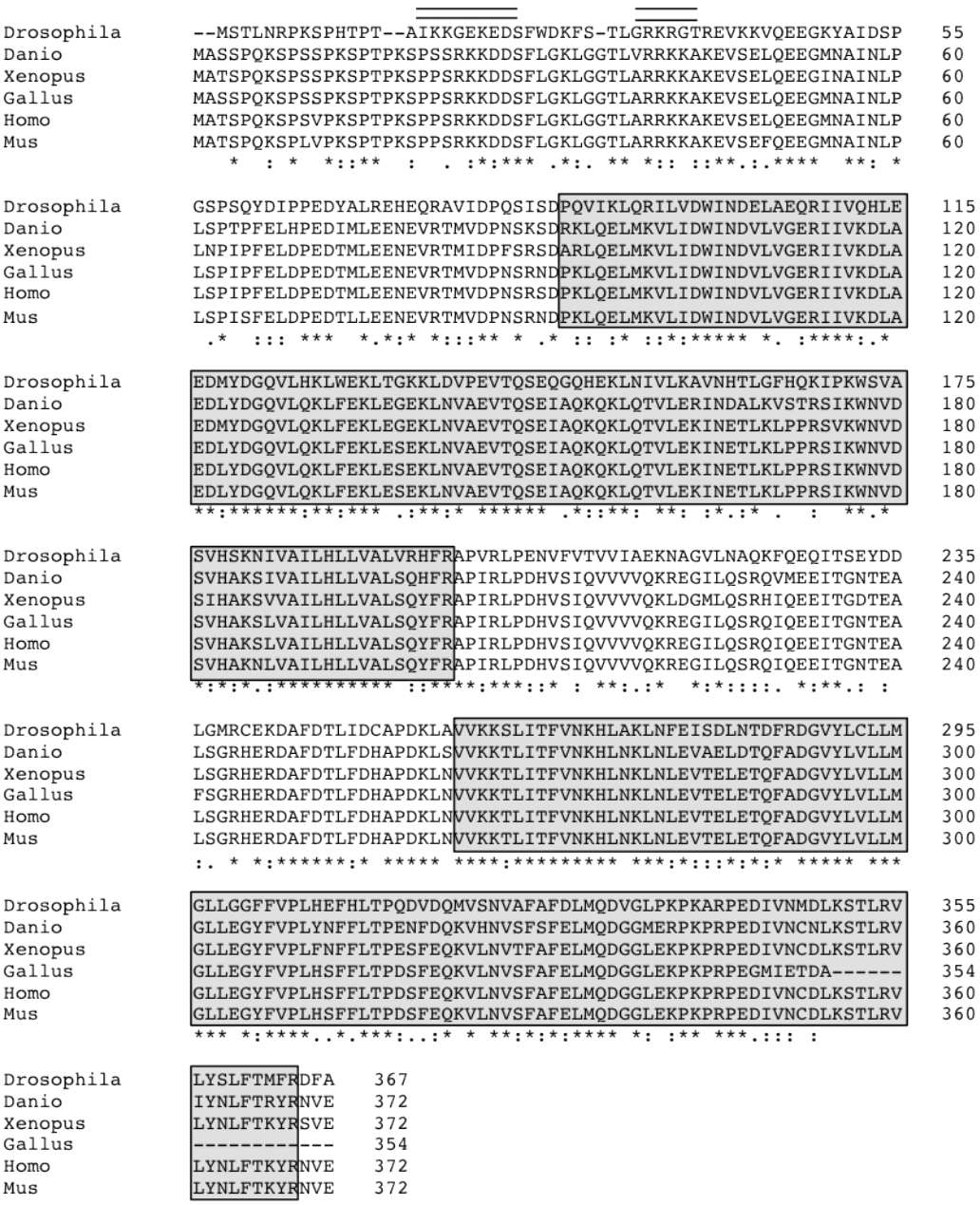
Drosophila --MSTLNRPKSPHTPT--AIKKGEKEDSFWDKFS-TLGRKRGTREVKKVQEEGKYAIDSP 55
Danio MASSPQKSPSSPKSPTPKSPSSRKKDDSFLGKLGGTLVRRKKAKEVSELQEEGMNAINLP 60
Xenopus MATSPQKSPSSPKSPTPKSPPSRKKDDSFLGKLGGTLARRKKAKEVSELQEEGINAINLP 60
Gallus MASSPQKSPSSPKSPTPKSPPSRKKDDSFLGKLGGTLARRKKAKEVSELQEEGMNAINLP 60
Homo MATSPQKSPSVPKSPTPKSPPSRKKDDSFLGKLGGTLARRKKAKEVSELQEEGMNAINLP 60
Mus MATSPQKSPLVPKSPTPKSPPSRKKDDSFLGKLGGTLARRKKAKEVSEFQEEGMNAINLP 60
GSPSQYDIPPEDYALREHEQRAVIDPQSISDPQVIKLQRILVDWINDELAEQRIIVQHLE 115
LSPTPFELHPEDIMLEENEVRTMVDPNSKSDRKLQELMKVLIDWINDVLVGERIIVKDLA 120
LNPIPFELDPEDTMLEENEVRTMIDPFSRSDARLQELMKVLIDWINDVLVGERIIVKDLA 120
LSPIPFELDPEDTMLEENEVRTMVDPNSRNDPKLQELMKVLIDWINDVLVGERIIVKDLA 120
LSPIPFELDPEDTMLEENEVRTMVDPNSRSDPKLQELMKVLIDWINDVLVGERIIVKDLA 120
LSPISFELDPEDTLLEENEVRTMVDPNSRNDPKLQELMKVLIDWINDVLVGERIIVKDLA 120
EDMYDGQVLHKLWEKLTGKKLDVPEVTQSEQGQHEKLNIVLKAVNHTLGFHQKIPKWSVA 175
EDLYDGQVLQKLFEKLEGEKLNVAEVTQSEIAQKQKLQTVLERINDALKVSTRSIKWNVD 180
EDMYDGQVLQKLFEKLEGEKLNVAEVTQSEIAQKQKLQTVLEKINETLKLPPRSVKWNVD 180
EDLYDGQVLQKLFEKLESEKLNVAEVTQSEIAQKQKLQTVLEKINETLKLPPRSIKWNVD 180
EDLYDGQVLQKLFEKLESEKLNVAEVTQSEIAQKQKLQTVLEKINETLKLPPRSIKWNVD 180
EDLYDGQVLQKLFEKLESEKLNVAEVTQSEIAQKQKLQTVLEKINETLKLPPRSIKWNVD 180
SVHSKNIVAILHLLVALVRHFRAPVRLPENVFVTVVIAEKNAGVLNAQKFQEQITSEYDD 235
SVHAKSIVAILHLLVALSQHFRAPIRLPDHVSIQVVVVQKREGILQSRQVMEEITGNTEA 240
SIHAKSVVAILHLLVALSQYFRAPIRLPDHVSIQVVVVQKLDGMLQSRHIQEEITGDTEA 240
SVHAKSLVAILHLLVALSQYFRAPIRLPDHVSIQVVVVQKREGILQSRQIQEEITGNTEA 240
SVHAKSLVAILHLLVALSQYFRAPIRLPDHVSIQVVVVQKREGILQSRQIQEEITGNTEA 240
SVHAKNLVAILHLLVALSQYFRAPIRLPDHVSIQVVVVQKREGILQSRQIQEEITGNTEA 240
LGMRCEKDAFDTLIDCAPDKLAVVKKSLITFVNKHLAKLNFEISDLNTDFRDGVYLCLLM 295
LSGRHERDAFDTLFDHAPDKLSVVKKTLITFVNKHLNKLNLEVAELDTQFADGVYLVLLM 300
LSGRHERDAFDTLFDHAPDKLNVVKKTLITFVNKHLNKLNLEVTELETQFADGVYLVLLM 300
FSGRHERDAFDTLFDHAPDKLNVVKKTLITFVNKHLNKLNLEVTELETQFADGVYLVLLM 300
LSGRHERDAFDTLFDHAPDKLNVVKKTLITFVNKHLNKLNLEVTELETQFADGVYLVLLM 300
LSGRHERDAFDTLFDHAPDKLNVVKKTLITFVNKHLNKLNLEVTELETQFADGVYLVLLM 300
GLLGGFFVPLHEFHLTPQDVDQMVSNVAFAFDLMQDVGLPKPKARPEDIVNMDLKSTLRV 355
GLLEGYFVPLYNFFLTPENFDQKVHNVSFSFELMQDGGMERPKPRPEDIVNCNLKSTLRV 360
GLLEGYFVPLFNFFLTPESFEQKVLNVTFAFELMQDGGLEKPKPRPEDIVNCDLKSTLRV 360
GLLEGYFVPLHSFFLTPDSFEQKVLNVSFAFELMQDGGLEKPKPRPEGMIETDA------ 354
GLLEGYFVPLHSFFLTPDSFEQKVLNVSFAFELMQDGGLEKPKPRPEDIVNCDLKSTLRV 360
GLLEGYFVPLHSFFLTPDSFEQKVLNVSFAFELMQDGGLEKPKPRPEDIVNCDLKSTLRV 360
LYSLFTMFRDFA 367
IYNLFTRYRNVE 372
LYNLFTKYRSVE 372
------------ 354
LYNLFTKYRNVE 372
LYNLFTKYRNVE 372

Figure 24. α and β-Parvin amino acid alignment and evolutionary relationship. A) Alignment of *Xenopus laevis* β-Parvin (Genbank accession number NP_001089519.1) and *Xenopus laevis* α-Parvin (Genbank accession number NM_134508.3) amino acid sequences was performed using Clustal Omega (http://www.ebi.ac.uk/Tools/msa/clustalo/). Identical amino acids, conservative amino acid substitutions and semi-conservative substitutions are represented by an asterisk, colon and period under the sequence respectively. Deletions in the sequence are denoted by a dash in the sequence. Double lines above the sequence mark putative nuclear localization signals and calponin homology domains 1 and 2 are highlighted. B) α-Parvin amino acid sequences listed in Figure 25 were compared with *Xenopus laevis* (Genbank accession number NP_001089519.1), *Gallus gallus* (Genbank accession number XP_416459.2), *Homo sapiens* (Genbank accession number AAG27171.1), *Mus musculus* (Genbank accession number AAG27172.1), *Danio rerio* (Genbank accession number NP_956020.1) β-Parvin amino acid sequences to form a phylogenetic tree using Simple Phylogeny (http://www.ebi.ac.uk/Tools/phylogeny/simple_phylogeny/).

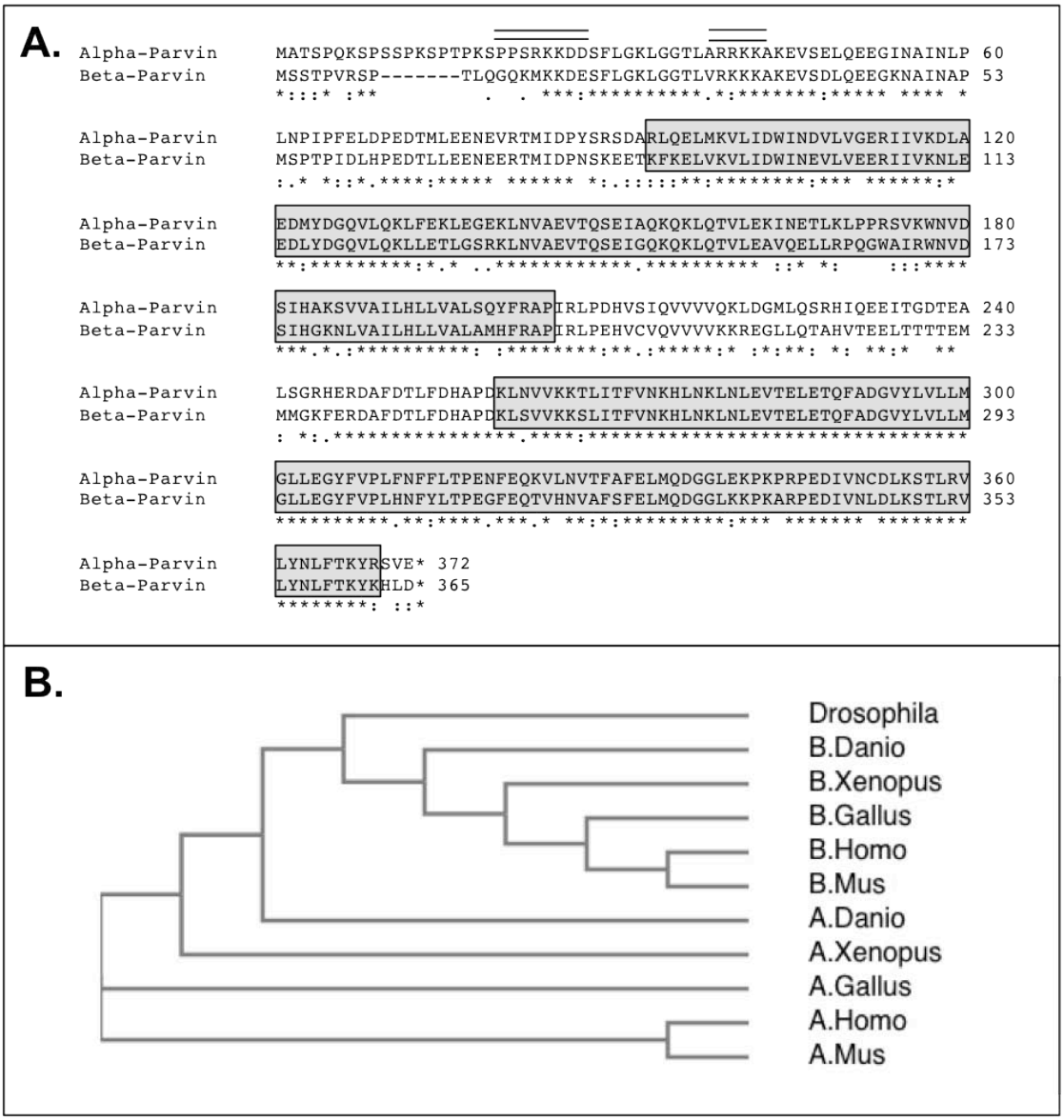
A.
Alpha-Parvin MATSPQKSPSSPKSPTPKSPPSRKKDDSFLGKLGGTLARRKKAKEVSELQEEGINAINLP 60
Beta-Parvin MSSTPVRSP-------TLQGQKMKKDESFLGKLGGTLVRKKKAKEVSDLQEEGKNAINAP 53
Alpha-Parvin LNPIPFELDPEDTMLEENEVRTMIDPYSRSDARLQELMKVLIDWINDVLVGERIIVKDLA 120
Beta-Parvin MSPTPIDLHPEDTLLEENEERTMIDPNSKEETKFKELVKVLIDWINEVLVEERIIVKNLE 113
Alpha-Parvin EDMYDGQVLQKLFEKLEGEKLNVAEVTQSEIAQKQKLQTVLEKINETLKLPPRSVKWNVD 180
Beta-Parvin EDLYDGQVLQKLLETLGSRKLNVAEVTQSEIGQKQKLQTVLEAVQELLRPQGWAIRWNVD 173
Alpha-Parvin SIHAKSVVAILHLLVALSQYFRAPIRLPDHVSIQVVVVQKLDGMLQSRHIQEEITGDTEA 240
Beta-Parvin SIHGKNLVAILHLLVALAMHFRAPIRLPEHVCVQVVVVKKREGLLQTAHVTEELTTTTEM 233
Alpha-Parvin LSGRHERDAFDTLFDHAPDKLNVVKKTLITFVNKHLNKLNLEVTELETQFADGVYLVLLM 300
Beta-Parvin MMGKFERDAFDTLFDHAPDKLSVVKKSLITFVNKHLNKLNLEVTELETQFADGVYLVLLM 293
Alpha-Parvin GLLEGYFVPLFNFFLTPENFEQKVLNVTFAFELMQDGGLEKPKPRPEDIVNCDLKSTLRV 360
Beta-Parvin GLLEGYFVPLHNFYLTPEGFEQTVHNVAFSFELMQDGGLKKPKARPEDIVNLDLKSTLRV 353
Alpha-Parvin LYNLFTKYRSVE* 372
Beta-Parvin LYNLFTKYKHLD* 365
B.
Drosophila
B.Danio
B.Xenopus
B.Gallus
B.Homo
B.Mus
A.Danio
A.Xenopus
A.Gallus
A.Homo
A.Mus

and reveals that α-Parvin groups more closely to other α-Parvins than to β-Parvin (Figure 24B). Furthermore, both α-Parvin and β-Parvin group more closely to fish and avian orthologs than to mammalian orthologs. Based on new sequence data, primers were designed (refer to section 2.1.5) to amplify *alpha-parvin* from cDNA collected at various stages of *Xenopus laevis* development. *Alpha-parvin* is expressed as a maternal transcript, at stages 2 through 7, and continues to be expressed zygotically during gastrulation (stages 10 through 12), neurulation (stage 17), and organogenesis (stage 28) (Figure 25). *Alpha-parvin* expression appears elevated during the early stages of gastrulation (stage 10) and this is consistent with RNA-seq data (Session et al., 2016).

Table 10. Amino acid comparison of *Xenopus laevis* α-Parvin with known orthologs and *Xenopus laevis* β-Parvin

Percent identity (I) and similarity (S) with *Xenopus laevis* alpha-parvin (XP_018115789.1)	I (%)	S (%)
Homo sapiens (NM_018222.5)	94.1	97.9
Mus musculus (AF237774)	92.5	97.3
Gallus gallus (XM_025151217.1)	91.8	97.2
Danio rerio (NM_001002872.2)	87.6	95.9
Drosophila melanogaster (NM_134508.3)	56.4	83.3
Xenopus laevis β-Parvin (NP_001089519.1)	72.3	89.8

An amino acid sequence comparison of *Xenopus laevis* α-Parvin with orthologs from *Homo sapiens, Mus muculus, Gallus gallus, Danio rerio* and *Drosophila melanogaster* as well β-Parvin from *Xenopus laevis*. Genebank accession numbers are indicated in the brackets.

Figure 25. Temporal expression pattern of *alpha-parvin* during early *Xenopus laevis* development. RT-PCR was used to amplify endogenous *alpha-parvin* transcripts (1119bp) from cDNA isolated at the developmental stage indicated. Stages 2 and 5 (A) represent maternally derived transcripts and stages 10-28 (B) represent transcripts of zygotic origin. *Alpha-parvin* is expressed at all stages during early *Xenopus laevis* development. (L) 1Kb molecular weight ladder.

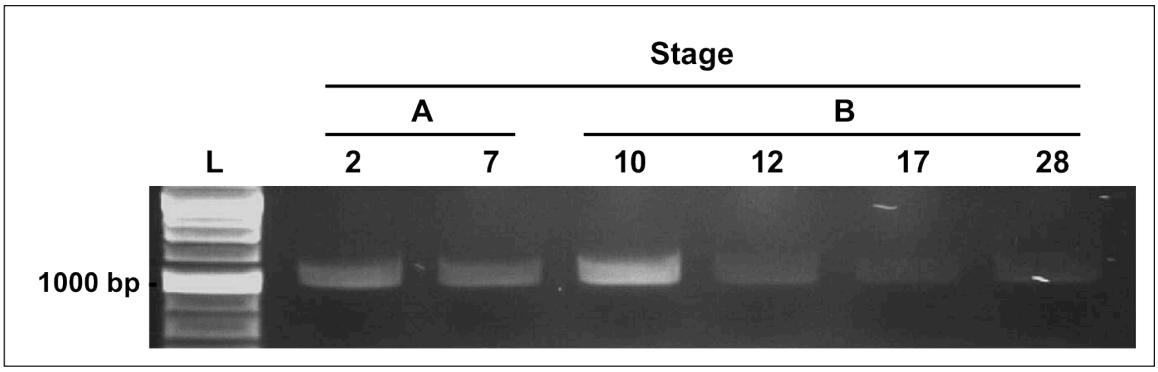
Stage
A
B
L
2
7
10
12
17
28
1000 bp

4.0 Discussion

The *Xenopus laevis* embryo provides a uniquely powerful and simple *in vivo* model to examine the modulation of integrin and cadherin function. Specifically, α5β1 integrin regulates a number of critical cell behaviours during gastrulation through interaction with the ECM protein FN. There are two distinct α5β1 dependent events: first, α5β1 assembles a FN matrix along the blastocoel roof and tissue boundaries (Lee et al., 1984). Second, cells use α5β1 to adhere to this FN matrix and transmit signals permissive for the cell rearrangements that drive gastrulation (Marsden and DeSimone, 2001). Blocking α5β1-FN ligation using function blocking antibodies or knocking down FN using morpholino oligonucleotides inhibits epiboly and CE during *Xenopus laevis* gastrulation (Marsden and DeSimone, 2001 and 2003; Davidson et al, 2006). Interestingly, sequestering molecules that interact with β1 integrin cytoplasmic tails also inhibits epiboly and CE (Marsden and DeSimone 2003). Therefore, signals emanating from both α5β1-FN ligation and β1 cytoplasmic tails are critical for the cell movements during gastrulation.

During the course of gastrulation, cadherin based adhesions are also regulated in a position specific manner. Cells in the BCR display higher C-cadherin mediated adhesion than cells in the post-involution mesoderm (Lee and Gumbiner, 1995). C-cadherin dependent adhesion is reduced in response to growth factor signaling as cells move through the Spemann organizer to the interior of the embryo (Reintsch and Hausen, 2001). It is also clear that there is interplay between integrin and cadherin receptors. α5β1 integrin dependent assembly of FN requires tissue tension created by the

modulation of cadherin adhesion (Dzamba et al, 2009). Reducing cadherin adhesion with a dominant negative construct does not inhibit α5β1-FN ligation but impairs FN assembly (Dzamba et al, 2009). Furthermore, integrin ligation modulates cadherin adhesion in post-involution mesoderm (Marsden and DeSimone 2003). Therefore, evidence suggests that integrins and cadherins functionally interact to co-ordinate cell movements, but the molecules responsible for this crosstalk are not as well defined.

4.1 Role of β-Parvin during *Xenopus laevis* gastrulation

β-Parvin is a scaffolding molecule that links the ECM to intracellular signaling pathways through β1 and β3 integrins (reviewed in Sepulveda and Wu, 2006). To fully ascertain the mechanisms of β-Parvin function, attempts were made to perform loss-of-function experiments using a morpholino oligonucleotide (MO). Since *Xenopus laevis* is tetraploid, the genome includes two copies of β-Parvin, β-Parvin (L) and β-Parvin (S), on chromosome 3 long and short arms respectively. A previously designed β-Parvin MO, designed to target β-Parvin (L) (β-Parvin MO1, Appendix A Figure A2A), failed to cause a defect when injected into embryos (Studholme, 2013). β-Parvin MO1 displayed poor binding kinetics and was the only MO we could design due to the limited amount of 5'untranslated region sequence data available. I designed a second MO (β-Parvin MO2, Appendix A Figure 2A) targeting the 5'UTR of β-Parvin (S). Injection of β-Parvin MO2 also failed to produce a defect in the embryo (Appendix A Figure A2B). Using RT-PCR it was determined that the β-Parvin (S) transcript only represents a small fraction of the total β-Parvin mRNA present in the embryo (Appendix A Figure A2C). Therefore, the β-Parvin (L) transcript is the only β-Parvin transcript expressed at a functional level in the

embryo. Given these findings, I attempted 5'RACE to determine the sequence of β-Parvin (L) 5'UTR, in an attempt to design an efficient and specific β-Parvin MO. A new protocol outlined in Appendix A, Figure A3 (Dallmeier and Neyts, 2012) and subsequent kit based protocols (Clontech SMART^{TM} RACE cDNA Amplification Kit and Sigma 5'/3' RACE Kit) were unsuccessful at amplifying the 5'UTR of β-Parvin (Stronks, 2017). The 5'end of β-Parvin's coding region contains many repetitive sequences and is GC rich, which may have been interfering with primer annealing during these protocols. As a result, the 5'UTR of β-Parvin was not isolated. In addition, genomic sequence data at the β-Parvin (L) 5'UTR locus is still incomplete suggesting that structurally this region of the genome is particularly hard to sequence. Therefore a method of performing loss-of-function experiments was not available.

Due to the inability to perform loss-of-function experiments using MOs I resorted to over-expression studies using β-Parvin domain deletion constructs. β-Parvin contains two tandem calponin homology (CH) domains: an N-terminal CH1 domain (RP1) and a C-terminal CH2 domain (RP2). Disruption of β-Parvin signaling in *Xenopus laevis* embryos produced gross morphological defects in gastrula stage embryos (Studholme, 2013), however the cell behaviors producing these defects were not examined. In the pre-involution DMZ, radially directed cell intercalations drive epiboly. At stage 10.5 cells in the deep layers of the pre-involution DMZ rapidly interdigitate, indicated by a change to a "sharks tooth" cell shape, undergo radial intercalations and result in the thinning of this tissue. Over-expression of RP1 and RP2 inhibit these cell shape changes and the DMZ fails to thin, indicating that there is a failure in epiboly

(Figure 7 and Figure 8). Previously it has been demonstrated that integrin signals emanating from α5β1 drive epiboly in the pre-involution DMZ (Marsden and DeSimone, 2001). Therefore it is likely that over-expression of the β-Parvin constructs is inhibiting α5β1 integrin mediated signals (Figure 4B).

In the post-involution mesoderm, mediolateral cell intercalations drive CE. At stage 10.5 cells in the post-involution DMZ elongate (increased length/width ratio), acquire polarized cell protrusions (Keller et al., 2000), and undergo medial-lateral cell intercalations to narrow and elongate this tissue. Over-expression of RP1 and RP2 inhibits the development of polarity in these cells and is reflected in a decreased length/width ratio (Figure 8 and 9). Therefore CE movements in RP1 and RP2 injected embryos failed to extend the anterior-posterior axis (Figure 8) of the embryo *in vivo,* resulting in shortened tadpoles (Studholme, 2013). The defects are similar to the phenotypes observed in embryos lacking a FN matrix (Marsden and DeSimone, 2001 and 2003). Indeed, while RP1 and RP2 over-expression inhibits FN matrix assembly, a mechanistic approach suggests they act through distinct mechanisms. RP2 inhibits α5β1-FN interactions resulting in a defective FN matrix. Similarly, inhibiting α5β1 integrin with function blocking antibodies, or knocking down FN with a MO also results in the loss of FN matrix as well as loss of polarized protrusions in post-involution mesoderm (Davidson et al, 2006). This suggests that RP2 may be inhibiting cell intercalation through the loss of interactions with FN and is supported by the observation that RP2 decreases the ability of embryonic cells to adhere to a FN substrate (discussed in section 4.2; Figure A4B). The molecular mechanism behind RP1

inhibition appears to be different as assessing CE movements in isolation with *ex vivo* animal cap explants demonstrated that RP1 over-expression permits CE in the absence of FN assembly (Studholme, 2013). Previous studies have shown that injecting embryos with a 70 kD N-terminal fragment of FN blocks FN assembly, but doesn't inhibit α5β1-FN ligation at the cell surface (Rozario et al., 2009). This demonstrated that fibrillar FN was required for epiboly, but was dispensable for medial-lateral cell intercalations of CE (Rozario et al., 2009). Considering α5β1-FN ligation would be functional in the presence of RP1, this would allow for cell intercalation *ex vivo*. Defects in the embryo caused by RP2 over-expression are likely the result of inhibiting α5β1-FN ligation, while RP1 may be disrupting intracellular signaling pathways emanating from α5β1 cytoplasmic tails. While this mechanistic approach reveals distinct roles for RP1 and RP2 in *ex vivo* explants, in intact embryos both constructs inhibit epiboly and CE suggesting architectural restraints play a significant role in gastrulation.

The experiments discussed above indicate that β-Parvin plays a role in the development of cell polarity. Cell polarity is a basic property of eukaryotic cells and is manifested in a multitude of cellular phenotypes. The development of anterior-posterior polarity is required for persistent, directed cell migration (reviewed in Campanale et al., 2017). Over-expression of RP2 affects the ability of embryonic cells to migrate on FN in response to Activin A (member of the TGF- β superfamily, Smith et al., 1990; Studholme, 2013). Ho and Dagnino (2012) have demonstrated that ILK is directly involved in epidermal growth factor (EGF) mediated cell polarization. As β-Parvin and ILK are obligate partners, and RP2 mediates the interaction between β-Parvin and xILK in

Xenopus laevis (discussed in section 4.3; Figure 10), it is possible that signaling pathways downstream of xILK-β-Parvin play a role in the development of cell polarization in response to growth factor signaling.

β-Parvin has been demonstrated to modulate the activation of Rho GTPases, RhoA and Rac, which are critical components in the development of cytoskeletal polarity that is essential for cell motility (Studholme, 2013; Campanale et al., 2017). The formation of a xILK-β-Parvin complex may serve as a hub to recruit Rho-GTPases and is a potential mechanism by which β-Parvin may modulate cell behaviours. How Rac and Rho are activated downstream of β-Parvin, in *Xenopus laevis*, remains to be determined, but studies in cell culture have demonstrated that the CH1 domain of β-Parvin interacts with α Pix, a guanine nucleotide exchange factor (GEF) that activates GTPases, at the leading edge of lamellipodia (Mishima et al, 2004).

4.2 β-Parvin compartmentalization correlates with cell behaviours

β-Parvin mRNA transcript has previously been shown to localize to tissues whose behavior is regulated by α5β1 integrin during *Xenopus laevis* gastrulation (Ramos et al., 1996; Studholme, 2013). The CH2 domain of β-Parvin (RP2) regulates subcellular compartmentalization of full-length β-Parvin and RP2 at sites of α5β1 integrin clustering during gastrulation (Figure 5). In support of this finding, previous *in vitro* studies have demonstrated that the CH2 domain of β-Parvin mediates its localization to integrin adhesion complexes known as focal adhesions (FA, Studholme, 2013; Olski et al., 2001; Yamaji et al., 2001). In addition to accumulating at FA's of well-spread cultured cells, β-Parvin also accumulates in membrane blebs present during the very early phase of cell

spreading. Other FA proteins such as focal adhesion kinase (FAK) and vinculin are absent during this stage of adhesion suggesting the possibility that β-Parvin is required early in FA formation (Yamaji et al., 2001). However, as described earlier this could be important in either an inside/out signal modulating α5β1-FN adhesion, or outside/in, propagating a post ligation signal. In cell adhesion assays over-expression of RP2 decreased the ability of embryonic cells to adhere to a FN substrate (the sole α5β1 ligand) in comparison to β-Parvin and RP1 over-expressing cells (Figure 4B). Yamaji et al. (2001) demonstrated that CH2 domain over-expression in Chinese hamster ovary (CHO) cells inhibits the formation of FAs and stress fibers. The initial phase in the spreading process was completely blocked in these cells. Since RP2 does not eliminate FN adhesion this indicates that β-Parvin likely plays a role in the maintenance of integrin adhesions.

As described earlier RP1 and RP2 do not act in the same manner to disrupt gastrulation. This is reflected in the compartmentalization of the constructs. While RP2 regulates recruitment to sites of α5β1 integrin accumulation, RP1 regulates the compartmentalization of β-Parvin at the cell periphery (Figure 5 and 6). This suggests a possible role in cell-cell interactions. This is supported by the observation that, β-Parvin was found to accumulate at nascent cell-cell adhesions in dissociated embryonic cells, although the molecular interactions mediating this recruitment have not been identified (Studholme, 2013). Significantly, ILK, a partner of β-Parvin, has been shown to localize to sites of cell-ECM adhesion as well as cell-cell adhesion. The domains of ILK responsible for this compartmentalization are distinct (Vespa et al., 2005) supporting a similar role for the above observation in β-Parvin.

The above observations suggest an interaction with C-cadherin exists during *Xenopus laevis* gastrulation. Over-expressing RP1 in embryonic cells significantly decreases adhesion to a cadherin substrate (FC-C-cadherin, Figure 4C) indicating a regulatory role for β-Parvin in cadherin adhesion. This role in cell-cell adhesion can further explain the observation that RP1 disrupts FN assembly. Assembly of FN along the BCR requires the modulation of cadherin adhesion, increasing tension across the BCR. Ectopic expression of cadherin in the BCR, leads to increased tissue tension leading to the precocious assembly of FN fibrils. Thus while FN assembly is a α5β1 dependent process it requires cadherin mediated tissue tension (Dzamba et al., 2009). My data suggest that over-expression of RP1 decreases cadherin adhesion and with a subsequent loss of tissue tension consequently inhibits the assembly of a FN matrix. This is supported by the observation that BCR cells show rounded profiles, indicative of low tissue tension (Figure 8 and 9). Combined, the evidence indicates that the defects in embryos over-expressing RP1 *in vivo* is due to reduced tissue tension due to altered cadherin adhesion.

4.3 Recruitment of β-Parvin to integrin adhesions

While the embryonic defects caused by β-Parvin deletion construct over-expression are well characterized the molecular mechanisms underlying these phenotypes and the compartmentalization of β-Parvin are not. My results demonstrate that the CH2 domain of *Xenopus laevis* β-Parvin mediates the interaction with xILK as full-length β-Parvin and RP2 are recruited to xILK (Figure 10). This is consistent with previous studies revealing that β-Parvin interacts with ILK through the CH2 domain in

cultured cell lines, at muscle adhesion sites (MAS) and wing epithelium in the developing *Drosophila* embryo (Yamaji et al. 2001; Chountala et al. 2012). In addition, my results suggest that the interaction between β-Parvin and xILK is dependent on the interaction of xILK with α5β1 integrin. In experiments using xILK constructs that have the integrin interaction domain deleted (xILK E359K, xILK ΔKIN, xILK ΔINT), there is a failure to recruit β-Parvin to xILK (Figure 11B-C). This suggests that the interaction between xILK and β-Parvin is driven at least in part through xILK- α5β1 interaction. This β-Parvin-xILK interaction is also dependent on outside/in signals resulting from α5β1-FN ligation. In dissociated embryonic cells, xILK is able to recruit β-Parvin when plated on FN, but not when plated on PLL (Figure 12). This shows a hierarchy of molecular recruitments where α5β1-FN ligation leads to the recruitment of xILK. Subsequently, α5β1 bound xILK recruits β-Parvin. This supports my conclusions in section 4.2 that β-Parvin signaling is down-stream of integrin ligation and likely plays a role in the maintenance of these adhesions. Interestingly, molecular differences in the assembly of integrin adhesion complexes have been demonstrated. In mammalian cell culture, the binding of β-Parvin to ILK precedes recruitment to adhesion sites (Zhang et al., 2002). During *Drosophila* development, ILK controls the stability and recruitment of parvin at muscle adhesion sites. However, like in mammalian cell culture, parvin and ILK are interdependent for complex assembly in the wing epithelium (Zhang et al., 2002; Vakaloglou et al., 2012). In *Xenopus laevis*, xILK appears to be playing the role of master regulator, as in *Drosophila* MAS, controlling the recruitment of β-Parvin to sites of adhesion. Furthermore, the IPP complex does not appear to exist during *Xenopus laevis*

gastrulation as co-immunoprecipitation experiments reveal β-Parvin is not found associated with PINCH (Appendix A, Figure A4). While I have described an integrin driven recruitment of β-Parvin in early embryos, the regulation of integrin adhesion is segregated spatially and temporally in the embryo, therefore the hierarchy of recruitment could also be tissue and stage dependent.

The results of RP1 and RP2 expression indicate a dynamic role for β-Parvin during gastrulation. In *Xenopus laevis* movement of cells through the Spemann organizer at the dorsal lip alters the properties of both integrin (Ramos et al., 1996) and cadherin (Brieher and Gumbiner, 1994) a process that can be mimicked *ex vivo* using Activin A. The ability of xILK to recruit β-Parvin is decreased in the presence of Activin A (Figure 13). This is coincident with dissociated embryonic cells acquiring a migratory phenotype in the presence of Activin A. The ability to migrate on FN is dependent on integrin-mediated recognition of the synergy site in FN and this lies downstream of Activin A signaling (Ramos et al, 1996; Ramos and DeSimone, 1996). Therefore, this suggests that as cells come under the influence of growth factors found in the Spemann organizer β-Parvin recruitment to xILK is altered and this may contribute to changes in integrin adhesion. Previous experiments demonstrated that the over-expression of RP2 inhibits the ability of embryonic cells to migrate on FN (Studholme, 2013) further supporting such a role for β-Parvin. Taken together, the normal function of β-Parvin is likely mediated by the CH2 domain binding to xILK and likely transmitting signals through the CH1 domain to downstream effector molecules. This suggests that while α5β1 integrin ligation recruits xILK and β-Parvin, the change in activation state and consequently the

recognition of the synergy site in FN is controlled by inside/out signaling that result in the release of β-Parvin complexes from the cytoplasmic tail. These inside/out signals stem from growth factor signaling, Activin A *ex vivo* and the growth factors secreted from the Spemann organizer *in vivo*.

4.4 Recruitment of β-Parvin to cadherin adhesions

Given the observation that RP1 was being compartmentalized to the cell periphery and not sites of integrin-mediated adhesion (Figure 5 and 6), and that over-expression of RP1 reduced adhesion of cells to a cadherin substrate (Figure 4C), I assessed the interaction of β-Parvin with C-cadherin during gastrulation. My results demonstrate that the CH1 domain of β-Parvin has the ability to interact with C-cadherin in *Xenopus laevis* (Figure 14). Full-length β-Parvin and RP1 were pulled down in a complex with endogenous C-cadherin, while RP2 was not (Figure 14). This is the first study showing a molecular link of β-Parvin to sites of cadherin adhesion. ILK has been reported to localize to sites of cell-cell adhesion in epidermal keratinocytes (Nakrieko et al, 2008). Therefore, I assessed the interaction of xILK with C-cadherin. xILK was not pulled down in a complex with C-cadherin (Figure 15) indicating that xILK does not link β-Parvin to sites of C-cadherin adhesion. Additionally, in embryos over-expressing full-length xILK or a xILK construct that cannot interact with β-Parvin (xILK E359K), β-Parvin was equally recruited to C-cadherin (Figure 16). Therefore the domains in β-Parvin responsible for association with C-cadherin are separate from those mediating association with xILK indicating the recruitment of β-Parvin to cadherin in *Xenopus laevis* is independent of xILK.

Significantly, the β-Parvin-C-cadherin interaction is increased in response to Activin A (Figure 17). C-cadherin dependent cell-cell adhesion decreases in response to cells passing through the Spemann organizer during involution (Lee and Gumbiner, 1995) and is also reduced in the presence of Activin A (Brieher and Gumbiner, 1994). Interestingly, the change in C-cadherin adhesive activity coincides with the change in integrin activity (Ramos et al., 1996), which appears to be regulated through the dissociation of β-Parvin and xILK (Figure 13). This brings up the possibility that β-Parvin moves from sites of α5β1 adhesion to sites of C-cadherin adhesion during involution.

4.5 β-Parvin interacts with β-catenin

Given that β-Parvin interacts with C-cadherin, I asked if this interaction was mediated through one of the catenins. β-Parvin and RP1 were pulled down in a complex with β-catenin from stage 12, embryo lysate (Figure 19). However, β-Parvin was not retrieved in a complex with Plakoglobin (PG, Figure 18). β-catenin and PG bind to the distal cytoplasmic tail of cadherins in a competitive manner and mediate an association between cadherins and the actin cytoskeleton, at adherens junctions (McCrea and Gottardi, 2015). PG also facilitates the association of cadherins with intermediate filaments at desmosomal junctions (Leonard et al, 2008). Given that there is no association with PG it is likely that, β-Parvin is found in adherens type junctions. Despite finding an interaction between B-catenin and β-Parvin, β-catenin is not required for the interaction between β-Parvin and C-cadherin (Figure 20B). In experiments using C-cadherin constructs that have the β-catenin binding domain deleted (ΔBCAT), β-Parvin was still recruited to C-cadherin (Figure 20B). However, in these experiments, much less

β-Parvin was recruited to C-cadherin in the absence of the β-catenin binding site. Furthermore, using a C-cadherin construct that increases interactions with β-catenin (ΔJMD) increased the amount of β-Parvin recruited to C-cadherin (Figure 20B-C). This suggests that β-catenin is involved in the interaction of β-Parvin with C-cadherin. It remains unclear if these results stems from an interaction with β-catenin or due to structural effects of the deletions. However, it is clear that β-catenin is not an obligate partner in the β-Parvin-cadherin interaction.

In addition to cell adhesion, β-catenin plays essential roles in Wnt-mediated transcriptional activation by interacting with DNA binding factor, T-cell factor (TCF, reviewed in McEwen et al., 2012). When over-expressed, C-cadherin acts as a stoichiometric inhibitor of β-catenin transcriptional signaling, suggesting that cadherins antagonize β-catenin mediated transcription during *Xenopus laevis* development by sequestering the cytosolic β-catenin pool to the membrane (Fagotto et al, 1996). Interestingly, I revealed that β-catenin can exist in populations that distinguish between C-cadherin and xTCF during *Xenopus laevis* gastrulation (Figure 21). In sequential pull-down assays, β-catenin was recruited to xTCF in lysate cleared of the C-cadherin interacting pool of β-catenin (Figure 21). This suggests that the cell adhesion and transcriptional populations of β-catenin are biochemically separated during *Xenopus laevis* gastrulation. Given that β-Parvin interacts with β-catenin protein complexes, I asked whether β-Parvin displayed preferential association to the C-cadherin or xTCF selective population. In sequential pull-down experiments, β-Parvin was found to interact with both C-cadherin and xTCF, suggesting that β-Parvin can interact with both

populations of β-catenin (Figure 22). In enteroendocrine L cells, two biochemically distinct populations of β-catenin have been demonstrated by sequential pull-down analysis (Gottardi and Gumbiner, 2004). However, E-cadherin phosphorylation permits the binding of β-catenin that was previously TCF selective to cadherin. This suggests that the β-catenin pools are distinguished by the biochemical form of β-catenin itself and conformational changes in the ligand. As β-Parvin does not distinguish distinct β-catenin populations it would be interesting to determine if a similar ligand driven segregation of β-catenin exists in *Xenopus laevis*.

The interaction of β-Parvin and β-catenin suggests a possible role for β-Parvin in regulating gene expression. The RP1 construct contains two NLS, possibly regulating the nuclear trafficking of β-Parvin. When over-expressed in embryos RP1 displays a relative decrease in nuclear localization compared to RP2 and full-length β-Parvin (Figure 5 and 6). In this case the NLS appears to be required for the nuclear exclusion of β-Parvin. While the regulation of β-Parvin nucleo-cytoplasmic shuttling has not been examined, the nuclear localization of β-Parvin has been acknowledged in cell culture (Johnstone, et al., 2008). Interestingly, the β-Parvin partner in integrin adhesion, ILK, is actively transported into the nucleus (Nakrieko et al, 2008). Therefore, another possibility for the differences in nuclear localization could be the interaction of β-Parvin with xILK. Given that β-Parvin interacts with the transcriptional populations of β-catenin, and displays regulated nuclear localization, this suggests a potential nuclear role for β-Parvin.

4.6 α-Parvin is expressed during early *Xenopus laevis* development

I have performed a preliminary examination of *Xenopus laevis* α-Parvin (α-Parvin) amino acid sequence and initial analysis of α-Parvin transcript expression during early *Xenopus laevis* development. Previous studies characterizing the structure and function of α-Parvin have been primarily examined in mammalian cell lines (Olski et al., 2001; Zhang et al., 2005; Yang et al., 2005; Wang et al., 2008; Montanez et al., 2009; Pignatelli et al., 2012). Due to incomplete genomic sequence data it was previously believed that α-Parvin was not present in amphibians and birds. At the time, it was thought that α-Parvin was either functionally deleted or never arose in the genome through duplication (Studholme, 2013). Recently, sequence data has become available, from Xenbase (J-strain v9.1) that reveals a α-Parvin ortholog.

Analysis of *Xenopus laevis* α-Parvin amino acid sequence determined that it shared the greatest identity to human α-Parvin at 94.1% while identity to *Drosophila* showed the greatest divergence at 56.4% identity (Table 12). Furthermore, the high similarity between α-Parvin amino acid sequences suggests that the overall structure of the protein is well conserved across species (Table 12). Additionally, a comparison between mammalian α-Parvin and *Xenopus laevis* α-Parvin revealed 100% shared identity in residues that have been identified as nuclear localization signals, although a function in the nucleus has not been defined (Figure 23). Given the observation that the NLS in β-Parvin appears to be required for the nuclear exclusion of β-Parvin (Figure 5 and 6), it is possible that the subcellular localization of α-Parvin is regulated in a similar manner. Interestingly, α-Parvin displays greater conservation across metazoans than β-

Parvin. *Xenopus laevis* β-Parvin shares the greatest identity with human β-Parvin at 88% and greatest divergence with *Danio rerio* at 76% (Studholme, 2013). The higher conservation of α-Parvin across species suggests the function of α-Parvin across species is likely more restricted.

Consistent with findings for β-Parvin (Studholme, 2013), phylogenetic analysis reveals that α-Parvin groups more closely to fish and avian orthologs than to mammalian orthologs indicating that the evolution of α and β-parvin across species has taken a similar route. However, β-Parvin groups more closely to the lone *Drosophila melanogaster* Parvin homolog, suggesting that β-Parvin most likely represents the ancestral parvin gene (Figure 24B). Analysis of *Xenopus laevis* α-Parvin and β-Parvin amino acid sequences determined that they shared 72.3% identity and 89.8% similarity (Table 10). Significantly, the sequences display 90% identity within the CH2 domain that mediates the interaction with xILK (Figure 24A). Since previous studies have demonstrated that α and β-parvin form mutually exclusive complexes with ILK, it suggests that they may competitively bind xILK during *Xenopus laevis* gastrulation (Zhang et al., 2004). Taken together, the high interspecies amino acid sequence conservation of *Xenopus laevis* α-Parvin suggests the function may also be conserved among species.

During early *Xenopus laevis* development, *α-parvin* is expressed as a maternal transcript, through early cleavage (stage 2-7). Following the mid-blastula transition, *α-parvin* is zygotically transcribed during gastrulation (stage 10-12), neurulation (stage 17) and organogenesis (stage 28, Figure 25). Interestingly, *α-parvin* expression appears

elevated during the early stage of gastrulation (stage 10) suggesting a possible role during this period. This result is consistent with *α-parvin* RNA-seq data (Session et al., 2016), however a more quantitative analysis of *α-parvin* transcript levels will need to be conducted.

4.7 Conclusions

The present study has for the first time described the molecular mechanisms governing the function of β-Parvin in integrin-cadherin receptor crosstalk during *Xenopus laevis* gastrulation. This was accomplished using domain deletion over-expression since a method of gene knockdown was not available. Although potential neomorphic effects are a possibility with over-expression studies, CH1 and CH2 domain over-expression phenotypes suggest binary roles with opposite effects on cell behaviours and signaling. In addition, the over-expression of full-length β-Parvin had little effect on *Xenopus laevis* development (Studholme, 2013). Furthermore, a gene that causes an over-expression phenotype may not produce a knockdown phenotype due to functional redundancy of a related protein. Given the identification of α-Parvin, it is possible that the knockdown of β-Parvin may have been compensated by the functional redundancy of α-Parvin (Pitter et al., 2018). In this case, over-expression studies can provide functional insight, while knockdown cannot (reviewed in Prelich, 2012).

The CH1 and CH2 domains of β-Parvin mediate distinct inter-molecular interactions contributing to integrin-cadherin crosstalk. The CH1 domain mediates the interaction of β-Parvin at sites of C-cadherin adhesion, while the CH2 domain mediates

the interaction of β-Parvin at sites of α5β1 integrin adhesion. Additionally, TGF- β signaling influences the association of β-Parvin with these adhesion molecules.

β-Parvin is essential for the establishment of cell polarity and the regulation of integrin and cadherin adhesion during *Xenopus laevis* gastrulation. Figure 26 shows a proposed model of β-Parvin function. During the early stages of gastrulation, β-Parvin interacts with xILK downstream of FN ligation (Figure 26A). The CH2 domain of β-Parvin mediates this interaction. As cells pass through the Spemann organizer and move to the interior of the embryo, growth factor signaling causes a decrease in β-Parvin-xILK association and an increase in the interaction between β-Parvin and C-cadherin (Figure 26B). The CH1 domain of β-Parvin mediates the interaction with C-cadherin. Here, β-catenin stabilizes the interaction of β-Parvin with C-cadherin. In addition, the nuclear transport of β-Parvin appears to be regulated by the NLS within RP1. Combined with the observation that β-Parvin can also interact with the xTCF-selective population of β-catenin, these data suggest that β-Parvin may regulate gene expression (Figure 26C).

In addition to examining the molecular mechanism of β-Parvin function, I have provided the first preliminary study on α-Parvin in *Xenopus laevis*. *Alpha-parvin* is expressed throughout early *Xenopus laevis* development and the high conservation across species suggests the function may also be conserved.

4.8 Future directions

Given the results described in this thesis, future studies could examine a number of roles for β-Parvin in more detail. One of the interesting findings is the requirement of FN ligation (outside/in signal) for the recruitment β-Parvin to xILK. Performing Co-IP

Figure 26. Proposed model of β-Parvin function during *Xenopus laevis* gastrulation. A) In the BCR during the early stage of gastrulation, integrin-FN ligation recruits xILK-β-Parvin protein complexes to α5β1 tails. B) As cells migrate around the dorsal lip, they pass the Spemann organizer and growth factor signals result in the release of β-Parvin from xILK and increases the recruitment of β-Parvin to C-cadherin. β-catenin is involved but not required for the interaction of β-Parvin and C-cadherin. C) β-Parvin also interacts with the xTCF selective pool of β-catenin. The observation that β-Parvin nuclear translocation is regulated suggests that β-Parvin may regulate gene transcription.

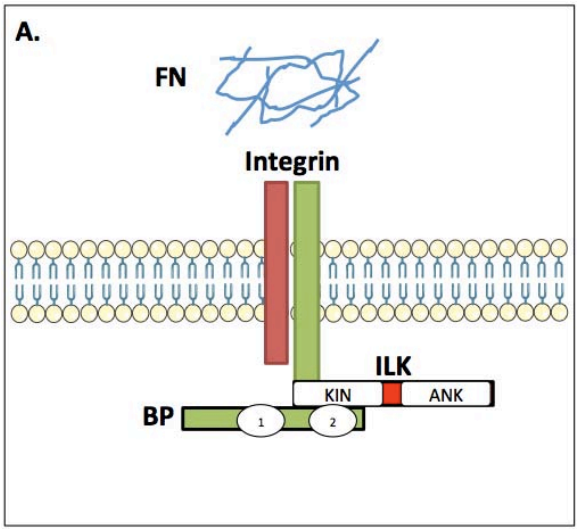
A.
FN
Integrin
ILK
KIN
ANK
BP
1
2

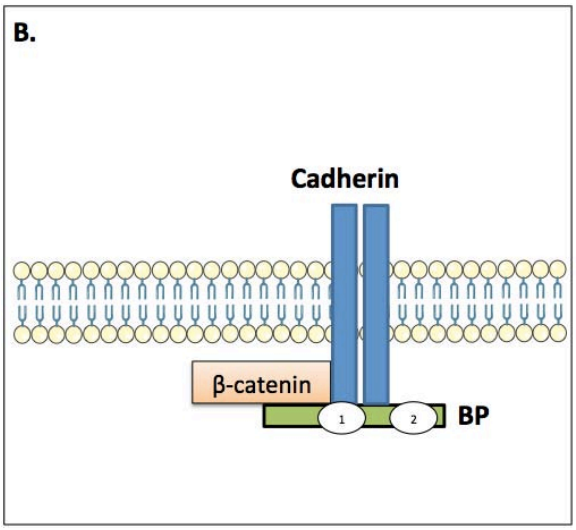
B.
Cadherin
β-catenin
1
2
BP

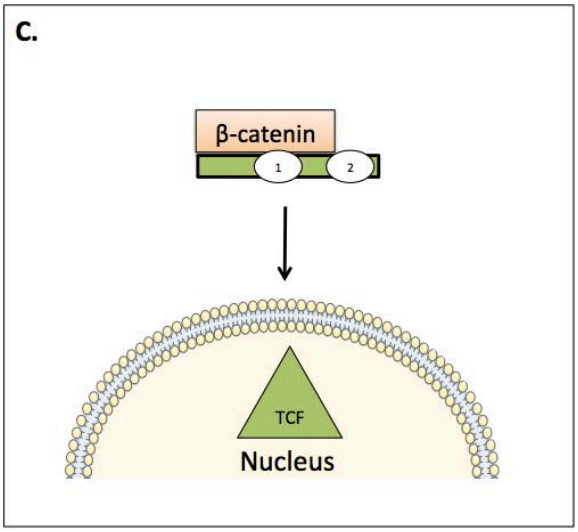
C.
β-catenin
1
2
TCF
Nucleus

experiments using dissociated embryonic cells plated on a FN or PLL substrate are technically difficult to perform. Therefore, it would be useful to repeat these experiments using embryos injected with a FN MO or function blocking antibodies, that block α5β1-FN interactions, to confirm the requirement of an outside/in signal in the formation of a β-Parvin-xILK complex.

My results in section 3.2 demonstrate that the nuclear localization of β-Parvin is regulated by sequences located in the amino terminus of β-Parvin. It is expected that the two NLS within this region are responsible. In addition, β-Parvin was found to interact with both the C-cadherin and xTCF-selective pool of β-catenin (refer to section 3.10). Together, these data suggest that β-Parvin may play a functional role in the nucleus. Future studies examining the co-localization of β-Parvin and β-catenin in the nucleus using FRET and performing ChIP and RT-PCR analysis to examine the regulation of β-catenin target genes during gastrulation may shed light on this question. A GFP tagged β-Parvin ΔNLS deletion construct has been subcloned and will be used to determine the requirement of these sites for the nuclear transport of β-Parvin. Furthermore, it would be worth determining the region of β-catenin that mediates the interaction with β-Parvin using Co-IP experiments.

This study also demonstrated that Activin A signaling modulates the recruitment of β-Parvin to xILK and C-cadherin (Figure 26), suggesting the possibility that β-Parvin moves from sites of α5β1 adhesion to sites of C-cadherin adhesion during gastrulation. It has been previously demonstrated that the recruitment of PG to C-cadherin in post-involution mesendoderm requires the application of force (Weber et al., 2012). PG then

recruits keratin intermediate filaments to establish directed protrusive behaviour required for cell migration. It would be worth examining whether a similar situation occurs during the recruitment of β-Parvin to C-cadherin in post-involution mesoderm.

Given the identification of *Xenopus laevis* α-Parvin, it will be important that future studies examine the role of α-Parvin during gastrulation and dissect the interplay with β-Parvin to gain a better understanding of how parvin regulates cell adhesion. Determining the spatial expression pattern of *α-parvin* during *Xenopus laevis* development relative to *β-parvin* would help predict functional interplay. Since the CH domains are well conserved between α and β-Parvin, over-expression studies to examine the function of each CH domain would complement β-Parvin findings. Since β-Parvin regulates integrin and cadherin based adhesions (Figure 4), the requirement of α-Parvin at these adhesion complexes and the intermolecular interactions with known β-Parvin binding partners such as ILK, C-cadherin and β-catenin should be determined. Previously, α and β-Parvin have been described to compete for binding with ILK in cell culture (Zhang et al., 2004). Determining if a similar scenario exists in *Xenopus laevis* and whether these interactions are functionally antagonistic will be important. Additionally, the 5'UTR of *α-parvin* is much more complete (273 base pairs, Appendix A Figure A5) than β-Parvin, making designing a MO that efficiently and specifically knocks down α-Parvin expression a possibility. Conducting both over-expression and knockdown studies of α-Parvin would further elucidate the mechanism of α-Parvin and β-Parvin function.

References

Alfandari, D., Whittaker, C. A., DeSimone, D. W., and Darribere, T. 1995. Integrin aV subunit is expressed on mesodermal cell surfaces during amphibian gastrulation. *Dev. Bio.* 170, 249-61

Boulter, E., and Obberghen-Schilling, E. V. 2006. Integrin-linked kinase and its partners: a modular platform regulating cell-matrix adhesion dynamics and cytoskeletal organization. *European J. of Cell Bio.* 85, 255-63.

Brieher, W. M., and Gumbiner, B. 1994. Regulation of C-cadherin function during activin induced morphogenesis of Xenopus laevis animal caps. *J. Cell Biol.* 126, 519-27.

Bjerke, M. A., Dzamba, B. J., Wang, C., and DeSimone, D. W. 2014. FAK is required for tension-dependent organization of collective cell movements in Xenopus laevis mesendoderm. *Dev. Biol*. 394, 340-56.

Bouvard, D., Pouwels, J., DeFranceschi, N., Ivaska, J. 2013. Integrin Inactivators: balancing cellular functions *in vitro* and *in vivo*. *Nature*. 14, 430-442.

Chomczynski, P., and Sacchi, N. 1987. Single-Step Method of RNA Isolation by Acid Guanidinium Thiocyanate-Phenol-Chloroform Extraction. *Analytical Biochemistry*. 162, 156-159.

Chountala, M., Vakaloglou, K. M., and Zervas, C. G. 2012. Parvin over-expression uncovers tissue-specific genetic pathways and disrupts F-actin to induce apoptosis in the developing epithelia in *Drosophila*. *Plos one.* 7, e47355.

Clarke, D. M., Brown, M. C, Lalonde, D.P., and Turner, C. E. 2004. Phosphorylation of actopaxin regulates cell spreading and migration. *J. Cell. Biol*.166, 901-12.

Dagnino, L. 2011. Integrin-linked kinase: a scaffold protein unique among its ilk. *J. Cell. Commun. Signal*. 5, 81-83.

Dallmeier, K., and Neyts, J. 2012. Simple and inexpensive three-step amplification of cDNA 5' ends using 5' phosphorylated primers. *Analytical Biochemistry*. 432, 1-3.

Davidson, L. A., Marsden, M., Keller, R., and DeSimone, D. W. 2006. Integrin $\alpha 5\beta 1$ and fibronectin regulate polarized cell protrusions required for *Xenopus laevis* convergence and extension. *Current Biology*. 16, 833-44.

Dzamba, B. J., Jakab, K. R., Marsden, M., Schwartz, M. A., and DeSimone, D. W. 2009. Cadherin adhesion, tissue tension, and noncanonical Wnt signaling regulate fibronectin matrix organization. *Developmental Cell.* 16, 421-432.

Evren, S. 2010. EphA4 Receptor Tyrosine Kinase and PAK1 Signaling: Novel Regulators of Xenopus laevis Brachyury Expression and Involution Movements During Gastrulation. MSc. Thesis.

Fagotto, F., Funayama, N., and Gumbiner, B, M. 1996. Binding to cadherins antagonizes the signaling activity of beta-catenin during axis formation in Xenopus laevis. *J. Cell Biol.* 132, 1105.

Fagotto, F. 2013. Looking beyond the Wnt pathway for the deep nature of β-catenin. *EMBO Rep*. 14, 422-33

Fagotto, F. 2014. The cellular basis of tissue separation. *Development*. 141: 3303-3318.

Gioma, M., Djinovic-Carugo, K., Kranewitter, W. J., and Winder, S.J. 2002. Functional plasticity of CH domains. *FEBS Letters.* 513, 98-106.

Gottardi, C, J., and Gumbiner, B, M. 2001. Adhesion signaling: how β-catenin interacts with its partners. *Curr. Biol.* 11, 792-4.

Gottardi, C, J., and Gumbiner, B, M. 2004. Distinct molecular forms of β-catenin are targeted to adhesive or transcriptional complexes. *J Cell Biol.* 167, 339-349.

Gumbiner, B. 2000. Regulation of Cadherin Adhesive Activity. *Journal of Cell Biology*. 148: 399-403.

Gumbiner, B. 2005. Regulation of Cadherin-Mediated Adhesion in Morphogenesis. *Nature*. 6: 622-634.

Hannigan, G. E., Leung-Hagesteijn, C., Fitz-Gibbon, L., Coppolino, M. G., Radeva, G., Filmus, J., Bell, J. C., and Dedhar, S. 1996. Regulation of cell adhesion and anchorage-dependent growth by a new beta 1-integrin-linked protein kinase. *Nature*. 379, 91-96.

Hardin, J. D. and Keller, R. 1988. The role of bottle cells in gastrulation of Xenopus laevis. *Development*. 103, 210–230.

Ho, E., and Dagnino, L. 2012. Epidermal growth factor induction of front-rear polarity and migration in keratinocytes is mediated by integrin-linked kinase and ELMO2. *Molecular Biology of the Cell.* 23, 492-502.

Hoffstrom, B. G. 2002. Integrin function during Xenopus laevis gastrulation. *Thesis*. Univeristy of Virginia.

Howard, S., Deroo, T., Fujita, Y., and Itaski, N. 2011. A Positive Role of Cadherin in Wnt/β-Catenin Signaling during Epithelial-Mesenchymal Transition. *Plos One*. 6, e23899.

Hynes, R. O., and Zhao, Q. 2000. The evolution of cell adhesion. *J. of Cell Bio*. 150, F89.

Hynes, R. O. 2002. Integrins: Bidirectional, allosteric signaling machines. *Cell.* 110, 673-87.

Johnstone, C. N., Mongroo, P. S., Rich, A. S., Schupp, M., Bowser, M. J., deLemons, A. S., Tobias, J. W., Liu, Y., Hannigan, G. E., and Rustgi, A. K. 2008. Parvin- β inhibits breast cancer tumorigenicity and promotes CDK9-mediated peroxisome proliferator-activated receptor gamma 1 phosphorylation. *Mol. and Cell Bio.* 28, 687-704.

Joos, T. O., Whittaker, C. A., Meng, F., DeSimone, D. W., Gnau, V., and Hausen, P. 1995. Integrin alpha 5 during early development of *Xenopus laevis. Mech. Dev*. 50, 187-99.

Joos, T. O., Reintsch, W. E., Brinker, A., Klein, C., and Hausen, P. 1998. Cloning of Xenopus laevis integrin alpha(v) subunit and analysis of its disruption during early development*. Int. J. Dev. Bio.* 42, 171-79.

Keller, R. 1978. Time-lapse cinemicrographic analysis of superficial cell behavior during and prior to gastrulation in *Xenopus laevis*. *J. Morphol*. 157, 223-48.

Keller, R. 1980. The cellular basis of epiboly: an SEM study of deep cell re-arrangement during gastrulation in Xenopus laevis. *J. Embryol. Exp. Morphol.* 157, 223-47.

Keller, R., Davidson, L., Edlund, A., Elul, T., Ezin, M., Shook, D., and Skoglund, P. 2000. Mechanisms of convergence and extension by cell intercalation. *Phil. Trans. R. Soc. Lond. B*. 355, 897-922.

Keller, R., Davidson, D. A., and Shook, D. R. 2003. How we are shaped: The biomechanics of gastrulation. *Differentiation.* 71, 171-205.

Keller, R., Shih, J., and Domingo, C. 1992. The patterning and functioning of protrusive activity during convergence and extension of the *Xenopus laevis* organizer. *Dev. Suppl*. 81-91.

Lee, G., Hynes, R., and Kirschner, M. 1984. Temporal and spatial regulation of fibronectin in early *Xenopus laevis* development. *Cell*. 36, 729-40.

Lee, C., and Gumbiner, B. 1995. Disruption of Gastrulation movements on Xenopus laevis by a Dominant Negative Mutant for C-Cadherin. *Developmental Biology*. 171: 363-373.

Legate, K. R., Montanez, E., Kudlacek, O., and Fassler, R. 2006. ILK, PINCH, and parvin: the tIPP of integrin signaling. *Nat. Rev. Mol. Cell. Biol*. 1, 20-31.

Leonard, M., Chan, Y., and Menko, A. S. 2008. Identification of a novel intermediate filament-linked N-cadherin/γ-catenin complex involved in the establishment of the cytoarchitecture of differentiated lens fiber cells. *Dev. Biol*. 319, 298-308.

Levi, G., Ginsberg, D., Girault, J. M., Sabanay, I., Thiery, J. P and Geiger, B. 1991. EP-cadherin in muscles and epithelia of *Xenopus laevis* embryos. *Dev*. 113, 1335-44.

Marsden, M., and DeSimone, D. W. 2001. Regulation of cell polarity, radial intercalation and epiboly in Xenopus laevis: novel roles for integrin and fibronectin. *Development*. 128, 3635-3647.

Marsden, M., and DeSimone, D.W. 2003. Integrin-ECM interactions regulate cadherin-dependent cell adhesion and are required for convergent extension in *Xenopus. Curr. Biol.* 13, 1182-91.

McCrea, P. D., and Gottardi, C. J. 2015. Beyond β-catenin: prospects for a larger catenin network in the nucleus. *Nature Reviews: Molecular Cell Biology.* 17, 55-64.

McCrea, P. D., Maher, M. T., and Gottardi, C. J. 2015. Nuclear signaling from cadherin adhesion complexes. *Curr. Top Dev. Biol.* 112, 129-96.

McEwen, A. E., Escobar, D. E., and Gottardi, C. 2012. Signaling from Adherens Junction. *Subcell Biochem*. 60, 171-196.

Mishima, W., Suzuki, A., Yamaji, S., Yoshimi, R., Ueda, A., Kaneko, T., Tanaka, J., Miwa, Y., Ohno, S., and Ishigatsubo, Y. 2004. The first CH domain of affixin activates Cdc42 and Rac1 through alphaPIX, a Cdc42/Rac1-specific guanine nucleotide exchange factor. *Genes Cells.* 9, 193-204.

Montanez, E., Wickstrom, S. A., Altstatter, J., Chu, H., and Fassler, R. 2009. α-parvin controls vascular mural cell recruitment to vessel wall by regulating RhoA/ROCK signaling. *The EMBO Journal*. 28, 3132-44.

Mui, K. L., Chen, C. S., and Assoian, R. K. 2016. The mechanical regulation of integrin-cadherin crosstalk organizes cells, signaling and forces. *J. Cell Sci.* 129, 1093-1100.

Na, J., Marsden, M., and DeSimone, D.W. 2003. Differential regulation of cell adhesive functions by integrin α subunit cytoplasmic tails *in vivo. J. of Cell Sci*. 116, 2333-43.

Nagel, M., and Winklbauer, R. 2018. PDGF-A suppresses contact inhibition during

directional collective cell migration. Dev. 145, dev162651.

Nakrieko, K., Vespa, A., Mason, D., Irvine, T. S., D'Souza, S. J. A., and Dagnino, L. 2008a. Modulation of integrin-linked kinase nucleo-cytoplasmic shuttling by ILKAP and CRM1. *Cell Cycle*. 7 (14), 2157-66.

Nakrieko, K., Welch, I., Dupuis, H., Bryce, D., Pajak, A., St. Arnaud, R., Dedhar, S., D'Souza, S. J A., and Dagnino, L. 2008b. Impaired hair follicle morphogenesis and polarized keratinocyte movement upon conditional inactivation of integrin-linked kinase in the epidermis. *Mol. Bio. Cell.* 19, 1462-73.

Nanadasa, S., Tao, Q., Menon, N. R., Heasman, J., and Wylie, C. 2009. N- and E-cadherins in Xenopus laevis are specifically required in the neural and non-neural ectoderm, respectively, for F-actin assembly and morphogenic movements. *Dev*. 136, 1327-38.

Nikolopoulos, S.N., and Turner, C.E. 2000. Actopaxin, a new focal adhesion protein that binds paxillin LD motifs and actin and regulates cell adhesion. *J. Cell Biol*. 151, 1435-48.

Ninomiya, H., David, R., Damm, E.W., Fagotto, F., Niessen, C., and Winklbauer, R. 2012. Cadherin-dependent differential cell adhesion in *Xenopus laevis* causes cell sorting *in vitro* but not in the embryo. *J. Cell. Sci.* 125, 1877-83.

Novak, A., Hsu, S. C., Leung-Hagesteijn, C., Radeva, G., Papkoff, J., Montesano, R., Roskelley, C., Grosschedl, R., and Dedhar, S. 1998. Call adhesion and the integrin-linked kinase regulate the LEF-1 and beta-catenin signaling pathways. *Proc Natl Acad Sci USA.* 95 (8), 4374-9.

Olski, T. M., Noegel, A. A., and Korenbaum, E. 2001. Parvin, a 42 kDa focal adhesion protein, related to the alpha-actinin superfamily. *J. Cell. Sci*. 114, 525-38.

Parsons, J., Horwitz, A. R., and Schwartz, M. 2010. Cell Adhesion: Integrating cytoskeletal dynamics and cellular tension. *Nature*. 11, 633-43.

Pignatelli, J., LaLonde, S. E., LaLonde, D.P., Clarke, D., and Turner, C.E. 2012. Actopaxin (α-parvin) phosphorylation is required for matrix degradation and cancer cell invasion. *J. Biol. Chem*. 287, 37309-20.

Pitter, B., Werner, A. C., and Montanez, E. 2018. Parvins are required for endothelial cell-cell junctions and cell polarity during embryonic blood vessel formation. *Atheroscler Thromb Vasc Biol.* 38, 1147-1158.

Prelich, G. 2012. Gene Overexpression: Uses, Mechanisms and Interpretation. *Genetics. 190*, 841 – 845.

Rantala, J., Pouwels, J., Pellinen, T., Veltel, S., Laasola, P., Mattila, E., Potter, C. S., Duffy, T., Sundberg, J. P., Kallioniemi, O., Askari, J. A., Humphries, M. J., Parsons, M., Salmi, M., and Ivaska, J. 2011. SHARPIN is an endogenous inhibitor of β1-integrin activation. *Nature Cell Biology*. 13 (11): 1315-1325.

Ramos, J. W., Whittaker, C. A., and DeSimone, D. W. 1996. Integrin-dependent adhesive activity is spatially controlled by inductive signals at gastrulation. *Dev*. 122, 2873-83.

Ramos, J. W., and DeSimone, D. W. 1996. *Xenopus laevis* embryonic cell adhesion to fibronectin: position-specific activation of RGD/synergy site-dependent migratory behavior at gastrulation. *J. Cell Biol*. 134, 227-40.

Reintsch, W. E., and Hausen, P. 2001. Dorsoventral differences in cell-cell interactions modulate the motile behaviour of cells from the *Xenopus laevis* gastrula. *Dev. Biol.* 240, 387-403.

Rohani, N., Canty, L., Luu, O., Fagotto, F., Winklbauer, R. 2011. EphrinB/EphB Signaling Controls Embryonic Germ Layer Separation by Contact-Induced Cell Detachment. *PLOS Biology*. 9 (3), e1000597.

Rohani, N., Parmeggiani, A., Winklbauer, R., and Fagotto, F. 2014. Variable Combinations of Specific Ephrin Ligand/Eph Receptor Pairs Control Embryonic Tissue Separation. *PLOS Biology*. 12 (9), e1001955.

Rozario, T., Dzamba, B., Weber, G. F., Davidson, L. A., and DeSimone, D. W. 2009. The physical state of fibronectin matrix differentially regulates morphogenetic movements *in vivo*. *Dev. Biol.* 15, 386-98.

Rozario, T., and DeSimone, D. W. 2010. The extracellular matrix in development and morphogenesis: a dynamic view. *Dev. Biol.* 341, 126-40.

Sambrook, J., and Russell, D. W. 2006. Inverse PCR. *Cold Spring Harb. Protoc.* doi:10.1101/pdb.prot3487.

Shattil, S., Kim, C., and Ginsberg, M. 2010. The final steps of integrin activation: the end game. *Nature*. 11, 288-300.

Sepulveda, J. L., and Wu, C. 2006. The parvins. *Cell. Mol. Life* 63, 25-35

Session, A., et al. 2016. Genome evolution in the allotetraploid frog *Xenopus laevis*. *Nature*. 538, 336-343.

Smith, J. C., Price, B. M., Van Nimmen, K., and Huylebroeck, D. 1990. Identification of a potent Xenopus laevis mesoderm-inducing factor as a homolog of Activin A. *Nature*.

345, 729-731.

Stronks, K. 2017. Using 5'RACE to isolate the 5'untranslated region of β-parvin. *Undergraduate 499 Thesis. University of Waterloo.*

Studholme, C. 2013. β-parvin Mediates Adhesion Receptor Cross-Talk During *Xenopus laevis* Gastrulation. *PhD Thesis. University of Waterloo.*

Szabo, A., Cobo, I., Omara, S., McLachlan, S., Keller, R., and Mayor R. 2016. The molecular basis of radial intercalation during tissue spreading in early development. *Dev. Cell*. 37, 213-225.

Tada, M., and Heisenberg, C-. P. 2012. Convergent extension: using collective cell migration and cell intercalation to shape embryos. *Dev*. 139, 3897-3904.

Tu, Y., Huang, Y., Zhang, Y., Hua, Y.. and Wu, C. 2001. A new focal adhesion protein that interacts with integrin-linked kinase and regulates cell adhesion and spreading. *The Journal of Cell Biology.* 153 (3), 585-598.

Vakaloglou, K. M., Chountala, M. and Zervas, C. G. 2012. Functional analysis of parvin and different modes of IPP-complex assembly at integrin sites during *Drosophila* development. *J Cell Sci.* 125, 3221-32.

Vespa, A., D'Souza, S., and Dagnino, L. 2005. A novel role for integrin-linked kinase in epithelial sheet morphogenesis. *Molecular Biology of the Cell*. 16, 4084-4095.

Wang, X., Fukuda, K., Byeon, I., Velyvis, A., Wu, C., Gronenborn, A., and Qin, J. 2008. The Structure of α-Parvin CH2-Paxillin LD1 Complex Reveals a Novel Modular Recognition for Focal Adhesion Assembly. *J. Biol. Chem.* 283 (30), 21113-9.

Weber, G. F., Bjerke, M. A., DeSimone, D. W. 2011. Integrins and cadherins join forces to form adhesive networks. *J. Cell Sci.* 124, 1183-1193.

Weber, G, F., Bjerke, M, A., and DeSimone, D, W. 2012. A mechano-responsive cadherin-keratin complex directs polarized protrusive behaviour and collective cell migration. *Dev. Cell.* 22, 104-115

Winklbauer, R. 1998. Conditions for fibronectin fibril formation in the early *Xenopus laevis* embryo. *Dev. Dyn*. 212, 335-45.

Winklbauer, R. and Schürfeld, M. 1999. Vegetal rotation, a new gastrulation movement involved in the internalization of the mesoderm and endoderm in Xenopus laevis. *Development*. 126, 3703– 3713.

Wolfenson, H., Lavelin, I., and Geiger, B. 2013. Dynamic Regulation of the Structure and Functions of Integrin Adhesions. *Developmental Cell*. 24: 447-458.

Wu, C., Keightley, S. Y., Leung-Hagesteijn, C., Radeva, G., Coppolino M., Goicoechea, S., McDonald J. A., and Dedhar, S. 1998. Integrin-linked protein kinase regulates fibronectin matrix assembly, E-cadherin expression, and tumorigenicity. *J Biol. Chem*. 273 (1), 528-36.

Yamaji, S., Suzuki, A., and Sugiyama, Y. 2001. A novel integrin-linked kinase-binding protein, affixin, is involved in the early stage of cell-substrate interaction. *J. Cell. Biol.* 153, 1251-65.

Yang, Y., Guo, L., Blattner, S. M., Mundel, P., Kretzler, M., and Wu, C. 2005. Formation and Phosphorylation of PINCH-1-Integrin Linked Kinase-α-Parvin Complex Are Important for Regulation of Renal Glomerular Podocyte Adhesion, Architecture, and Survival. *J. Am Soc Nephrol*. 16, 1966-76.

Yasunaga, T., Kusakabe, M., Yamanaka, H., Hanafusa, H., Masuyama, N., and Nishida, E. 2005. *Xenopus laevis* ILK (integrin-linked kinase) is required for morphogenetic movements during gastrulation. *Genes Cells* 10, 369-79.

Zervas, C. G., Psarra, E., Williams, V., Solomon, E., Vakaloglou, K. M., and Brown, N. H. 2011. A central multifunctional role of integrin-linked kinase at muscle attachment sites. *J. Cell. Sci*. 124, 1316-27.

Zhang, Y., Chen, K., Tu, Y., Velyvis, A., Yang, Y., Qin, J., and Wu, C. 2002. Assembly of the PINCH-ILK-CH-ILKBP complex precedes and is essential for the localization of each component to cell-matrix adhesion sites. *J Cell Sci*. 115, 4777-86.

Zhang, Y. J., Chen, K., Tu, Y. Z., and Wu, C. Y. 2004. Distinct roles of two structurally closely related focal adhesion proteins, α-parvins and β-parvins, in regulation of cell morphology and survival. *J. Biol. Chem*. 279, 41695-705.

Zhong, C., Chrzanowaska-Wodnicka, M., Brown, J., Shaub, A., Belkin, A. M., and Burridge, K. 1998. Rho-mediated contractility exposes cryptic site in fibronectin and induces fibronectin matrix assembly. *J. Cell Biol.* 141, 539-51.

Zhong, Y., Brieher, W. M., and Gumbiner, B. M. 1999. Analysis of C-cadherin regulation during tissue morphogenesis with an activating antibody. *J. Cell Biol*. 144, 351-3

Appendix A

Figure A1. β-Parvin CH2 domain regulates β-Parvin nuclear localization. HA tagged RP1 (RP1) and HA tagged RP2 (RP2) were injected into the dorsal blastomeres of four-cell stage embryos at sub-phenotypic levels. Embryos were collected at the gastrula stage and fixed in MEMFA. Immunocytochemistry was performed to detect over-expressed HA tagged proteins. RP1 displays a relative decrease in nuclear localization in comparison to HA tagged RP2 (RP2). This is consistent with the results observed with GFP tagged RP1 and RP2 constructs. Scale bar represents 100µm.

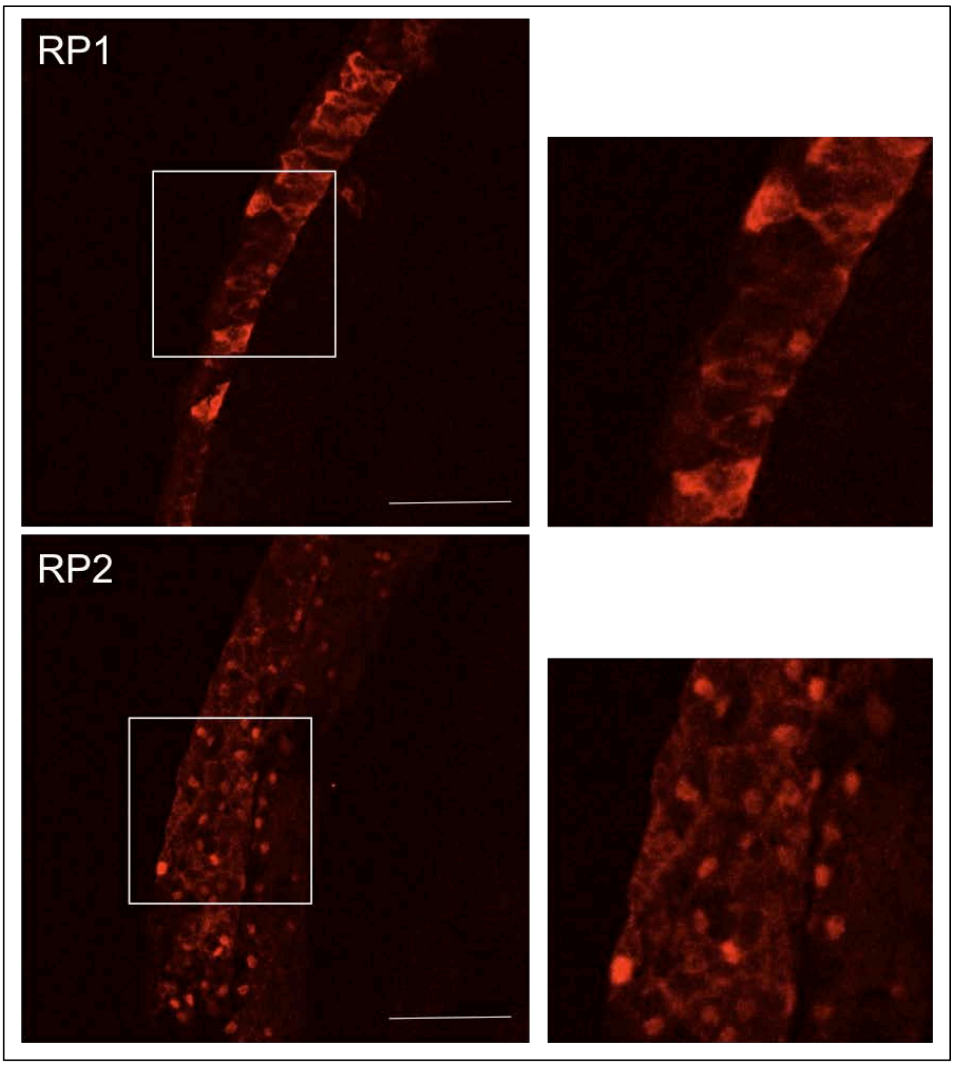
RP1
RP2

Figure A2. Injection of β-Parvin morpholinos fail to cause defects during *Xenopus laevis* gastrulation. A) The *Xenopus laevis* genome includes two copies of β-Parvin, β-Parvin L and β-Parvin S. Available 5'UTR sequences of β-Parvin L and β-Parvin S are shown. The coding sequence is identified with red text. Two morpholino oligonucleotides (MO) were designed to knock down β-Parvin expression. The first was designed to target the 5'UTR of β-Parvin L and second was designed to target the 5'UTR of β-Parvin S (β-Parvin MO2). The binding site of each MO is marked with a red line. B) Sagittal view. β-Parvin MO2 was injected into the animal cap of one-cell stage embryos. Embryos were left to develop until mid gastrulation and fixed. 20 or 40ηg injections failed to produce a defect in gastrula stage embryos. C) RT-PCR analysis. Primer pairs were designed to amplify either both copies of β-Parvin, or β-Parvin S. β-Parvin S (BP (S)) only represents a small fraction of the total β-Parvin mRNA (BP (S+L)) present in the embryo

A.

BP MO1

BP(L):5′…ACATGAGCTCAGGGTGCTGCTGAGGGGCACCCACACCCCAGGGGAG
CAGCATGTCC…3′

BP MO2

BP(S):5′…CTGCTGATAAGACTGAGCTTCAGCTCCACATCCTGTTCCTTCATCA
CATGAGCTCAGGGTGCTGCTGAGAGGCACCCACACCATGTCC…3′

B.

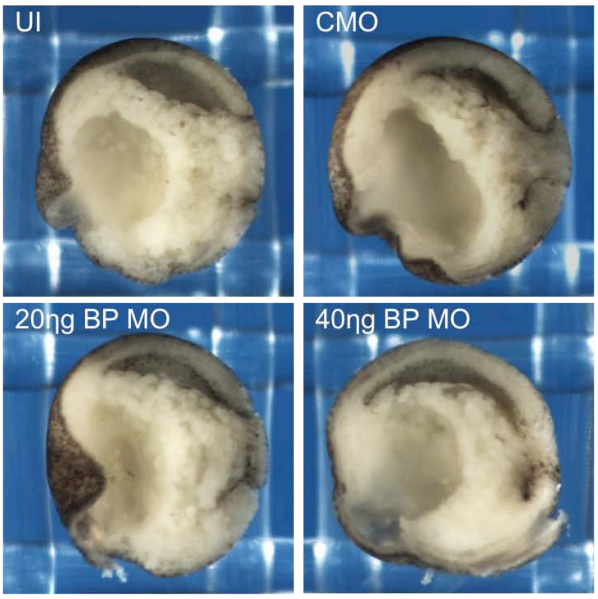

C.

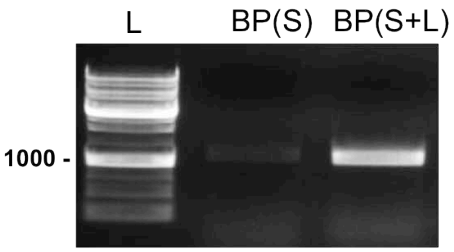

Figure A3. Modified 5'RACE protocol to identify 5'UTR sequence of β-Parvin. A) Workflow schematic of 5'RACE protocol. Reverse transcription (RT) was performed with 5' phosphorylated primer specific to β-Parvin L (*beta-parvin)*. Amplified cDNA was circularized with T4 RNA Ligase 1. T4 DNA polymerase was then used to degrade non-circularized cDNA. Subsequent inverted PCR reactions were performed to amplify the 5'UTR sequence. This protocol was unsuccessful at isolating the 5'UTR of β-Parvin. B) PCR was used to determine the step at which the 5'RACE protocol was failing. PCR to amplify the RP1 region of β-Parvin was used as a control. RP1 is amplifies from cDNA not treated with T4 DNA polymerase (NT). RP1 is not amplified with cDNA treated with T4 DNA polymerase (T). Therefore, cDNA was not circularized with T4 RNA ligase 1 and subsequently degraded by T4 DNA polymerase. (Protocol adapted from Dallmeier and Neyts, 2012).

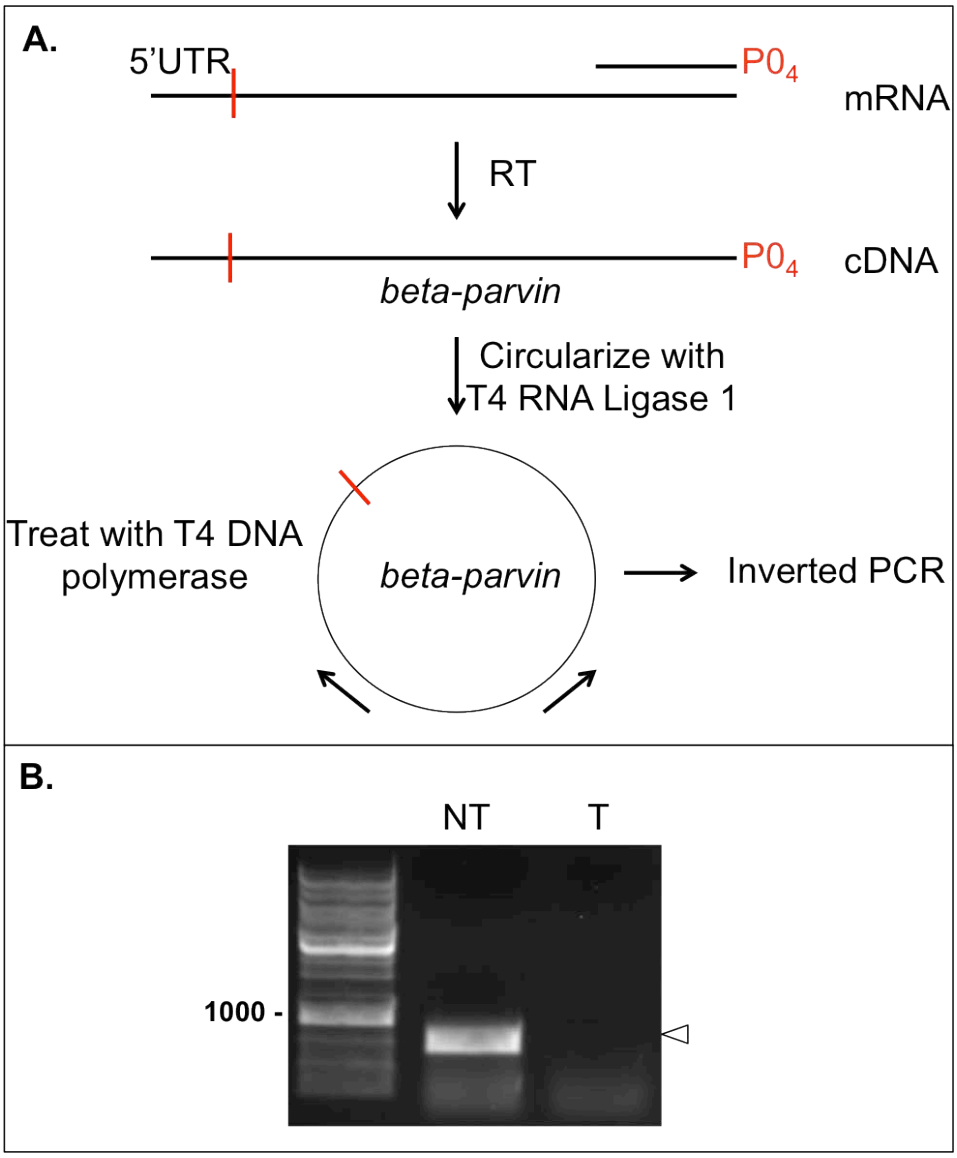
A.
5'UTR
P0$_4$
mRNA
RT
P0$_4$
cDNA
beta-parvin
Circularize with
T4 RNA Ligase 1
Treat with T4 DNA
polymerase
beta-parvin
Inverted PCR
B.
NT
T
1000 -

Figure A4. β-Parvin and PINCH do not interact during *Xenopus laevis* gastrulation. Embryos were co-injected with HA tagged β-Parvin and control GFP or GFP tagged PINCH-xILK and cultured until stage 11. HA tagged BP (BP-HA) was immunoprecipitated from protein lysate using a mouse anti-HA antibody. The immunoprecipitated samples were then subjected to SDS-PAGE and western blot analysis to detect GFP (GFP) and GFP-PINCH (GFP-PINCH). Control GFP and GFP-PINCH are expressed in embryos (Lysate). GFP-PINCH is not pulled down with BP-HA (IP). HA antibody heavy chain runs at 55kDa and is indicated with an outlined triangle.

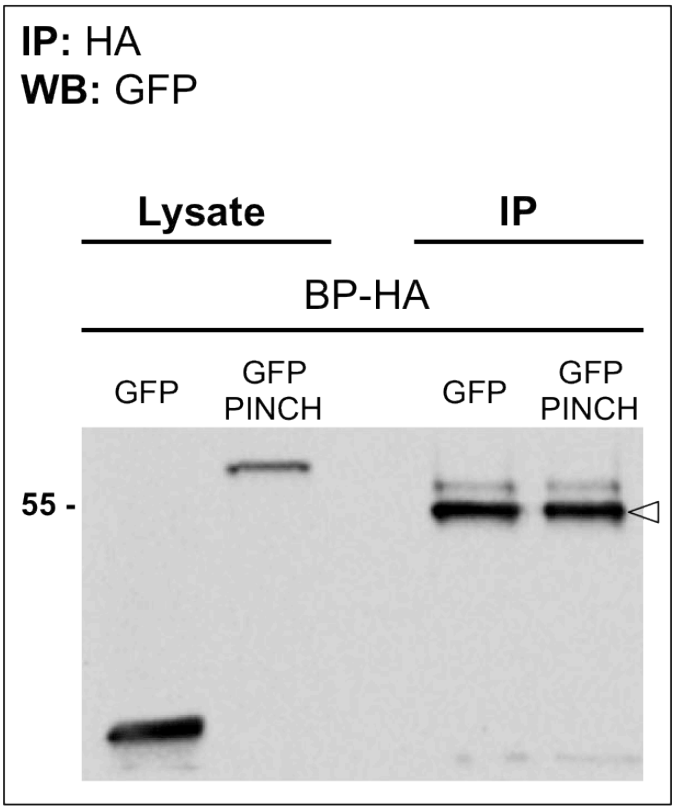
IP: HA
WB: GFP
Lysate
IP
BP-HA
GFP
GFP PINCH
GFP
GFP PINCH
55 -

Figure A5. α-parvin L 5'UTR and coding sequence. The *Xenopus laevis* genome includes two copies of α-parvin, α-parvin L and α-parvin S. α-parvin L is expressed at a functional level in the embryo. The 5'UTR is indicated by bold font. The coding sequence start site is indicated in red. 273 base pairs of α-parvin L 5'UTR are sequenced.

AP(L):5′**CTGAAACGCAAGGAAGTAACGAGTTCCCTTTATAGAGACACTTCCAGCCGGAAT**
AAATGGGGGAGACGTGGGGGAGGGGCAGAGAGGAGCCCAAGATTTAGCAGTGGGAGAGGAA
TGTGGGGGCAGCAGGCTGAGTCTGGTGGGGGGGACAGAGGGATGTCATGTGTCTAATCCAG
TCCCAGGCGGGGTCGGGGAGAGGGAGGATCGCGGCTGAGAAGATTCCGGTTCCGCCTCCGA
CCCTCCCCTCAGTGCAGCGCTGCGCCTCTCCCAGTCATGGCAACGTCCCCCCAAAAATCTC
CTTCCAGCCCGAAATCCCCCACTCCCAAGTCTCCCCCTTCTAGGAAGAAAGATGATTCGTT
CCTGGGCAAGCTGGGGGGCACCCTGGCACGGAGAAAGAAAGCCAAGGAGGTATCCGAGCTC
CAGGAGGAAGGGATCAATGCTATTAACTTGCCGCTCAACCCCATTCCCTTTGAGCTGGACC
CCGAGGACACGATGCTTGAGGAAAATGAAGTCCGAACGATGATCGACCCATTCTCAAGGAG
TGATGCGAGACTGCAAGAGCTGATGAAGGTTCTGATCGATTGGATCAATGATGTGCTGGTT
GGAGAGAGAATCATTGTCAAGGATCTAGCGGAGGATATGTACGATGGGCAAGTTCTGCAGA
AGCTTTTCGAGAAACTGGAAGGGGAGAAACTAAATGTCGCCGAAGTCACACAGTCGGAAAT
CGCTCAGAAGCAGAAGCTGCAGACGGTGCTGGAGAAAATCAACGAAACGCTCAAGCTGCCC
CCGAGGAGCGTCAAGTGGAACGTGGACTCAATTCATGCAAAATCTGTAGTAGCCATCCTTC
ATCTTCTGGTTGCCCTGTCGCAGTATTTCCGGGCCCCCATCCGACTACCAGATCATGTATC
AATTCAGGTCGTCGTCGTCCAGAAGTTGGACGGAATGTTGCAGTCTCGGCACATCCAGGAG
GAAATCACCGGTGACACAGAGGCGCTGTCAGGAAGGCACGAGAGAGATGCGTTTGACACCC
TGTTCGACCACGCTCCAGACAAACTTAATGTGGTGAAAAAGACTCTCATCACGTTTGTCAA
CAAACACCTCAATAAACTGAACCTGGAAGTAACAGAACTGGAAACCCAGTTTGCAGATGGA
GTGTACCTGGTGCTTCTGATGGGTCTCCTGGAAGGATATTTTGTGCCTCTGTTCAACTTCT
TCTTGACGCCAGAGAGCTTTGAACAAAAGGTTCTGAATGTGACATTTGCTTTTGAACTCAT
GCAAGACGGAGGCCTGGAGAAGCCCAAACCGCGGCCAGAAGATATTGTCAACTGTGACCTG
AAATCCACTCTGAGGGTCCTCTACAATCTGTTCACCAAGTACAGAAGCGTGGAGTGA…3′

Appendix B

The importance of each xILK mutant during *Xenopus laevis* gastrulation was assessed using over-expression experiments. As a first step, I over-expressed full-length xILK and each xILK deletion construct in the dorsal tissues of gastrulating embryos and assessed gross morphological defects. At stage 12 it was clear that the morphology of embryos injected with each xILK construct was severely disrupted (Figure B1). In full-length xILK over-expressing embryos (xILK) the DMZ has failed to thin through epiboly, the post-involution mesoderm has not converged and extended through CE movements and a normal archenteron has failed to form. In xILK ΔANK (ΔANK) over-expressing embryos, the DMZ also failed to thin through epiboly however the post-involution mesoderm appears to have undergone CE movements and an archenteron is visible. Embryos over-expressing xILK constructs that cannot bind β-Parvin (ΔINT (ΔINT) and xILK ΔKIN (ΔKIN)) also fail to undergo epiboly and CE, however these defects appeared more severe than in embryos over-expressing xILK constructs capable of binding β-Parvin (xILK and ΔANK, Figure B1). Additionally, cell-cell contacts in the endoderm and yolk plug area of xILK ΔKIN injected embryos appeared more dissociated than cell-cell junctions in xILK, xILK ΔANK and xILK ΔINT injected embryos. In control un-injected embryos, the DMZ has undergone epiboly and CE, and a normal archenteron has formed. These results suggest that xILK plays a role in regulating the cellular rearrangements required for gastrulation.

The defects produced by xILK construct over-expression resemble those seen in embryos lacking a FN matrix (Marsden and DeSimone, 2001). Therefore I assessed the formation of a FN matrix along the BCR using immunocytochemistry. Control

Figure B1. xILK construct overexpression inhibits gastrulation. Embryos were injected at the four-cell stage with full-length FLAG tagged xILK or one of the FLAG tagged xILK deletion constructs. Un-injected (UI) control embryos display tissue architecture of a normally gastrulating embryo. Over-expression of FLAG-xILK (xILK) causes defects in the pre and post-involution tissues undergoing epiboly and CE. The pre-involution DMZ has failed to thin through epiboly and the post-involution mesoderm has failed to extend through CE. An archenteron has not formed. Injection of FLAG-xILK ΔANK (ΔANK) also prevents DMZ tissue thinning through epiboly, but CE appears to have occurred and an archenteron has formed. Overexpression of FLAG-xILK ΔINT (ΔINT) and FLAG-xILK ΔKIN (ΔKIN) also prevents epiboly and CE and an archenteron fails to form. Cell-cell contacts in ΔKIN-injected embryos are dissociated in the endoderm and area of the yolk plug.

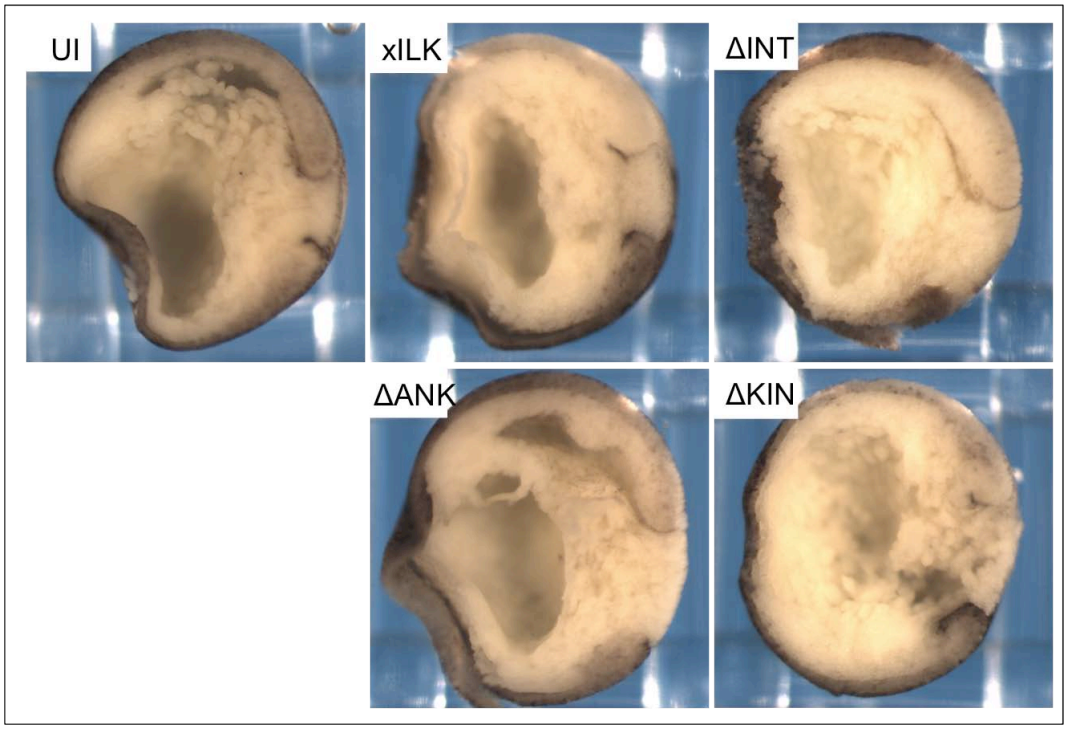
UI
xILK
ΔINT
ΔANK
ΔKIN

Control un-injected (UI) embryos assemble a FN matrix (Figure B2). Embryos over-expressing full-length xILK (xILK) exhibit a small decrease in FN assembly compared to controls. xILK ΔANK (ΔANK) displays a larger decrease in FN assembly compared to xILK. Over-expression of xILK constructs that cannot bind β-Parvin (xILK ΔINT (ΔINT) and xILK E359K (E359K)) display an even greater reduction in assembled FN. Short FN punctae are still visible on the cell surface, indicating functioning FN-integrin ligation (Figure B2). These results demonstrate that xILK is required for the assembly of a FN matrix.

To better understand the role xILK-β-Parvin complex formation plays during gastrulation, the cellular rearrangements of xILK and xILK E359K injected embryos were examined by confocal microscopy. Control un-injected embryos have undergone epiboly and display proper cell arrangement in the post-involution mesoderm to drive CE movements (Figure B3). Embryos over-expressing xILK do not appear to have undergone epiboly and the cells in the post-involution mesoderm are disorganized. Embryos over-expressing xILK E359K also appear to have failed epiboly and the cells in the post-involution mesoderm took no obvious orientation (Figure B3). Although similar the defects observed with xILK E359K are more severe than those produced by xILK. Together, the more severe morphological defects and greater inhibition of FN matrix assembly caused by the over-expression of a xILK construct that cannot interact with β-Parvin, suggests that the xILK-β-Parvin complex is important during these processes.

Figure B2. xILK is required for FN fibrillogenesis. Embryos were injected at the four-cell stage with full-length FLAG tagged xILK or one of the FLAG tagged xILK deletion constructs and cultured until stage 12. Immunocytochemistry was performed to detect FN. Un-injected (UI) embryos exhibit normal FN matrix assembly. Embryos injected with FLAG-xILK (xILK) and FLAG-xILK ΔANK (ΔANK) display a large reduction in FN assembly. However, FN fibrils are still visible. Overexpression of FLAG-xILK ΔINT (ΔINT) and FLAG-xILK E359K (E359K) inhibits FN assembly. Very few fibrils are present.

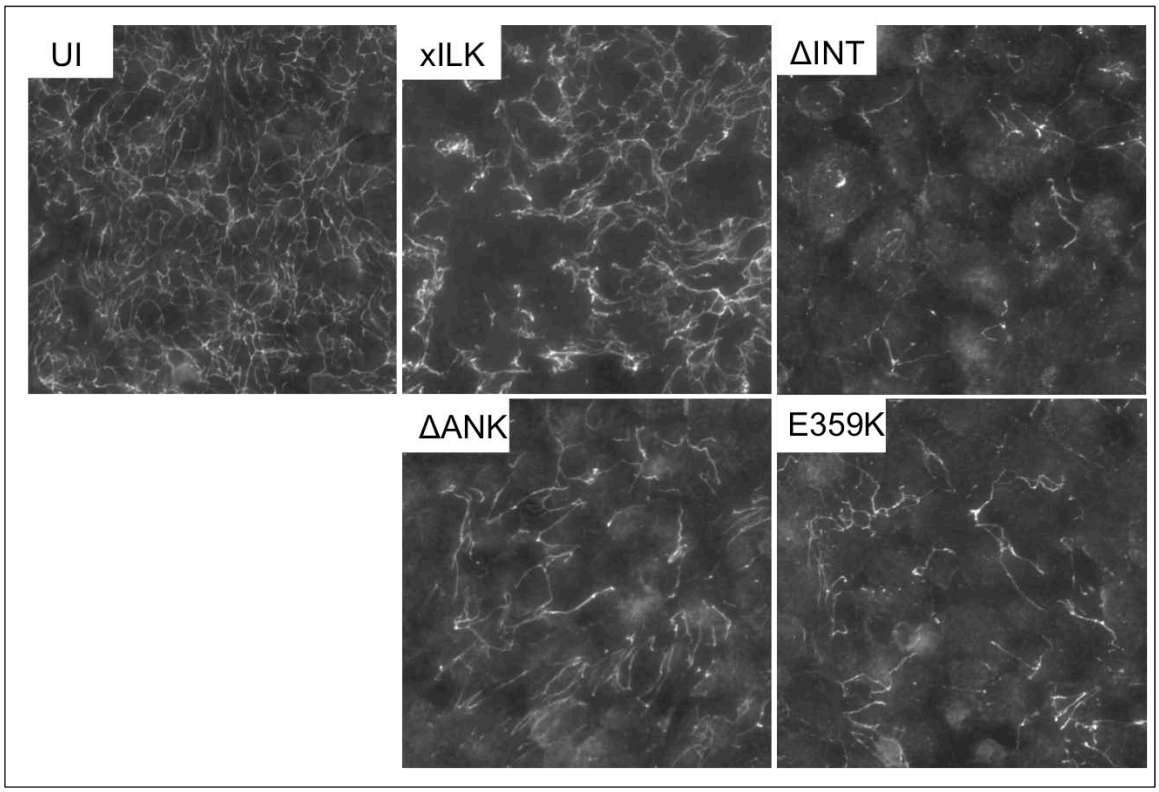
UI
xILK
ΔINT
ΔANK
E359K

Figure B3. xILK and xILK E359K overexpression inhibits epiboly and cell polarization in the DMZ. Stage 12 embryos. Control GFP (GFP) injected embryos have undergone epiboly and also display proper cell arrangement in the post-involution mesoderm. The DMZ has thinned slightly and cells in the post-involution mesoderm are disorganized in GFP-xILK (xILK) injected embryos. The DMZ failed to thin and the post-involution mesoderm is severely disorganized in GFP-xILK E359K (E359K) injected. Black box represents the approximate field of view in the lower panels. Double-headed white arrow represents the thickness of the pre-involution DMZ and the single headed white arrow points to the involuted mesoderm. Scale bars represent 100µm.

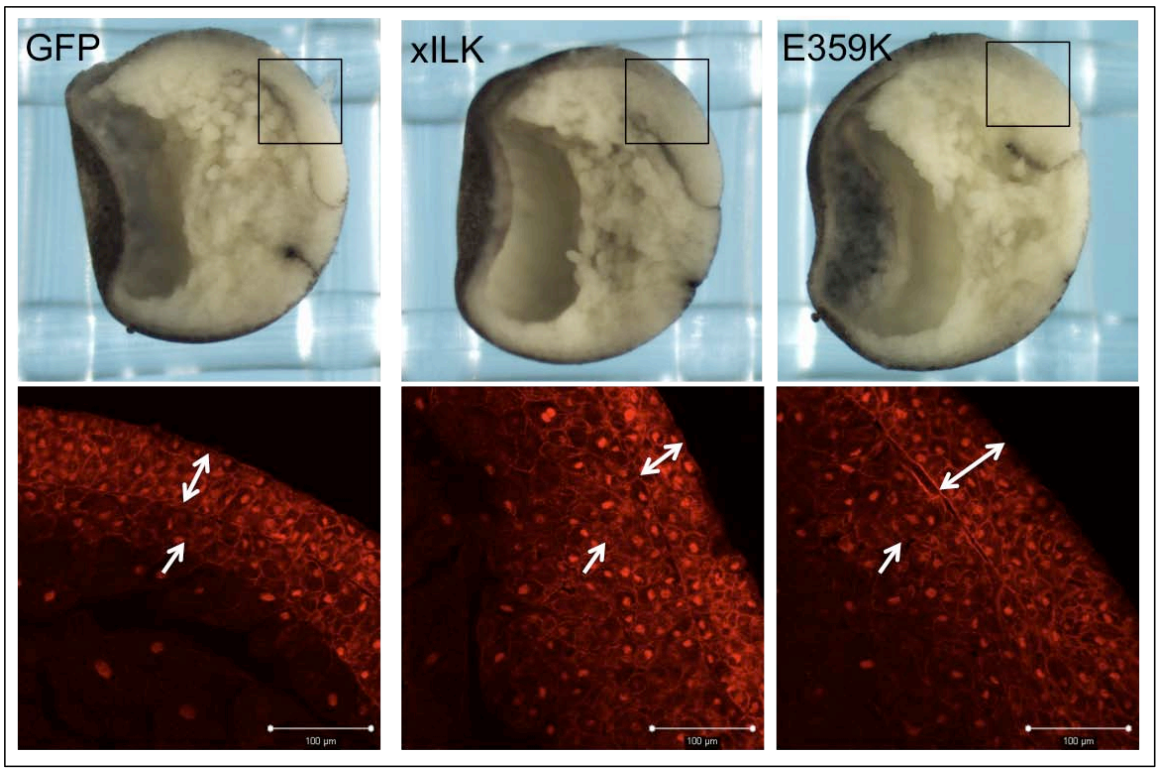
GFP
xILK
E359K
100 µm
100 µm
100 µm